

**Donor-Acceptor Block Copolymers
for Charge Separation
at Nanostructured Interfaces**

Dissertation

for the award of the academic degree of
Doctor of Natural Science (Dr. rer. nat.)
from the Faculty of Biology, Chemistry and Geosciences
University of Bayreuth

submitted by
Stefan M. Lindner
born in Bayreuth

Bayreuth, 2006

Die vorliegende Arbeit wurde in der Zeit von Oktober 2002 bis März 2006 am Lehrstuhl für Makromolekulare Chemie I der Universität Bayreuth angefertigt.

Vollständiger Abdruck der von der Fakultät Biologie, Chemie und Geowissenschaften der Universität Bayreuth genehmigten Dissertation zur Erlangung des akademischen Grades Doktor der Naturwissenschaften (Dr. rer. nat.).

Datum der Einreichung der Arbeit: 09.03.2006

Datum des wissenschaftlichen Kolloquiums: 21.07.2006

Prüfungsausschuß:

Prof. Dr. K. Seifert (*Vorsitzender*)

Prof. Dr. M. Thelakkat (*Erstgutachter*)

Prof. Dr. G. Krausch (*Zweitgutachter*)

Prof. Dr. H. G. Alt

*Für meinen Vater
Manfred Lindner
† 10.12.2004*

*,,Neue Wege entstehen,
indem wir sie gehen.“*

Friedrich Nietzsche

Danksagung

Herrn Professor Dr. Mukundan Thelakkat danke ich für die Möglichkeit auf diesem sehr interessanten Themengebiet zu arbeiten. Neben der Diskussionsbereitschaft, der persönlichen Unterstützung und der Teilnahme an internationalen Fachtagungen, möchte ich mich besonders für die Freiheit im wissenschaftlichen Arbeiten bedanken.

Herrn Prof. Dr. Hans-Werner Schmidt danke ich für die Möglichkeit an seinem Lehrstuhl zu promovieren und für das Bereitstellen eines sehr gut ausgestatteten Laborplatzes.

Herrn Prof. Dr. Georg Krausch, Dr. Arnaud Chiche und Sven Hüttner möchte ich für die Zusammenarbeit auf dem Gebiet der Morphologie in organischen Solarzellen danken.

Für die Zusammenarbeit bei der Entwicklung von neuen lichtabsorbierenden Fullerenderivaten möchte ich mich bei Herrn Prof. Dr. Andreas Hirsch und Michaela Ruppert, Universität Erlangen-Nürnberg, bedanken.

Ich möchte mich bei allen Mitarbeitern des Lehrstuhls bedanken, die durch ihre fachliche Unterstützung zu dieser Arbeit beigetragen haben. Aber vor allem auch bei denen, die durch verschiedene Aktivitäten eine positive und motivierende Arbeitsatmosphäre geschaffen haben und zu guten Freunden geworden sind. Ich möchte hierbei Frank Abraham, Dr. Katja Fischer, Doris Hanft, Nils Mohmeyer, Martin Sonntag und Dr. Heiko Thiem besonders hervorheben. Außerdem möchte ich meinen Nachfolgern Nadine Kaufmann und Michael Sommer für die Fortentwicklung der Forschungsgebiete danken und ihnen viel Erfolg wünschen.

Für die finanzielle Unterstützung möchte ich mich bei der Deutschen Forschungsgemeinschaft, Sonderforschungsbereich 481, bedanken.

Meiner Familie möchte ich für die Unterstützung während des Studiums und dem Erstellen meiner Doktorarbeit herzlich danken, da sie diese Arbeit überhaupt erst ermöglichten.

List of Abbreviations

a.u.	arbitrary unit
AM 1.5	air mass 1.5 solar spectrum
CuPc	copper phthalocyanine
DBU	1,8-diazabicyclo[5.4.0]undec-7-ene
DSC	differential scanning calorimetry
DSSC	dye-sensitized nanocrystalline TiO ₂ solar cells
DTCB	2-[(2E)-3-[4-(tert-butyl)phenyl]-2-methylprop-2-enylidene]malononitrile
Fc	ferrocene
FTO	fluorinated tin oxide
GPC	gel permeation chromatography
HOMO	highest occupied molecular orbital
HTM	hole transport material
IPCE	incident photon to current conversion efficiency
I _{sc}	short circuit current
ITO	indium tin oxide
L _D	exciton diffusion length
LUMO	lowest unoccupied molecular orbital
MALDI-TOF	matrix-assisted laser desorption ionization - time of flight
M _n	number average molecular weight
nc	nanocrystalline
NMR	nuclear magnetic resonance
NMRP	nitroxide mediated controlled radical polymerization
NPD	N,N'-di(1-naphthyl)-N,N'-diphenyl-1,1-biphenyl-4,4'-diamine
OD	optical density
P3HT	poly(3-hexylthiophene)
PB	perylene benzimidazole
PCBM	[6,6]phenyl-C ₆₁ -butyric acid methyl ester
PDI	polydispersity
PEDOT:PSS	poly(3,4-ethylenedioxythiophene) / polystyrene sulfonate
PPTS	pyridinium <i>para</i> -toluenesulfonate

PPV	poly(<i>para</i> -phenylene vinylene)
RAFT	reversible addition - fragmentation chain transfer
<i>spiro</i> -OMeTAD	2,2',7,7'-tetrakis(N,N-di- <i>p</i> -methoxy-phenylamine)-9,9'-spirofluorene
TBAB	tetrabutyl ammonium bromide
TEM	transmission electron microscopy
TEMPO	2,2,6,6-tetramethylpiperidinyloxy
T _g	glass transition temperature
TGA	thermo gravimetric analysis
THF	tetrahydrofuran
T _m	melting point
TPA	triphenylamine
TPD	N,N,N',N'-tetraphenyl-1,1-biphenyl-4,4'-diamine
UV/vis	ultraviolet / visible
V _{oc}	open circuit voltage
WAXS	wide angle X-ray scattering

Table of Contents

1. Introduction	1
1.1 Organic Electronics	1
1.2 Organic/Hybrid Solar Cells	2
1.2.1 Vapor Deposited Multi-Layer Solar Cells	2
1.2.2 Hybrid Solar Cells	4
1.2.3 Polymer Blend Solar Cells	6
1.3 Nitroxide Mediated Controlled Radical Polymerization.....	9
2. Overview of Thesis	12
2.1 Motivation and Aim	12
2.2 Fluorescent Acceptor Dye Labeled Polymers carrying Hole Transport Pendant Groups.....	15
2.2.1 Synthesis.....	15
2.2.2 Results and Discussion.....	17
2.3 Novel Soluble Perylene Bisimide - Fullerene Dyads	22
2.3.1 Synthesis.....	22
2.3.2 Results and Discussion.....	23
2.4 Block Copolymers for Nanostructured Organic Electronics.....	28
2.4.1 Synthesis.....	28
2.4.2 Results and Discussion.....	32
2.5 Photovoltaic Devices	43
2.5.1 Methods.....	43
2.5.2 Solar Cell Results	45
2.5.3 Additional Results	49
2.6 Statement	51

3. Summary	53
4. Zusammenfassung.....	58
5. Appendix	63
A1 Fluorescent Acceptor Labeled Polymers carrying Hole Transport Pendant Groups.....	63
A2 Synthesis, Photophysical and Electrochemical Characterization of Novel Soluble Perylene Bisimide - Fullerene Dyads.....	81
A3 Nanostructures of n-Type Organic Semiconductor in a p-Type Matrix via Self-Assembly of Block Copolymers	95
A4 Nanostructured Semiconductor Block Copolymers: π - π Stacking, Optical and Electrochemical Properties	110
A5 Charge Separation at Self-Assembled Nanostructured Bulk Interfaces in Block Copolymers	124

1. Introduction

1.1 Organic Electronics

The interest in the use of low molecular or polymeric compounds for organic electronics is rapidly growing. The main reason for this is that on the one hand there are already the first products on the market, but on the other hand most of the potential applications are still under development. Normally polymers or low molecular organic compounds are known to be insulators. But in 1977 it was discovered that with doping polyacetylene also conducting polymers could be achieved¹. “For the discovery and development of conductive polymers” the Nobel Prize in chemistry 2000 was awarded to Alan Heeger, Alan MacDiarmid and Hideki Shirakawa. Organic materials have found potential applications in many opto-electronic devices such as organic light emitting diodes (OLED)², organic field effect transistors (OFET)³, optical switches⁴, organic lasers⁵, organic solar cells⁶, and many more.

Organic light emitting diodes and displays constitute one of the successful stories in the field of electro-optical applications with organic materials. They are already commercially available for small displays with a low resolution like cell phones. Another application for organic electronics are organic field effect transistors (OFET)³. These transistors can be used for example in RFID (radio frequency identification) tags⁷. These chips are used for the storage of information and can be read out by radio waves. They may be used instead of barcodes on prize labels as no direct contact is needed.

Especially for these low cost applications, organic materials are the ideal candidates. They can be easily processed, are applicable to large areas and are compatible with flexible substrates^{8,9}. Another advantage of organic materials compared to inorganic materials is that the properties of organic molecules can be tailored on a molecular level.

¹ H. Shirakawa, E. J. Louis, A. G. MacDiarmid, C. K. Chiang, A. J. Heeger *J. Chem. Soc. Chem. Commun.* **1977**, 578-580.

² C. W. Tang, S. A. VanSlyke *Appl. Phys. Lett.* **1987**, 51, 913-915.

³ C. J. Drury, C. M. J. Mutsaers, C. M. Hart, M. Metters, D. M. de Leeuw *Appl. Phys. Lett.* **1998**, 73, 108-110.

⁴ M. P. O’Neil, M. P. Niemczyk, W. A. Svec, D. Gosztola, G. L. Gaines III, M. R. Wasielewski *Science* **1992**, 257, 63-65.

⁵ R. Gvishi, R. Reisfeld, Z. Burshtein *Chem. Phys. Lett.* **1993**, 213, 338-344.

⁶ C. W. Tang *Appl. Phys. Lett.* **1986**, 48, 183-185.

⁷ R. Butscher *Bild der Wissenschaft* **2005**, 6, 100-110.

⁸ G. Malliaras, R. Friend *Phys. Today* **2005**, 58, 53-58.

⁹ C. J. Brabec, J. A. Hauch, P. Schilinsky, C. Waldauf *MRS Bull.* **2005**, 30, 50-52.

1.2 Organic / Hybrid Solar Cells

A very interesting and emerging technology based on organic materials is the organic photovoltaics. As fossil fuels are limited and their combustion produces carbon dioxide which boosts the green house effect, alternative energy sources are of great interest. Inorganic solar cells like the silicon solar cells are well established, but the prize is high as the production processes are energy and cost intensive. Therefore organic solar cells are interesting candidates towards inexpensive renewable energy sources.

Organic solar cells can be divided into several classes by different approaches. They may be distinguished into small molecules and polymer solar cells, or into solution processed and vapor deposited, or on their charge creation mechanism and so on. But the focus of this chapter should be the similarities and not the differences of the different approaches.

1.2.1 Vapor Deposited Multi-Layer Solar Cells

The first and best understood systems are vapor deposited thin-layer devices. This concept was introduced by Tang⁶ in 1986. Two organic layers were deposited between a transparent ITO electrode and a metal electrode (Tang cell, see figure 1-1). The organic layers consisted of perylene benzimidazole (PB) as an electron transport material (electron acceptor, n-type material) and copper phthalocyanine (CuPc) as a hole transport material (electron donor, p-type material). The combination of a p-type and an n-type material, the so-called p/n heterojunction is a basic concept for all efficient organic solar cells. There are many advantages of the vapor deposited thin layer solar cells. The thickness and the composition (two stacked layers or a mixed layer) of the layers can be controlled precisely, the purity of the materials is very high (train sublimation) and also insoluble materials may be vapor deposited.

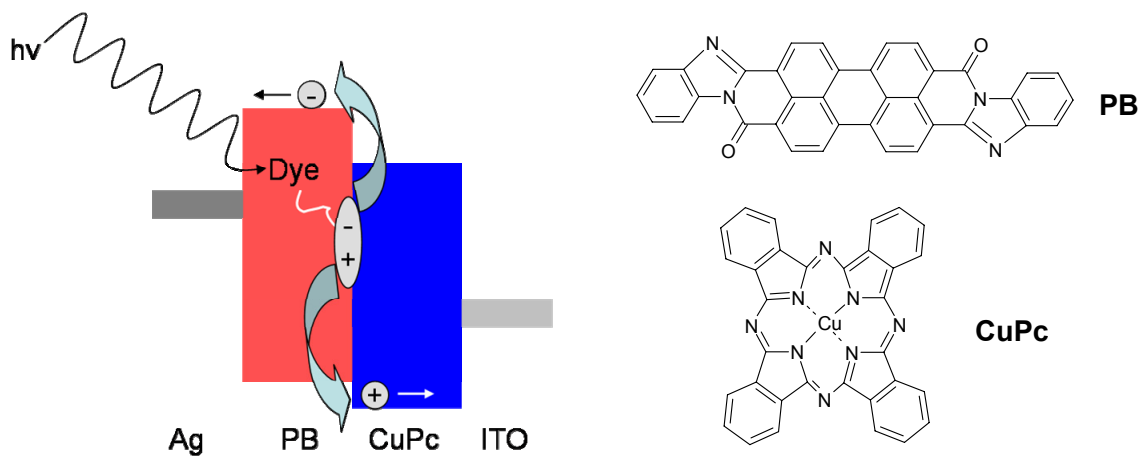


Figure 1-1: Schematic processes in a Tang cell and the chemical structures of the used materials.

In figure 1-1 a scheme of the physical processes in organic solar cells is shown. For simplicity a basic model of the Tang cell is used, but for other organic solar cells the steps are actually comparable. There are more complex models shown in the literature^{10,11}. The first step is the absorption of light to build an exciton (bound electron-hole pair). The exciton binding energy is with 0.4 – 1.4 eV very strong¹², therefore strong fields of about 10^6 V/cm are necessary for efficient exciton dissociation¹³. So the exciton has to diffuse to the interface between the n-type and p-type material, because only there the exciton can be dissociated into an electron and hole. The electron is then transported through the electron transport material and the hole through the hole transport material to the electrodes if transport pathways are available. The charge carrier transport in amorphous organic semiconductors is described by a so-called hopping process from one molecule to the next one.

The limiting factor in this system is the exciton diffusion length L_D . Typical exciton diffusion lengths are about 2-20 nm for organic materials. Therefore only excitons which are created near the interface can reach the interface. For this reason the layer thicknesses in vapor deposited solar cells are about 5-35 nm. But the insufficient absorption in these layers is limiting the efficiency of the device.

¹⁰ C. J. Brabec, N. S. Sariciftci, J. C. Hummelen *Adv. Funct. Mat.* **2001**, *11*, 15-26.

¹¹ J. Nelson *Current Opinion in Solid State & Materials Science* **2002**, *6*, 87-95.

¹² I. G. Hill, A. Kahn, Z. G. Soos, R. A. Pascal *Chem. Phys. Lett.* **2000**, *327*, 181-188.

¹³ P. Peumans, A. Yakimov, S. R. Forrest *J. Appl. Phys.* **2003**, *93*, 3693-3723.

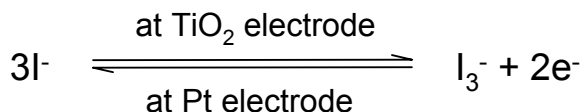
Interesting attempts to solve this problem by using mixed layers^{14,15,16} of p-type and n-type materials and by using tandem cells¹⁷ have been developed. Tandem cells consist actually of two solar cells which are connected in series by a recombination zone. The layer thickness and structure were adjusted to obtain high optical field intensities. The efficiency of such tandem cells has already reached high values (~ 5%)¹⁷, but the vapor deposition of a series of up to eleven layers with an exact thickness (1 nm – 5 nm) is complicated and costly.

Therefore, other concepts were introduced to combine the exciton diffusion length of some nanometers with optical thick samples that require 100 nm to 500 nm thick devices. These systems have to be nanostructured to have interfaces in the range of the exciton diffusion length. There are two major concepts which fulfill this requirement: Dye-sensitized nanocrystalline TiO₂ solar cells (DSSC) and blends of polymers and low molecular materials.

1.2.2 Hybrid Solar Cells

In order to get a large interface in a photovoltaic device, Brian O'Regan and Michael Grätzel presented a concept¹⁸ which uses nanocrystalline (nc) TiO₂ as n-type semiconductor. The nc TiO₂ particles are deposited on a FTO substrate by screen printing from a colloidal suspension of TiO₂ followed by sintering. In this way a mesoporous layer of TiO₂ is created. The resulting interface is 1000 times higher than that for a flat device. A Ru-dye is chemisorbed onto the surface of the TiO₂ particles. The cell is then filled with an I⁻/I₃⁻ redox electrolyte in acetonitrile. As a counter electrode a platinum coated FTO substrate is used.

In this cell the light is absorbed by the Ru-dye. As there is only a monomolecular dye layer, an electron can be directly injected into the nc TiO₂ particles. The electron is transported through the TiO₂ to the electrode. The positively charged Ru-complex has to be regenerated by an electron donation. The I⁻/I₃⁻ redox couple acts as an electron donor and is regenerated itself at the platinum coated electrode.



The regeneration of the Ru-dye has to be very fast, otherwise recombination between the hole on the dye and the electron in the TiO₂ will occur. The power conversion efficiency of such

¹⁴ J. Rostalski, D. Meissner *Sol. En. Mat. & Solar Cells* **2000**, *61*, 87-95.

¹⁵ P. Peumans, S. Uchida, S. R. Forrest *Nature* **2003**, *425*, 158-162.

¹⁶ J. Xue, B. P. Rand, S. Uchida, S. R. Forrest *Adv. Mater.* **2005**, *17*, 66-71.

¹⁷ J. Xue, S. Uchida, B. P. Rand, S. R. Forrest *Appl. Phys. Lett.* **2004**, *85*, 5757-5759.

¹⁸ B. O'Regan, M. Grätzel *Nature* **1991**, *353*, 737-740.

1. Introduction

cells is with up to 10 % very good¹⁹, but the main problem is the drying up of the solvent. Although the devices are sealed, a loss of solvent over the time is barely to avoid. There are many attempts to solve this problem by using the I/I_3^- redox couple with high boiling solvents or by using organic gelators to have a quasi solid-state electrolyte²⁰ or by using ionic liquids²¹ but the efficiencies are in all cases lower due to the fact that the conductivity of I/I_3^- is decided by the viscosity of the medium.

To overcome this problem, the principle of using organic hole conductors instead of the I/I_3^- electrolyte was shown²² in 1997. The solid-state dye sensitized TiO_2 solar cell was further optimized by using doped *spiro*-OMeTAD as hole conductor and a blocking TiO_2 layer between the nanocrystalline TiO_2 and the FTO substrate was introduced²³. Also additives like N-lithiotrifluoromethanesulfonimide, the radical cation of *spiro*-OMeTAD and 4-*tert*-butyl pyridine²⁴ are used for better efficiency.

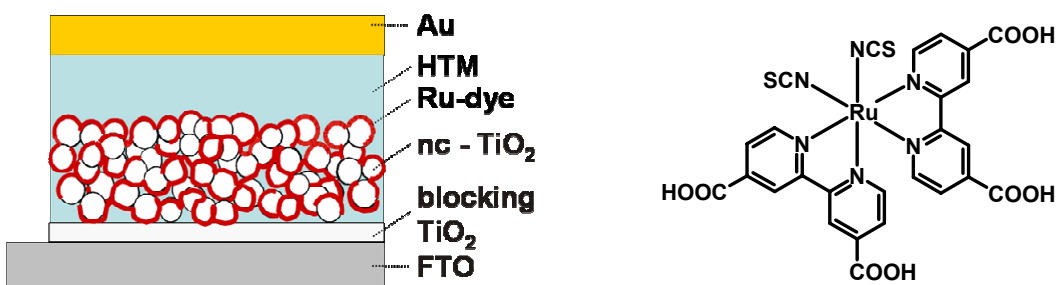


Figure 1-2: Device structure of a solid-state dye sensitized TiO_2 solar cell and the chemical structure of the Ru-dye N3.

The problem of evaporation of the solvent is solved, but the efficiency of such devices is still lower than those of the electrolyte cells. One problem in solid-state dye sensitized TiO_2 solar cells is the high recombination in such cells. Moreover, the dye regeneration occurs very fast with the redox electrolyte, but is slower for organic hole conductors. As the positive charge remains longer on the dye the probability of recombination increases. The recombination can

¹⁹ M. Grätzel *J.Photochem. Photobiol. C: Photochem. Rev.* **2003**, 4, 145-153.

²⁰ N. Mohmeyer, P. Wang, H.-W. Schmidt, S. M. Zakeeruddin, M. Grätzel *J. Mater. Chem.* **2004**, 14, 1905-1909.

²¹ P. Bonhôte, A.-P. Dias, N. Papageorgiou, K. Kalyanasundaram, M. Grätzel *Inorg. Chem.* **1996**, 35, 1168-1178.

²² J. Hagen, W. Schaffrath, P. Otschik, R. Fink, A. Bacher, H.-W. Schmidt, D. Haarer *Synth. Met.* **1997**, 89, 215-220.

²³ U. Bach, D. Lupo, J. E. Moser, F. Weissortel, J. Salbeck, H. Spreitzer, M. Grätzel *Nature* **1998**, 395, 583-585.

²⁴ J. Krüger, R. Plass, L. Cevey, M. Piccirelli, M. Grätzel, U. Bach *Appl. Phys. Lett.* **2001**, 79, 2085-2087.

1. Introduction

be suppressed²⁵ by using dual-functional dyes which enhances the efficiency²⁶. There a donor antenna group is attached to the Ru-dye which transfers the hole away from the TiO₂ surface to the donor. Another positive effect of these dyes is the enhanced light absorption and the compatibility with the organic hole conductor.

Most of the hybrid solar cells use TiO₂ nanoparticles which are commercially available in different particle sizes and in large quantities. But other semiconducting nanoparticles are also used. Especially colored particles like CdSe²⁷ are very interesting for this purpose as the additional dye layer can be avoided. There is ongoing research on this topic but the efficiencies are still lower than for dye sensitized nc TiO₂ solar cells and the problem of toxicity remains.

1.2.3 Polymer Blend Solar Cells

The creation of small domain sizes is also possible by blending polymers with low molecular weight materials. Most of the early work^{28,29} was done with PPV (poly(*p*-phenylene vinylene)) as hole conductor and PCBM ([6,6]phenyl-C₆₁-butyric acid methyl ester), a fullerene derivative as electron transport material. The chemical structures are shown in figure 1-3.

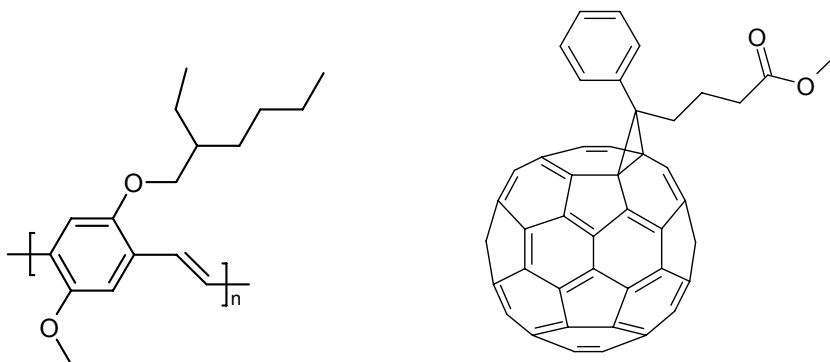


Figure 1-3: Chemical structures of MEH-PPV and PCBM.

The performance of these devices strongly depends on the ratio between PCBM and PPV and the morphology of the blend films. The power conversion efficiency is maximum for high amounts of PCBM (80%). This fact is astonishing as PCBM is barely absorbing in the solar spectrum and is in regard to light harvesting non-active. An efficient quenching of the

²⁵ S. A. Haque, S. Handa, K. Peter, E. Palomares, M. Thelakkat, J. R. Durrant *Angew. Chem. Int. Ed.* **2005**, 44, 5740-5744.

²⁶ K. Peter, H. Wietasch, B. Peng, M. Thelakkat *Appl. Phys. A* **2004**, 79, 65-71.

²⁷ W. U. Huynh, J. J. Dittmer, A. P. Alivisatos *Science* **2002**, 295, 2425-2427.

²⁸ N. S. Sariciftci, L. Smilowitz, A. J. Heeger, F. Wudl *Science* **1992**, 258, 1474-1476.

²⁹ G. Yu, J. Gao, J. C. Hummelen, F. Wudl, A. J. Heeger *Science* **1995**, 270, 1789-1791.

1. Introduction

fluorescence of PPV is already achieved with 2 % of PCBM, so for the exciton separation only low amounts are necessary³⁰. But it could be shown that the morphology strongly depends on the composition. Only for high amounts of PCBM a clear morphology could be shown. Actually there are two domains, a pure PCBM domain and a mixed phase of both compounds. These results clearly show the importance of the morphology for obtaining high efficient organic solar cells³¹.

The morphology and with it the performance is also strongly dependent on the film casting conditions. If chlorobenzene is used for spin coating instead of toluene, the efficiency is nearly tripled from 0.9 to 2.5 %³². It could be even shown that the domain sizes are one order of magnitude bigger for the toluene cast films³³.

This concept was even improved by changing the hole transport material from PPV to P3HT (poly(3-hexylthiophene)). P3HT is known to be a very good hole conductor with a high hole mobility and a broad absorption. Furthermore, the optimal ratio of PCBM to P3HT is with 1 to 1 better as the amount of dye for a constant device thickness could be enhanced³⁴. With this hole conductor efficiencies of up to 5.1 % could be realized³⁵. The performance strongly depends on the annealing conditions³⁶. Only after controlled tempering high efficiencies could be achieved. There are less morphology studies than for the PPV - PCBM system, but these results strongly suggest a morphology change resulting in ordered structures due to stacking of the P3HT chains.

Polymer / polymer blends were also investigated for the application in organic solar cells. As electron transport material a cyano derivative of poly(p-phenylene vinylene) (MEH-CN-PPV) is used together with MEH-PPV³⁷. But the efficiencies were quite low, even with other polymer systems^{38,39}. Therefore special preparation techniques were introduced to enhance the efficiency. For example by laminating two layers⁴⁰ the efficiency could be increased. The first layer consisted of 95 % poly[3-(4-octylphenyl)thiophene] (POPT) with 5 % MEH-CN-PPV

³⁰ J. K. J. van Duren, X. Yang, J. Loos, C. W. T. Bulle-Lieuwma, A. B. Sieval, J. C. Hummelen, R. A. J. Janssen *Adv. Funct. Mater.* **2004**, *14*, 425-434.

³¹ H. Hoppe, N. S. Sariciftci *J. Mater. Chem.* **2006**, *16*, 45-61.

³² S. E. Shaheen, C. J. Brabec, N. S. Sariciftci, F. Padinger, T. Fromherz, J. C. Hummelen *Appl. Phys. Lett.* **2001**, *78*, 841-843.

³³ H. Hoppe, M. Niggemann, C. Winder, J. Kraut, R. Hiesgen, A. Hinsch, D. Meissner, N. S. Sariciftci *Adv. Funct. Mater.* **2004**, *14*, 1005-1011.

³⁴ G. Li, V. Shrotriya, J. Huang, Y. Yao, T. Moriarty, K. Emery, Y. Yang *Nature Materials* **2005**, *4*, 864-868.

³⁵ W. Ma, C. Yang, X. Gong, K. Lee, A. J. Heeger *Adv. Funct. Mater.* **2005**, *15*, 1617-1622.

³⁶ J. Huang, G. Li, Y. Yang *Appl. Phys. Lett.* **2005**, *87*, 112105.

³⁷ J. J. M. Halls, C. A. Walsh, N. C. Greenham, E. A. Marseglia, R. H. Friend, S. C. Moratti, A. B. Holmes *Nature* **1995**, *376*, 498-500.

³⁸ A. C. Arias, J. D. MacKenzie, R. Stevenson, J. J. Halls, M. Inbasekharan, E. P. Woo, D. Richards, R. H. Friend *Macromolecules* **2001**, *34*, 6005-6013.

³⁹ Y. Kim, S. Cook, S. A. Choulis, J. Nelson, J. R. Durrant, D. D. C. Bradley *Chem. Mater.* **2004**, *16*, 4812-4818.

⁴⁰ M. Granström, K. Petritsch, A. C. Arias, A. Lux, M. R. Andersson, R. H. Friend *Nature* **1998**, *395*, 257-260.

1. Introduction

and the second layer of 5 % POPT and 95% MEH-CN-PPV. The layers were deposited individually on top of different electrodes on two different substrates. The MEH-CN-PPV rich layer and the POPT rich layer were put on each other and were laminated under pressure with high temperature to get a compact cell. This lamination process resulted in a large p/n heterojunction interface which leads to efficiencies up to 1.9 %.

Recently, also efficient spin-coated polymer / polymer blend systems could be realized. They also used a PPV derivate as hole conductor and a cyano substituted PPV ether as electron transport material⁴¹. In that study a vertically composition graded structure that is built during the spin-coating process, was proposed. This would be in somewhat similar to the laminated system which would explain the good efficiency of 1.7 %.

There were also several attempts to control the mixing of n-type and p-type materials on a molecular scale. The so-called double-cable polymers⁴² consist of a polythiophene backbone with covalently grafted fullerenes. These materials are intrinsic bipolar which is interesting for the morphological and electronic properties. In contrast to the PPV / PCBM composites the interface between the p-type backbone and the fullerene moieties is controlled by the spacers. But no microphase separation could be observed and the efficiencies were low in these systems.

It was also tried to use rod-coil block copolymers consisting of a PPV backbone which was functionalized with an alkoxyamine end-group to get starting groups for the polymerization⁴³. The second block was a statistical block of styrene and 4-chloromethyl styrene which was introduced by controlled radical polymerization. Fullerenes were covalently attached by the reaction with the chloromethyl group. It could be shown that the fullerenes were incorporated into the polymer but no phase morphology in the nanometer range was observed. One of the problems may be that the ATRA (atom transfer radical addition) of the fullerenes to the polymer chain is a radical process. The radicals may favor side reactions like cross-linking. So the resulting polymers were not sufficiently soluble. The polymer analogous reaction was changed by first introducing an azide group with which also fullerenes can be attached⁴⁴, but with less side reactions. With this change the introduction of the fullerene could be improved, but still no microphase separation could be observed.

⁴¹ T. Kietzke, H.-H. Hörrhold, D. Neher *Chem. Mat.* **2005**, *17*, 6532-6537.

⁴² A. Cravino, N. S. Sariciftci *J. Mater. Chem.* **2002**, *12*, 1931-1943.

⁴³ U. Stalmach, B. de Boer, C. Videlot, P. F. van Hutten, G. Hadzioannou *J. Am. Chem. Soc.* **2000**, *122*, 5464-5472.

⁴⁴ M. H. van der Veen, B. de Boer, U. Stalmach, K. I. van de Wetering, G. Hadzioannou *Macromolecules* **2004**, *37*, 3673-3684.

1.3 Nitroxide Mediated Controlled Radical Polymerization

Radical polymerization is known to be a very well developed technology with millions of tons of polymer produced every year. The importance in industry and science is based on the ease in use as radical polymerization is possible with all kinds of monomers with different functional groups and is stable in protic media like water.

As this polymerization technique is already widely used in industry, it is interesting that radical polymerization is in the focus of academic research again. This is due to the development of controlled radical polymerization techniques. Living polymerization techniques are mainly known for anionic and cationic polymerization methods. Especially with anionic polymerizations the synthesis of very well-defined polymers with low polydispersities and defined starting- and end-groups is possible. But the reaction conditions have to be very stringent. Ultra pure solvents and monomers have to be used and oxygen and water have to be strictly excluded. Also certain monomers and functional groups are not possible to polymerize in a controlled fashion due to side reactions.

With the development of controlled radical polymerization the controlled nature of the polymerization could be coupled with the tolerance to functional groups. Different kinds of controlled radical polymerization techniques like ATRP (Atom Transfer Radical Polymerization)^{45,46}, RAFT (Reversible Addition - Fragmentation chain Transfer)⁴⁷, and NMRP (Nitroxide Mediated controlled Radical Polymerization) were developed.

In the following the nitroxide mediated controlled radical polymerization will be discussed in detail. The mechanism is based on the reversible termination of the propagating polymer chain which reduces the concentration of the active radical. The equilibrium between the so-called dormant species and the active one is on the side of the dormant species. As the radical concentration is extremely low the termination by disproportionation or combination is suppressed.

⁴⁵ K. Matyjaszewski, J. Xia *Chem. Rev.* **2001**, *101*, 2921-2990.

⁴⁶ M. Kamigaito, T. Ando, M. Sawamoto *Chem. Rev.* **2001**, *101*, 3689-3745.

⁴⁷ J. Chieffari, Y. K. Chong, F. Ercole, J. Krstina, J. Jeffery, T. P. T. Le, R. T. A. Mayadunne, G. F. Meijis, C. L. Moad, G. Moad, E. Rizzardo, S. H. Thang *Macromolecules* **1998**, *31*, 5559-5562.

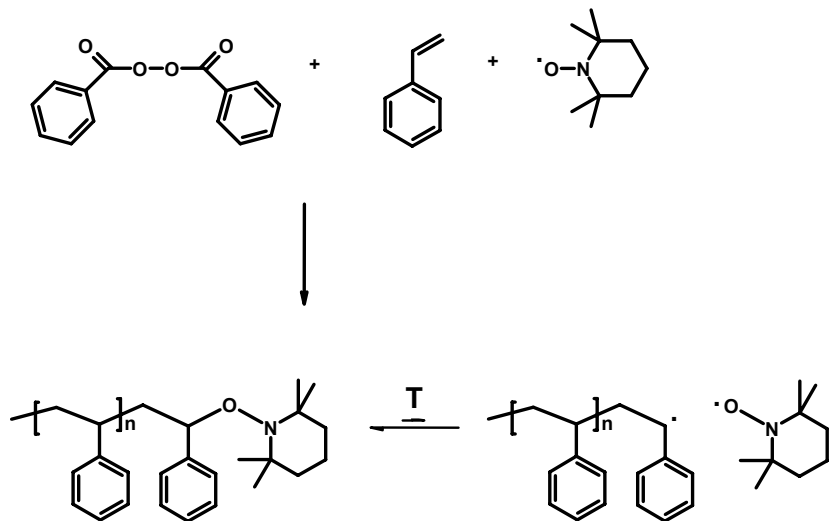


Figure 1-4: Reaction scheme of the controlled polymerization of styrene with TEMPO and BPO.

Originally TEMPO (2,2,6,6-tetramethylpiperidinyloxy) was used as termination fragment to shift the equilibrium towards the dormant species (figure 1-4). It was used together with styrene and benzoyl peroxide (BPO) as radical initiator at 130 °C to get well-defined polystyrene⁴⁸. At this temperature the C-O bond in the alkoxyamine can be reversibly opened by a homolytic cleavage. But this reaction was mainly limited to styrene. Other monomers like acrylates could not be polymerized in a controlled fashion. The next step was the use of unimolecular initiators. They consisted already of an alkoxyamine, so no radical initiator has to be added (figure 1-5).

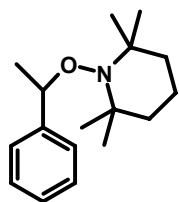


Figure 1-5: Chemical structure of unimolecular initiator for the nitroxide mediated radical polymerization.

A major improvement was the use of nitroxides which have a hydrogen atom at one of the α -carbons. Interestingly these compounds are normally considered as not very stable nitroxides. But this instability seems to be important for the polymerization. This concept was realized by

⁴⁸ M. K. Georges, R. P. N. Veregin, P. M. Kazmaier, G. K. Hamer *Macromolecules* **1993**, *26*, 2987-2988.

1. Introduction

using a benzylic hydrogen atom at the α -carbon⁴⁹ or by using a phosphonate substituted compound⁵⁰.



Figure 1-6: Chemical structures of nitroxides having hydrogen atoms at the α -carbon.

In contrast to the TEMPO mediated polymerization, it is possible with these new nitroxides (see figure 1-6) to polymerize a wide range of monomers in a controlled way. Acrylates, acrylamides, acrylonitriles and dienes can be used for the homo polymerization or for random and block copolymers⁵¹.

This versatility makes the nitroxide mediated controlled radical polymerization very interesting for the synthesis of block copolymers and other complex macromolecular architectures. Graft, dendritic, hyperbranched and star polymers^{52,53,54} were successfully prepared by the nitroxide mediated controlled radical polymerization technique. But also surface modifications using NMRP initiators are reported, resulting in polymer brushes⁵⁵. The stability of the alkoxyamine initiator and the controlled nature of the polymerization allow the preparation of different complex architectures in combination with different other polymerization techniques.

Especially for organic electronics another feature of NMRP is highly valuable. The synthesis is metal free. Metal ions have a very strong impact on the electronic properties as they are free charge carriers. The monomers can be purified by column chromatography and as the polymerization is metal free, the polymers can be simply purified by precipitation.

⁴⁹ D. Benoit, V. Chaplinski, R. Braslau, C. J. Hawker *J. Am. Chem. Soc.* **1999**, *121*, 3904-3920.

⁵⁰ D. Benoit, S. Grimaldi, S. Robin, J. P. Finet, P. Tordo, Y. Gnanou *J. Am. Chem. Soc.* **2000**, *122*, 5929-5939.

⁵¹ C. J. Hawker, A. W. Bosman, E. Harth *Chem. Rev.* **2001**, *101*, 3661-3688.

⁵² R. B. Grubbs, C. J. Hawker, J. Dao, J. M. J. Fréchet *Angew. Chem. Int. Ed.* **1997**, *36*, 270-272.

⁵³ A. W. Bosman, A. Heumann, G. Klaerner, D. Benoit, J. M. J. Fréchet, C. J. Hawker *J. Am. Chem. Soc.* **2001**, *123*, 6461-6462.

⁵⁴ A. W. Bosman, R. Vestberg, A. Heumann, J. M. J. Fréchet, C. J. Hawker *J. Am. Chem. Soc.* **2003**, *125*, 715-728.

⁵⁵ M. Huseman, E. E. Malmström, M. McNamara, M. Mate, D. Mecerreyes, D. G. Benoit, J. L. Hedrick, P. Mansky, E. Huang, T. P. Russell, C. J. Hawker *Macromolecules* **1999**, *32*, 1424-1431.

2. Overview of Thesis

The results of my thesis are summarized in this chapter. The detailed studies are listed in the appendix (chapter 5).

The fluorescent acceptor labeled polymers carrying hole transport pendant groups are presented in detail in appendix A1.

The perylene bisimide – fullerene dyads, which are strongly absorbing electron transport materials are specified in appendix A2.

The publication in appendix A3 describes mainly the synthesis, the thermal and optical properties as well as the microphase separation of block copolymers consisting of n-type and p-type organic semiconductors.

The manuscript in appendix A4 gives a detailed study of the optical and electrochemical properties, the π - π stacking of the perylene bisimide units as well as the synthesis and morphology of the block copolymers.

In appendix A5 the use of block copolymers for charge separation at self-assembled nanostructured interfaces in solar cells and the morphology in thin films are described.

2.1 Motivation and Aim

In organic solar cells realized with a donor / acceptor heterojunction, the morphology in the nanometer range is the key parameter for obtaining efficient devices. There are two well established concepts that combine the domain size in the nanometer range along with a sufficient thick layer for absorption. These are at the first glance contradictory requirements. They are needed as the exciton (bound electron–hole pair) diffusion length is in the order of some nanometer and within this range an interface between the organic hole and electron transport material is needed for the dissociation of the exciton into an electron and a hole. But on the other hand the photovoltaic devices have to be thick (100 nm – 500 nm) to absorb enough light.

This could be realized by using dye sensitized nanocrystalline TiO₂ solar cells and by blending polymers with low molecular weight organic materials.

My approach was to use block copolymers for obtaining microphase separation. Block copolymers exhibit domain sizes on a nanometer scale by the interplay between immiscibility and molecular connectivity of the two blocks. The microphase separation in bulk and in thin

films was shown by several studies^{56,57}. As the microdomains can be aligned for example by electrical fields⁵⁸ they exhibit a great potential for nanotechnology^{59,60} as well.

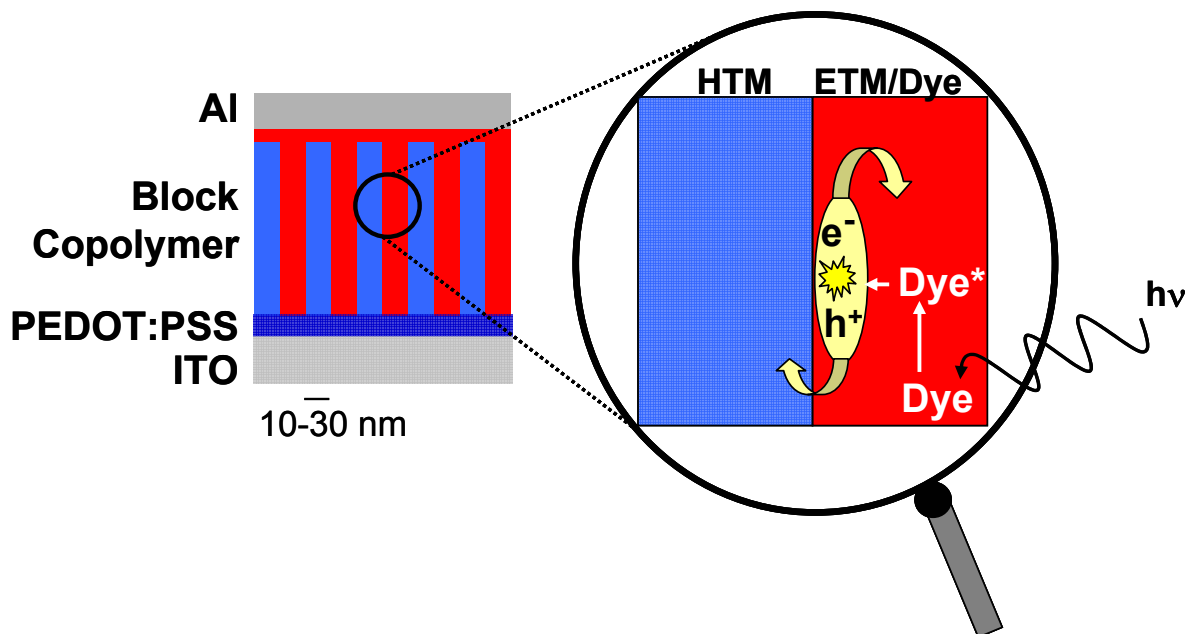


Figure 2-1: Schematic representation of the device structure of an aligned block copolymer solar cell and the physical processes in an organic solar cell.

In figure 2-1 an idealized block copolymer solar cell is shown. The dye is excited by a photon and the resulting exciton has to diffuse to the donor / acceptor interface. As the block copolymer is nanostructured, the interface is within the exciton diffusion length of several nanometers. There the exciton is dissociated into an electron and a hole. The charge carriers are transported through the corresponding organic semiconductors (n-type or p-type) to the different electrodes. As the morphology of the block copolymer is aligned, the domains act as percolation paths for electrons and holes. Therefore the use of block copolymers allows the creation of large interfaces with domain sizes on a nanometer scale and since the phase separation occurs throughout the bulk, thick layers can be utilized for device preparation.

With this approach the enormous potentials for organic electronics and nanotechnology can be combined. For the application in organic solar cells all the electronic requirements of an organic solar cell have to be fulfilled in the block copolymer using appropriate chemical

⁵⁶ A.-V.Ruzette, L. Leibler *Nature Materials* **2005**, 4, 19-31.

⁵⁷ M. J. Fasolka, A. M. Mayes *Ann. Rev. Mat. Res.* **2001**, 31, 323-355.

⁵⁸ T. Xu, A. V. Zvelindovsky, G. J. A. Sevink, K. S. Lyakhova, H. Jinnai, T. P. Russell *Macromolecules* **2005**, 38, 10788-10798.

⁵⁹ C. Park, J. Yoon, E.L. Thomas *Polymer* **2003**, 44, 6725–6760.

⁶⁰ I. W. Hamley *Angew. Chem. Int. Ed.* **2003**, 42, 1692-1712.

moieties. The block copolymer has to consist of a dye to absorb the light and of electron transport (acceptor) and hole transport (donor) moieties for the exciton dissociation and the charge carrier transport to the electrodes. The first task is to design a synthetic strategy for the sequential polymerization of functionalized monomers carrying electronic moieties. Perylene bisimide can be used as dye and electron transport moiety. They are known for their high chemical and photochemical stability and they have a high electron mobility^{61,62,63}. As they readily crystallize via π - π stacking they are also very interesting for supramolecular assemblies⁶⁴. Here the challenge is to functionalize the perylene bisimide unsymmetrically and obtain a suitable monomer with sufficient solubility. The other block has to consist of a hole transport material, for example a triphenylamine. Nitroxide mediated controlled radical polymerization can be used for the synthesis of the block copolymer as a wide range of monomers can be polymerized and the synthesis is metal free. The morphology and the charge separation of such block copolymers which exhibit a phase morphology on a nanometer scale will be investigated.

Besides the block copolymers for the nanostructured interfaces, also model compounds for electron and energy transfer processes have to be synthesized. An alkoxyamine which is covalently attached to a perylene bisimide unit can be used as initiator for the nitroxide mediated controlled radical polymerization. Using this initiator, different monomers with or without electron donors, will be polymerized. The photophysical properties of the resulting polymers, carrying a single electron acceptor in the polymer chain, should be studied. Depending on the pendant groups in the polymer chain, the thermal and optical properties can be varied.

Dyads consisting of fullerene and perylene bisimide are low molecular weight model compounds. The combination of two electron acceptors, which have similar LUMO values, are capable for studying energy and electron transfer processes in solution. In contrast to PCBM, these dyads are strongly absorbing light and are therefore interesting as electron acceptors in organic solar cells.

Finally optical, electrochemical and thermal properties of all these compounds should be studied in detail.

⁶¹ P. Ranke, I. Bleyl, J. Simmerer, D. Haarer, A. Bacher, H.-W. Schmidt *Appl. Phys. Lett.* **1997**, *71*, 1332-1334.

⁶² E. H. Magin, P.M. Borsenberger *J. Appl. Phys.* **1993**, *73*, 787-791.

⁶³ P. Malenfant, C. D. Dimitrakopoulos, J. D. Gelorme, L. L. Kosbar, T. O. Graham, A. Curioni, W. Anreoni *Appl. Phys. Lett.* **2002**, *80*, 2517-2519.

⁶⁴ F. Würthner *Chem Commun.* **2004**, *14*, 1564-1579.

2.2 Fluorescent Acceptor Dye Labeled Polymers carrying Hole Transport Pendant Groups

2.2.1 Synthesis

In this chapter a summary of the prepared model systems for electron transfer is given. The model systems are polymers with one perylene bisimide moiety as fluorescent electron acceptor in each polymer chain. The polymer chain can carry electron donors like triphenylamines or non-active groups as pendant groups. This assembly is possible by the use of a perylene bisimide initiator. In order to get well-defined polymers, an alkoxyamine was used as initiator for the nitroxide mediated controlled radical polymerization.

Perylene bisimides are known for their thermal, chemical and photochemical stability. They have a very strong fluorescence and a characteristic absorption spectra depending on their aggregation. The main problem of perylene bisimides is the low solubility in organic solvents. Most of the perylene bisimides used for organic electronics are not soluble at all in organic solvents and have to be evaporated by vacuum deposition. Another problem is that starting with 3,4:9,10-tetracarboxylic bisanhydride **1**, a pigment used for car paints, the products are normally twice substituted. Therefore an unsymmetrical synthesis has to be applied (see figure 2-2). But by the use of KOH the tetra potassium salt is formed which can be selectively transformed to the mono potassium salt **2**^{65,66}. With ammonia an unsymmetrical perylene monoanhydride monoimide **3** is formed. A so-called swallow-tail substituent is built by the reaction with 8-aminopentadecane. Swallow-tail substituted perylene bisimides⁶⁷ are in contrast to most other perylene bisimides highly soluble in organic solvents, even in poor solvents such as hexane. The other imide group was then reacted with a chloromethyl functionalized initiator **5** which was first reported by Hawker⁴⁹.

⁶⁵ H. Tröster *Dyes Pigm.* **1983**, *4*, 171-177.

⁶⁶ H. Kaiser, J. Lindner, H. Langhals *Chem. Ber.* **1991**, *124*, 529-535.

⁶⁷ H. Langhals, S. Demmig, T. Potrawa *Journal f. prakt. Chemie* **1991**, *333*, 733-748.

2. Overview of Thesis

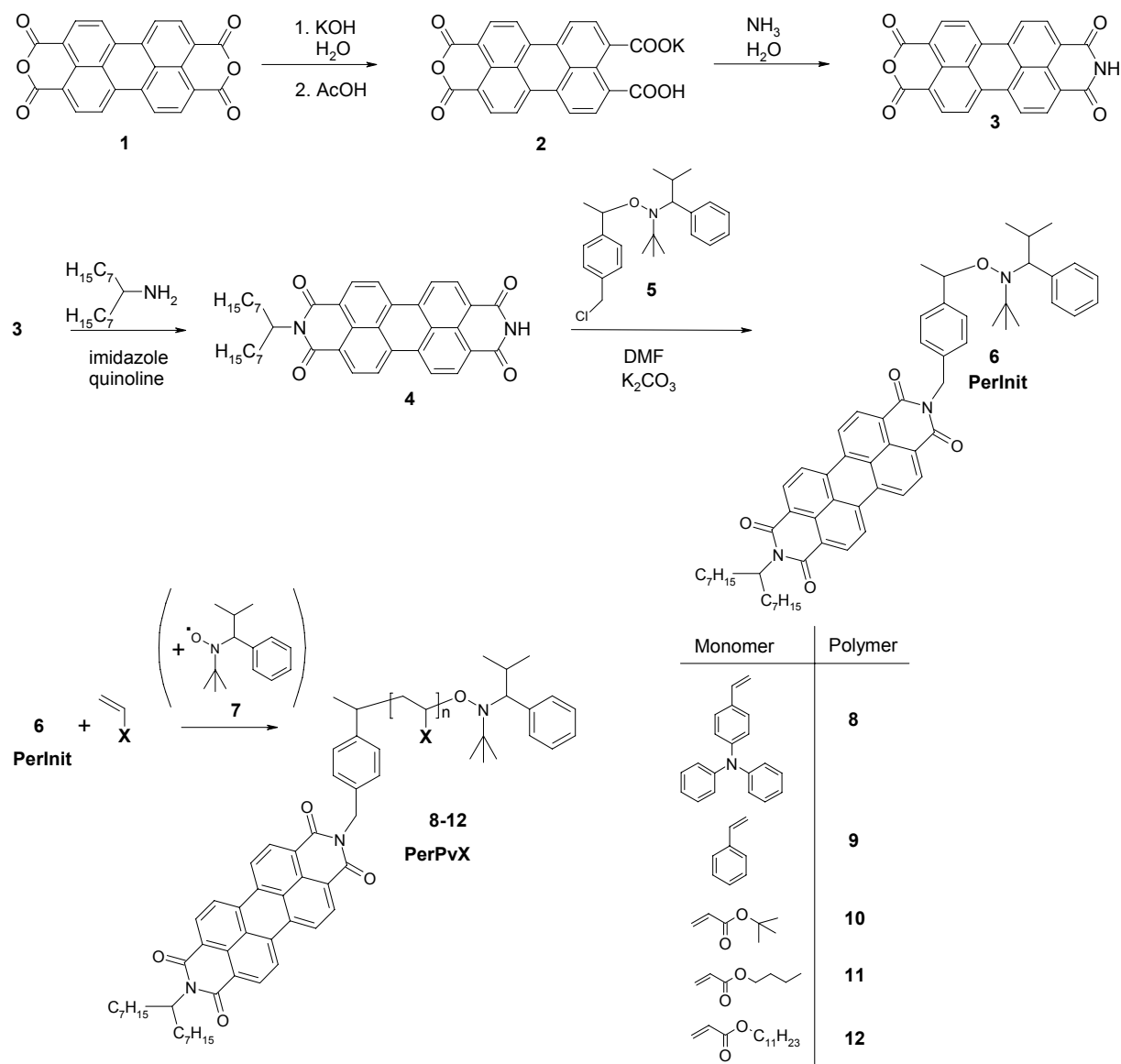


Figure 2-2: Synthesis of the perylene bisimide labeled initiator **PerInit 6** and the corresponding polymers **8-12**.

With the perylene bisimide labeled initiator **PerInit 6** different polymers could be synthesized by nitroxide mediated controlled polymerization. Depending on the monomers used, bifunctional polymers carrying electron donating moieties and a single electron acceptor unit (**8**) or polymers labeled with a single electron acceptor (**9-12**) can be prepared.

2.2.2 Results and Discussion

In order to examine the controlled nature of the polymerization time dependent GPC measurements were performed (figure 2-3). The PerInit **6** with 250 equivalents of styrene was heated at 125 °C.

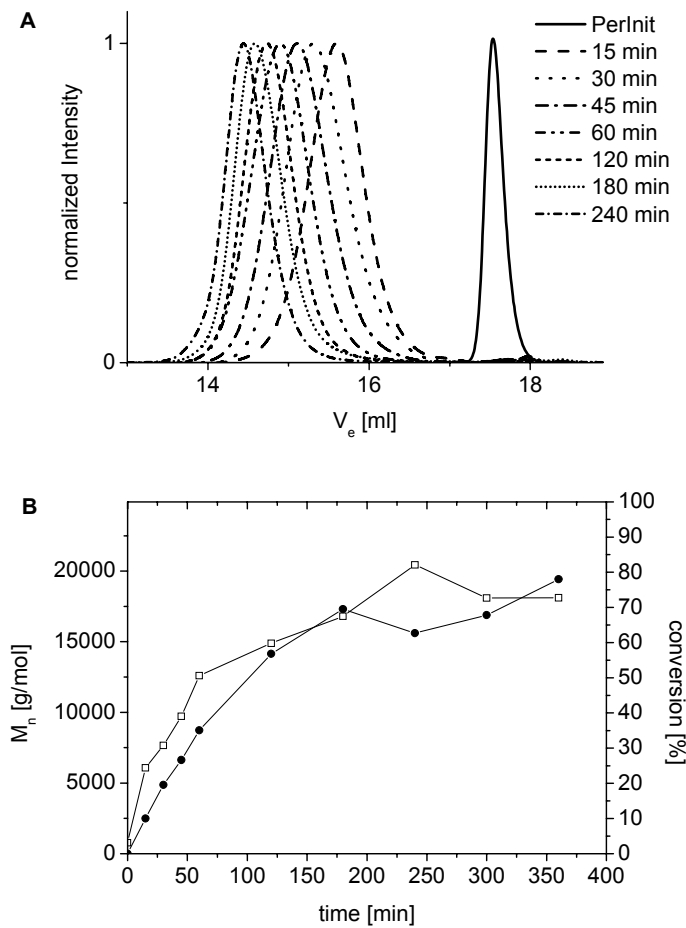


Figure 2-3: A) Evolution of GPC elution curves for the polymerization of styrene (250 equiv) with **6** at 125 °C. B) Evolution of M_n (□) and conversion (●) for the same reaction. M_n was determined with GPC and the conversion with 1H NMR.

In the beginning the conversion and M_n increased linear with time, but after one hour the increase became significantly lower. This behavior is due to the lower concentration of the monomer, but mainly due to the increase in viscosity. A series of different styrene or acrylate monomers were polymerized (table 2-1). Thus the properties of the resulting polymers could be tuned. For example, the glass transition temperature changes from -48°C for poly(*n*-butyl acrylate) to 133°C for poly(4-vinyltriphenylamine). As the polydispersities of the samples are

between 1.1 and 1.2, except for the polymerization of *tert*-butyl acrylate with a polydispersity of 1.3, the controlled nature of the polymerization is obvious.

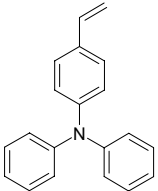
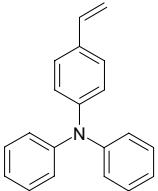
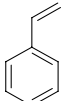
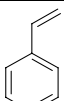
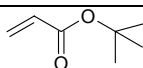
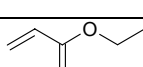
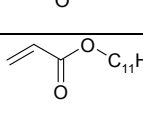
Polymer	monomer	mol% 7	reaction time	M _n [g/mol]	PDI	T _g [°C]	TGA-5% [°C]
8A		0.05	30 min	3050	1.10	114	331
8B		0.05	60 min	7510	1.23	133	355
9A		---	1 h	9560	1.15	97	344
9B		---	4 h	17950	1.10	99	352
10		0.05	18 h	25740	1.30	46	241
11		0.05	18 h	21950	1.19	-48	309
12		0.05	18 h	8300	1.19	-*	336

Table 2-1: Polymerization conditions of different monomers, polymer data and thermal properties (from DSC and TGA) of the dye labeled polymers; polydispersity and M_n were determined by GPC with polystyrene standards using THF as solvent.*only the melting point at -17 °C could be detected.

The incorporation of initiators into a polymer can be investigated by UV/vis spectroscopy for dyes⁶⁸ or by potentiometric titration for amino terminated polymers⁶⁹. We used MALDI-TOF mass spectrometry as it is a very straightforward method and shows the complete composition

⁶⁸ M. Rodlert, E. Harth, I. Rees, C. J. Hawker *J. Polym. Sci. Part A: Polym. Chem.* **2000**, *38*, 4749-4763.

⁶⁹ C. J. Hawker, J. L. Hedrick *Macromolecules* **1995**, *28*, 2993-2995.

of the polymer. The spectra were measured in the reflectron mode giving the isotopic resolution of the polymer molecule (figure 2-4).

The MALDI-TOF mass spectra consist only of discrete peaks which have the distance of one repeating unit (here: styrene). A silver and a hydrogen atom is added from the matrix. The calculated spectrum matches with the measured spectrum of the 25mer and 26mer (figure 2-4B) with every polymer chain having one perylene bisimide acceptor and one alkoxyamine group. This is not only the proof for one perylene bisimide unit in each chain, but also for the controlled polymerization and the stability of the alkoxyamine initiator. The polymer is not fragmented at all in the workup or the ionization process.

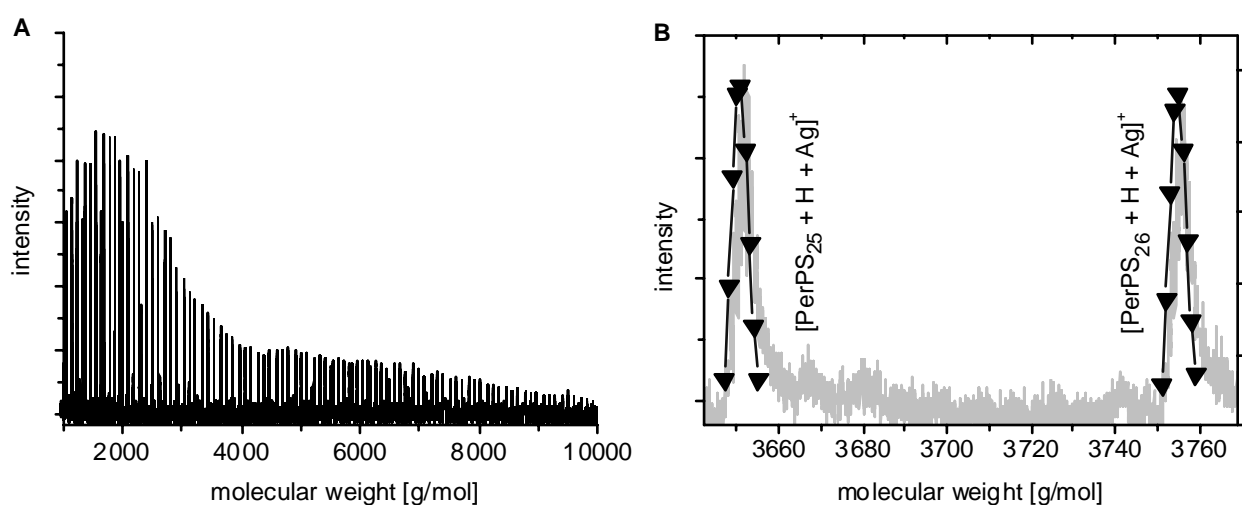


Figure 2-4: A) MALDI-TOF-mass spectra of a low molecular perylene bisimide labeled polystyrene sample measured in reflectron mode. B) Magnification of two measured peaks of the 25mer and the 26mer and the corresponding simulated spectra (\blacktriangledown) of PerPS_{25} and PerPS_{26} . Recorded with DTCB as matrix and silver triflate.

Cyclic voltammetry was used for the determination of the HOMO (Highest Occupied Molecular Orbital) and LUMO (Lowest Unoccupied Molecular Orbital) level. A three-electrode assembly with a Ag/AgNO_3 electrode and CH_2Cl_2 containing 0.1 M tetrabutylammonium hexafluorophosphate as solvent was used. The perylene bisimide initiator PerInit **6** has two reversible reduction peaks and one oxidation peak. From these, the HOMO and LUMO can be calculated using ferrocene (HOMO = -4.80 eV) as internal standard. The LUMO is -3.74 eV and the HOMO is -6.01 eV with respect to zero energy level. The electronic gap is 2.27 eV.

The optical and electro-optical properties were determined by UV/vis and fluorescence spectroscopy. In figure 2-5A the UV/vis absorption spectra of PerInit **6** and two triphenylamine substituted polymers **8A** ($M_n = 3050$ g/mol) and **8B** ($M_n = 7510$ g/mol) with different molecular weights are shown. The first vibronic transition of the electronic S_0 - S_1 transition is shifted from 544 nm in **6** to 530 nm in **8A** and 529 nm in **8B**. The change in UV/vis spectra is caused by the π - π stacking of the perylene bisimide.

The aggregation of perylene bisimide dyes also change the intensity of the transitions⁷⁰. The quotient of the second and the first vibronic transitions is introduced as a parameter for the degree of order between the perylene bisimide moieties. This quotient changes from 1.68 for the PerInit **6** to 1.11 for **8A** and 0.97 for **8B**, thus indicating that the aggregation decreases from **6** to **8A** and **8B**.

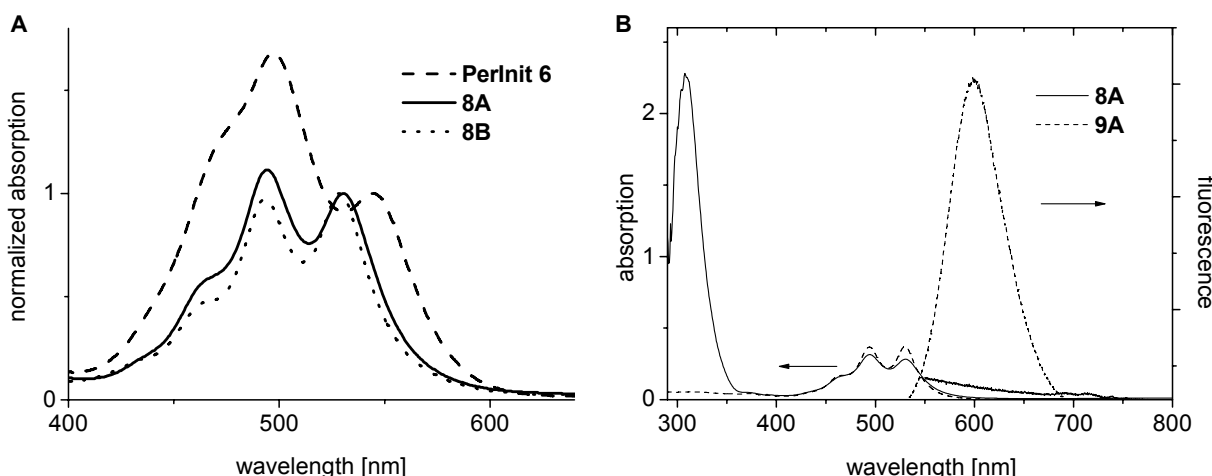


Figure 2-5: A) UV/vis spectra of PerInit **6** and the polymers **8A** and **8B** in film. The UV/vis spectra are normalized. B) UV/vis and fluorescence spectra of the **8A** and **9A** in film.

The opto-electronic properties can also be tailored by using different monomers. In figure 2-5B the UV/vis and fluorescence spectra of a perylene bisimide labeled polystyrene **9** and a poly(4-vinyltriphenylamine) **8A** are compared. PerPS **9A** shows a strong red fluorescence in contrast to PerPvTPA **8A** where the fluorescence is quenched completely. The triphenylamine quenches the fluorescence, most probably by an electron transfer. This is the same process as in block copolymer solar cells which will be discussed in the next chapters. By using polymers with a sufficient high molecular weight the stacking of the single perylene bisimide

⁷⁰ B. A. Gregg *J. Phys. Chem.* **1996**, *100*, 852-859.

2. Overview of Thesis

units can be avoided. The electron acceptor is then surrounded by electron donors which leads to a very fast fluorescence quenching.

Thus, perylene bisimide labeled initiators are suitable for the preparation of various dye labeled polymers. The polymerization has a controlled nature with low polydispersities and a complete incorporation of the perylene bisimide dye into the polymer chain is guaranteed. The polymers can be viscous or semi-crystalline depending on the monomers used. As perylene bisimides are very strong fluorescent dyes the polymers can be used for single-molecule imaging⁷¹. If electron donors like triphenylamines are used, the fluorescence is quenched, therefore the polymers can be used as model systems for energy and electron transfer studies.

⁷¹ N. B. Bowden, K. A. Willets, W. E. Moerner, R. M. Waymouth *Macromolecules* **2002**, *35*, 8122-8125.

2.3 Novel Soluble Perylene Bisimide - Fullerene Dyads

2.3.1 Synthesis

Two different dyads, $\text{Per}_1\text{C}_{60}$ (**15**) and $\text{Per}_2\text{C}_{60}$ (**17**) containing one or two perylene bisimide moieties were prepared. The synthetic route for the preparation of perylene bisimide – fullerene dyads is shown in figure 2-6. The reaction steps VI-VIII were carried out in the group of Prof. Dr. A. Hirsch, University of Erlangen-Nürnberg.

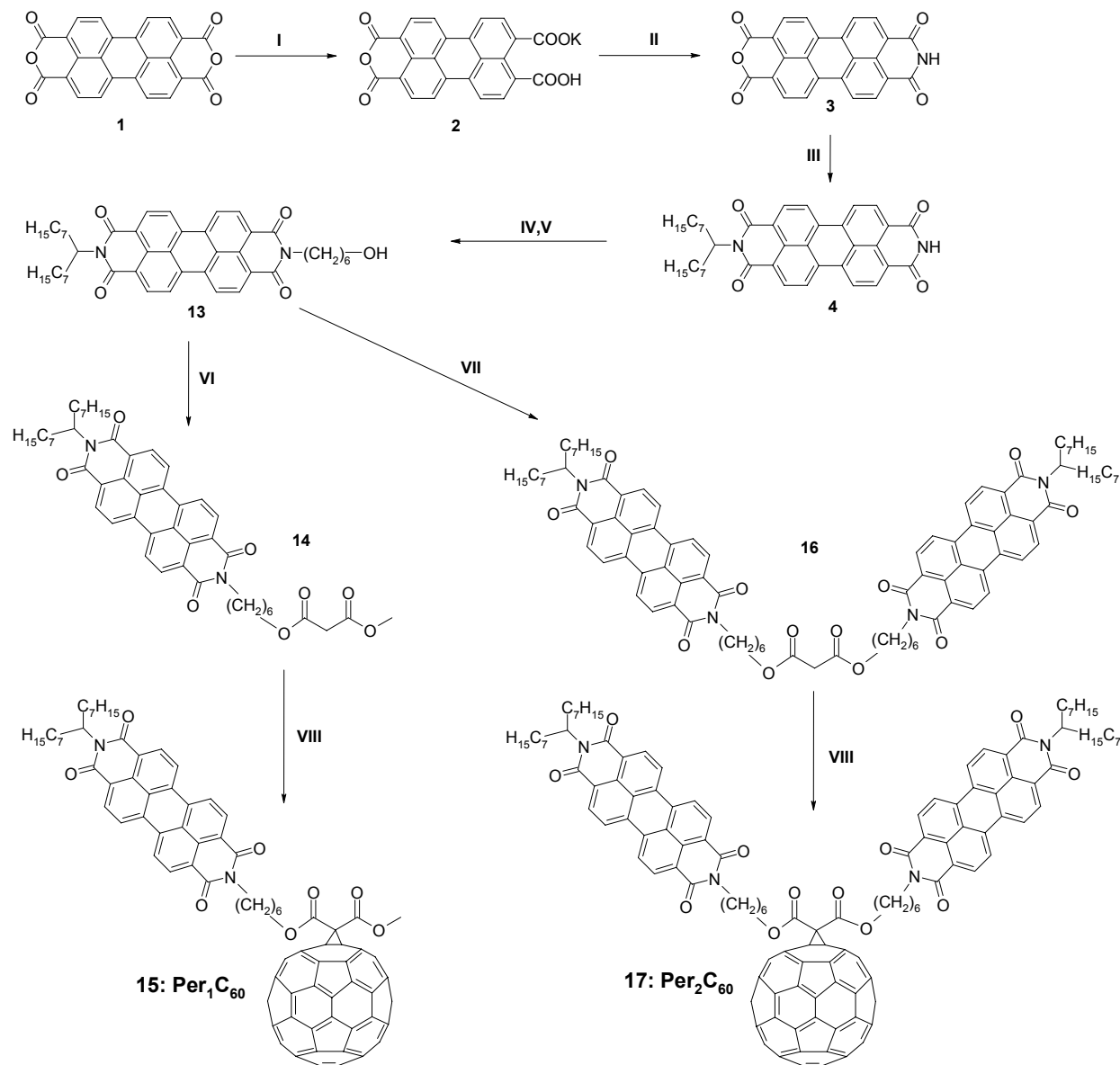


Figure 2-6: Scheme of synthesis of the perylene bisimide – fullerene dyad **15** and **17**. Reagents and conditions: (I) $\text{KOH}, \text{H}_2\text{O}; \text{AcOH}$; (II) $\text{NH}_3, \text{H}_2\text{O}$; (III) 8-aminodecane, imidazole, quinoline, 160°C ; (IV) $\text{Br}-(\text{CH}_2)_6-\text{OTHP}, \text{K}_2\text{CO}_3, \text{DMF}, \text{THF}, 60^\circ\text{C}$; (V) $\text{PPTS}, \text{HCl}, \text{THF}, \text{ethanol}, 55^\circ\text{C}$; (VI) methyl malonyl chloride, pyridine, CH_2Cl_2 ; (VII) malonyl dichloride, pyridine, CH_2Cl_2 ; (VIII) $\text{C}_{60}, \text{I}_2, \text{DBU}, \text{toluene}$.

The hydroxyl functionalized perylene bisimide **13** was prepared by coupling the unsymmetrical perylene bisimide **4** with 1-bromo-6-tetrahydropyranloxyhexane ($\text{Br}-(\text{CH}_2)_6-\text{OTHP}$). The free hydroxyl group was prepared by opening the THP protecting group under acidic conditions. The hydroxyl functionalized perylene bisimide **13** was reacted with methyl malonyl chloride or malonyl dichloride to get the mono (**14**) or disubstituted (**16**) malonates. The dyads **15** and **17** were synthesized by a cyclopropanation of C_{60} in a modified Bingel reaction⁷² with the malonate **14** or **16**, iodine and 1,8-diazabicyclo[5.4.0]undec-7-ene (DBU) in toluene⁷³. The resulting perylene bisimide – fullerenes dyads $\text{Per}_1\text{C}_{60}$ (**15**) and $\text{Per}_2\text{C}_{60}$ (**17**) have one and two covalently linked perylene bisimide units.

2.3.2 Results and Discussion

The optical and electrochemical properties of the synthesized molecules were studied and compared with the model compounds [6,6]phenyl-C₆₁-butyric acid methyl ester (PCBM) and N,N'-di(1-heptyloctyl)perylene-3,4:9,10-tetracarboxylic bisimide **18**.

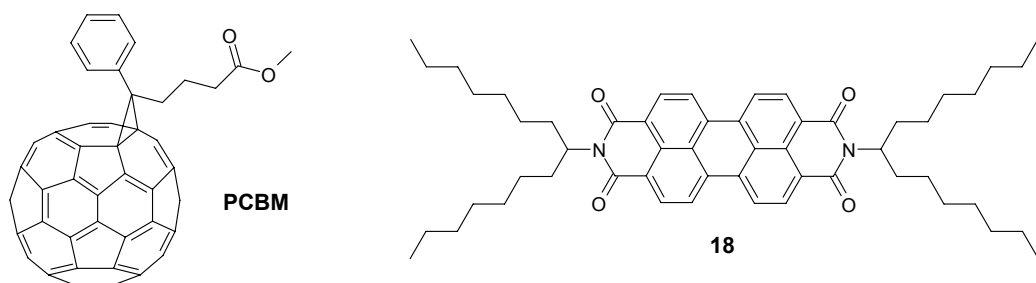


Figure 2-7: Chemical structures of the model compounds PCBM and the perylene bisimide **18**.

The perylene bisimide **18** has two reversible reduction peaks and one oxidation peak. The LUMO value could be calculated from the first reduction $E_{\text{red}1}$ as -3.71 eV and the HOMO from the first oxidation peak $E_{\text{ox}1}$ as -6.03 eV with respect to the zero energy level. The LUMO of PCBM is with -3.69 eV comparable to the value of the perylene bisimide **18** (figure 2-8A).

⁷² C. Bingel *Chem. Ber.* **1993**, *126*, 1957-1959.

⁷³ J.-F. Nierengarten, V. Gramlich, F. Cardullo, F. Diederich *Angew. Chem. Int. Ed.* **1996**, *35*, 2101-2103.

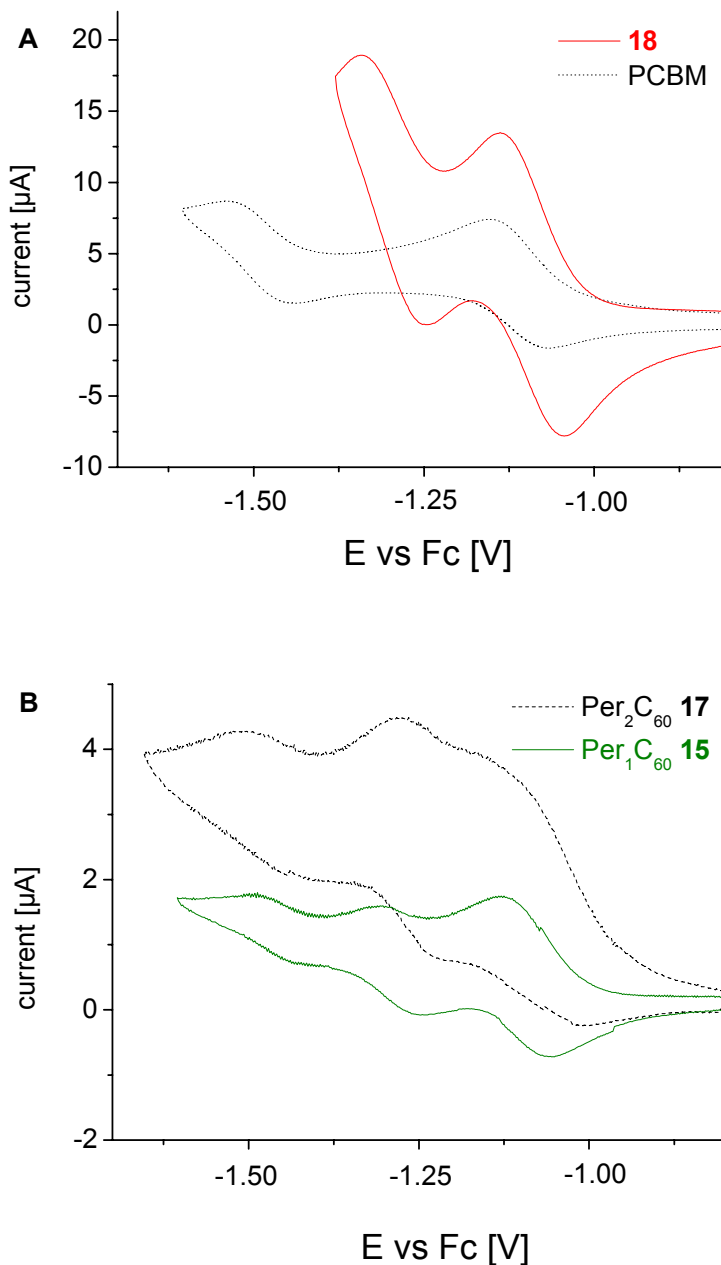


Figure 2-8: A) Cyclic voltammogramm of the perylene bisimide **18** and PCBM. B) Cyclic voltammogramm of $\text{Per}_1\text{C}_{60}$ (**15**) and $\text{Per}_2\text{C}_{60}$ (**17**). The measurements were conducted in CH_2Cl_2 containing 0.1 M tetrabutylammonium hexafluorophosphate with respect to ferrocene (Fc) at a scan rate of 50 mV s^{-1} .

Therefore the LUMOs of the dyads are also similar with -3.71 eV for $\text{Per}_1\text{C}_{60}$ (**15**) and -3.72 eV for $\text{Per}_2\text{C}_{60}$ (**17**). As the second reduction peaks of the fullerene derivative PCBM ($E_{\text{red}2}$ vs Fc = -1.49 V) and the perylene bisimide **18** ($E_{\text{red}2}$ vs Fc = -1.29 V) are different, three reduction peaks appear for the dyads $\text{Per}_1\text{C}_{60}$ (**15**) and $\text{Per}_2\text{C}_{60}$ (**17**) (figure 2-8B) corresponding to both the moieties. The values of the dyads and the model compounds are

similar (table 2-2) suggesting that no strong interaction within the dyads occur in the ground state.

	E _{red1} vs Fc [V]	E _{red2} vs Fc [V]	E _{red3} vs Fc [V]	LUMO [eV]
18	-1.09	-1.29	-	-3.71
PCBM	-1.11	-1.49	-	-3.69
Per ₁ C ₆₀ 15	-1.09	-1.28	-1.45	-3.71
Per ₂ C ₆₀ 17	-1.08	-1.25	-1.46	-3.72

Table 2-2: CV data for the model compounds **18** and PCBM and the dyads **15** and **17**. The measurement was conducted in CH₂Cl₂ containing 0.1 M tetrabutylammonium hexafluorophosphate in a three electrode assembly using Ag/AgNO₃ as a reference electrode. The values are given with respect to ferrocene (Fc).

The absorption spectra of the dyads **15** and **17** and the model systems **18** and PCBM are shown in figure 2-9. The main absorption of the fullerene derivative PCBM is in the ultraviolet part of the spectra with a characteristic peak at 327 nm, but it is barely absorbing light in the range between 400 and 600 nm. Both the dyads **15** and **17** show characteristic absorption of perylene bisimide and fullerene as if added together.

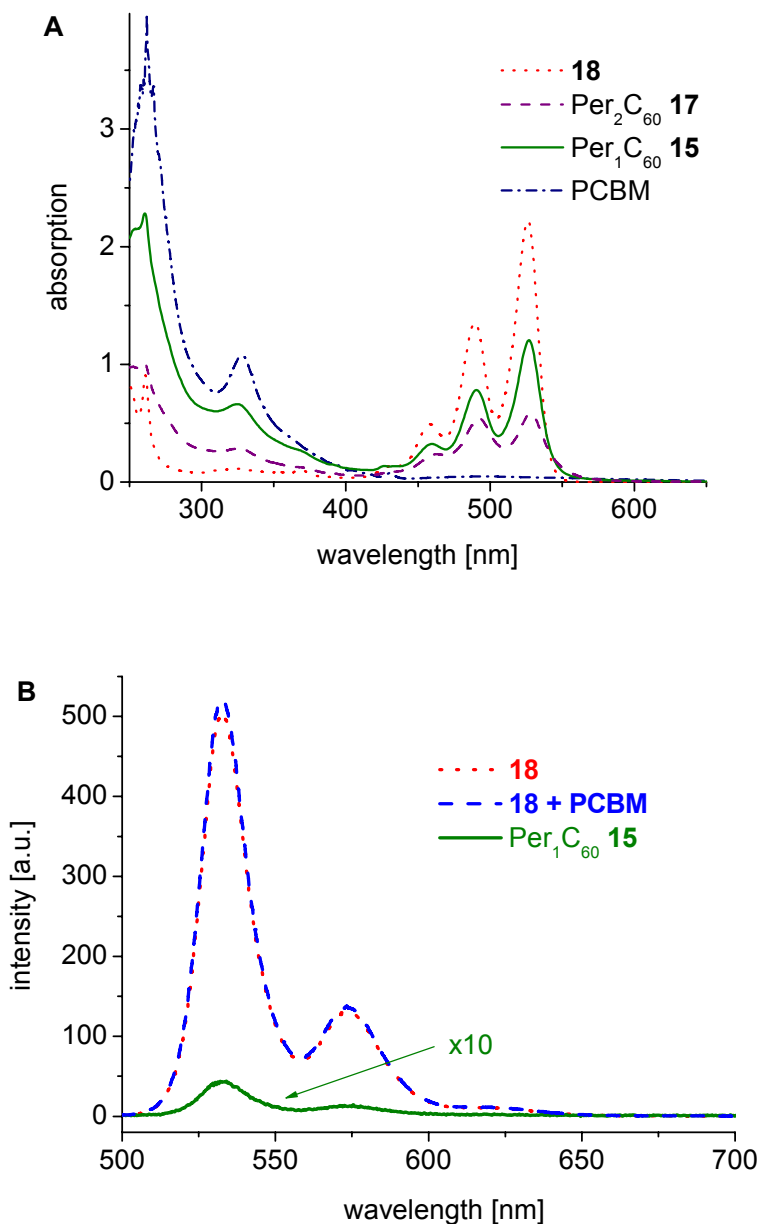


Figure 2-9: A) UV/vis spectra of the perylene bisimide **18**, PCBM, $\text{Per}_1\text{C}_{60}$ (**15**) and $\text{Per}_2\text{C}_{60}$ (**17**) measured in CHCl_3 (0.02 mg/ml). B) Fluorescence spectra of **18**, the dyad **15** (magnification: 10x) and a mixture of **18** and PCBM in CHCl_3 .

The dyads exhibit three characteristic peaks for the vibronic transition (527 nm, 491 nm, 459 nm) of the electronic S_0 - S_1 transition in the perylene bisimide moiety. The dyads **15** and **17** have high extinction coefficients, 91600 and 63900 $1 \text{ mol}^{-1} \text{ cm}^{-1}$ respectively at 527 nm. The molar extinction coefficient for $\text{Per}_1\text{C}_{60}$ (**15**) is remarkably higher than that for $\text{Per}_2\text{C}_{60}$ (**17**). This behavior can be attributed to stronger π - π stacking which is similar for polymers (see

chapter 2.4.2) or for cyclophanes⁷⁴ in solution. This effect is not observed for rigid bound perylene bisimides on a fullerene core⁷⁵. But with the flexible hexyl-bridge the perylene bisimide units interact strongly in solution which is also expressed by the quotient of the absorptions at the vibronic transitions. This optical parameter is a sign for the aggregation⁷⁰. The quotient of the absorption at the second and first vibronic transition changes from 0.65 for Per₁C₆₀ (**15**) to 0.93 for Per₂C₆₀ (**17**) which indicates a stronger aggregation in **17**. For **18** the quotient is with 0.61 similar to **15**, indicating that in **15** no strong interactions occur. The quotient is virtually independent of the concentration of dilute solution, exhibiting that it is an intramolecular effect in **17**.

Therefore the Per₁C₆₀ dyad **15** was used for the fluorescence studies as here only the interaction between the fullerene and the perylene bisimide moiety is pronounced in comparison to perylene bisimide – perylene bisimide interactions in **17**. The UV/vis and fluorescence spectra of the perylene bisimide **18**, the dyad **15** and 1:1 molar mixture of **18** and PCBM with the same molar concentrations in solution are compared in figure 2-9B. The pure perylene bisimide **18** solution shows a very strong fluorescence with three distinct transitions. The dyad **15** exhibits the same three transitions, but the fluorescence is quenched by 99% due to electron and energy transfer⁷⁶. As this transfer is strongly influenced by the distance of the donor and acceptor, the fluorescence of the mixture of **18** and PCBM, which has the same molar concentration as **15**, is not notably quenched.

The perylene bisimide labeled fullerenes are suitable for fundamental studies on energy and electron transfer processes in solution, but they are also interesting as electron transport materials. These dyads consisting of two electron acceptors are capable for the use in organic solar cells as these are dyes with a high extinction coefficient in contrast to PCBM, which is barely absorbing light in the visible spectrum.

⁷⁴ H. Langhals, R. Ismael *Eur. J. Chem.* **1998**, 1915-1917.

⁷⁵ R. Gomez, J. Segura, N. Martin, *Org. Lett.* **2005**, 7, 717-720.

⁷⁶ I. B. Martini, B. Ma, T. Da Ros, R. Helgeson, F. Wudl, B. J. Schwartz, *Chem. Phys. Lett.* **2000**, 327, 253-262.

2.4 Block Copolymers for Nanostructured Organic Electronics

2.4.1 Synthesis

The block copolymers were prepared by nitroxide mediated controlled radical polymerization of functional monomers. Another possibility to get functional polymers would be a polymer analogues reaction of reactive repeating units. But in the latter case side reactions can occur which lead for example to cross-linking or the conversion may not be complete. Also often metal salts are needed as catalysts for the reaction which have to be removed completely. Otherwise they would influence the properties of organic electronic devices. This is also the reason for the use of nitroxide mediated controlled radical polymerization. This technique not only offers the possibility of preparing block copolymers with a wide range of different functional groups, it is also metal free. As the monomers were purified by column chromatography the resulting polymers only have to be separated from the non converted monomer, which is possible by repeated precipitation or soxhlet extraction.

As hole transport material a vinyl substituted triphenylamine is used. Triphenylamines are common hole conductors as they are relatively stable with good mobilities and good film forming properties. 4-Vinyltriphenylamine **22** was synthesized by a Hartwig/Buchwald^{77,78} amination of 4-bromostyrene with diphenylamine. A catalytic system of Pd(OAc)₂ and P(*tert*-Bu)₃ provided high yields even for large amounts of more than 10 g.

Perylene bisimide was chosen as dye and electron transport material. Perylene bisimides and perylene bisanhydride are widely used dyes/pigments in industrial application like car paints. They are cheap, produced in large quantities and they are thermally, chemically and photochemically stable. For the use in organic electronics also other factors are important. They are electron transport materials with high electron mobility^{61,62,63} and they crystallize via π - π stacking. Such stacking of molecules is correlated with a good mobility and it leads to the formation of supramolecular assemblies⁶⁴.

But perylene derivates have also some distinct drawbacks. The main problem is the low solubility. Most of the perylene bisimides or perylene bisanhydride which are used for organic electronics are not soluble in organic solvents. They are evaporated by vacuum deposition. Another disadvantage is that, starting from perylene bisanhydride normally symmetrical substituted products evolve. But for the use as side-chain polymer an unsymmetrical

⁷⁷ J. F. Hartwig *Angew. Chem. Int. Ed.* **1998**, 37, 2046-2067.

⁷⁸ B. H. Yang, S. L. Buchwald *J. Organomet. Chem.* **1999**, 576, 125-146.

2. Overview of Thesis

substituted molecule is needed. These two problems had to be solved in order to get the desired monomers and polymers.

The unsymmetrical perylene bisimides were prepared by a method originally developed by Tröster⁶⁵ and modified by Langhals⁶⁶. The first step of the synthesis is the opening of one of the anhydride groups in the perylene-3,4:9,10-tetracarboxylic bisanhydride **1** to form the mono potassium salt **2** (figure 2-10). The ring is closed again with ammonia to get the monoanhydride monoimide **3**. As the resulting imide group is stable against basic and acidic reactions, only the anhydride group reacts in the next step with 8-aminopentadecane. The so-called swallow-tail substituent provides a very good solubility in organic solvents⁶⁷. But in contrast to other substituents for good solubility such as bulky benzene derivates⁷⁹ or a substitution at the bay-positions (1, 7 position of the perylene ring), the swallow-tail substituents do not enhance the perylene - perylene distance in the solid.

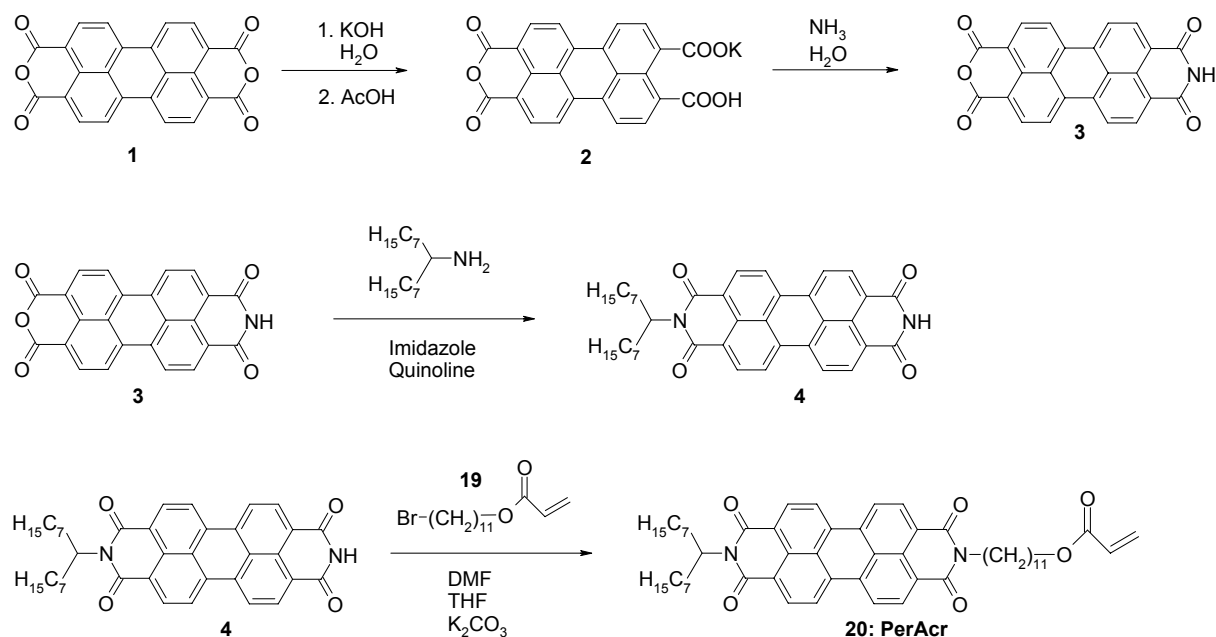


Figure 2-10: Synthesis of the perylene bisimide substituted acrylate PerAcr **20**.

The PerAcr monomer **20** could be obtained by coupling 11-bromoundecyl acrylate **19**, which was synthesized according to literature⁸⁰ with the unsymmetrically substituted perylene bisimide **4**. It has a good solubility in organic solvents with a low melting point ($T_{\text{onset}} = 120^{\circ}\text{C}$) which is in the range of the polymerization temperature at 125°C .

⁷⁹ A. Rademacher, S. Märkle, H. Langhals *Chem. Ber.* **1982**, *115*, 2927-2934.

⁸⁰ D. Joynes, D. C. Sherrington *Polymer* **1996**, *37*, 1453-1462.

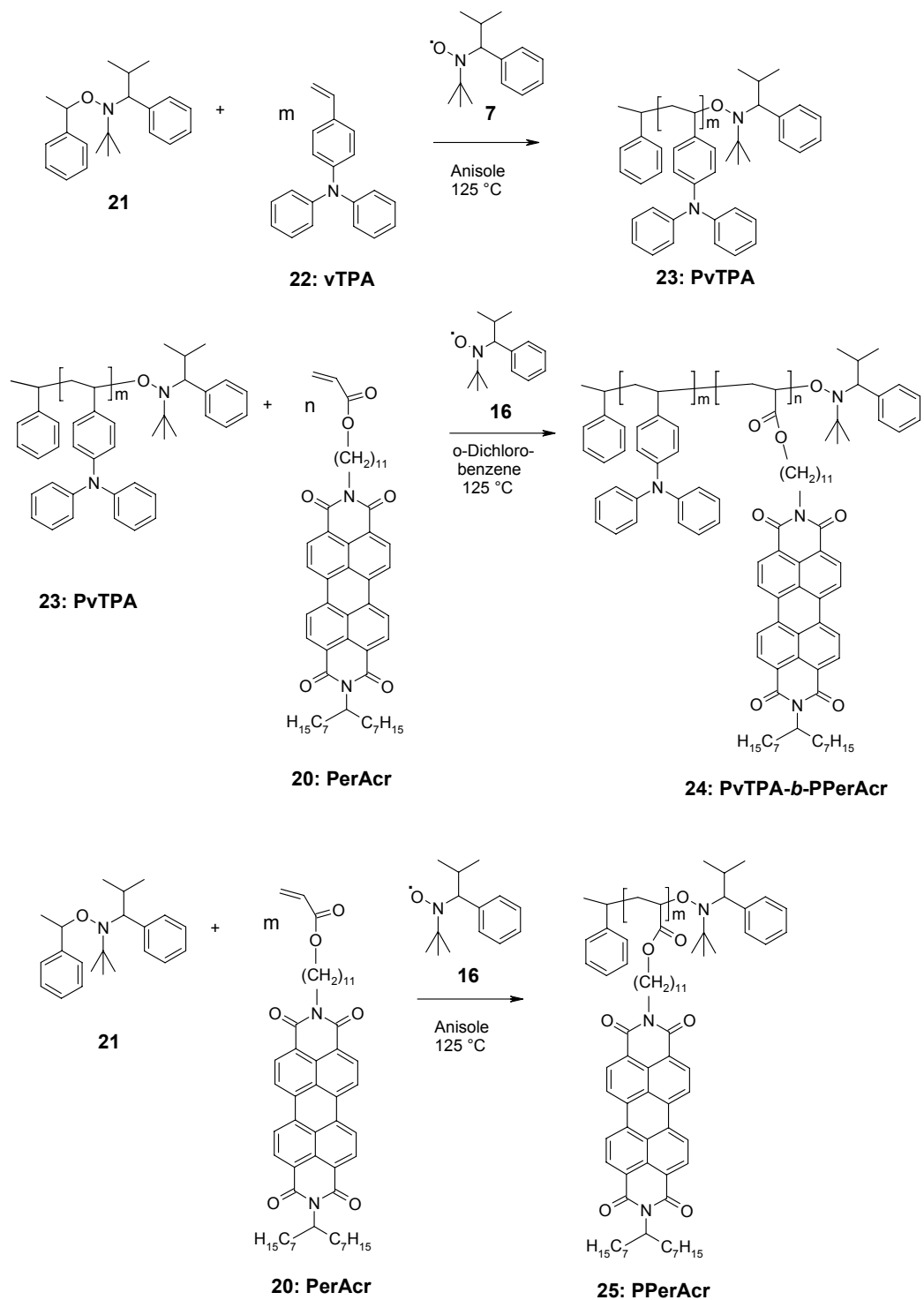


Figure 2-11: Controlled radical polymerization and block copolymerization of vTPA and PerAcr monomers via nitroxide mediated polymerization (NMRP).

These monomers were used for the preparation of the block copolymers and the homopolymers (figure 2-11). For the polymerization the free nitroxide **7** was added. The use of an additional free nitroxide besides the unimolecular initiator is described in literature to ensure the control of the polymerization of acrylates⁴⁹. Also for the polymerization of 4-vinyltriphenylamine the addition of the free nitroxide enhanced the control of the polymerization, resulting in lower polydispersities. Anisole was used as solvent for the homo polymerization of vTPA **22** as it reduces the viscosity of the reaction mixture. Otherwise the viscosity increases even after low conversion strongly resulting in a loss of control of the polymerization.

In order to check the control of the polymerization also time-dependant measurements were performed. In figure 2-12 the linear dependence between the time, the molecular weight and the conversion is shown.

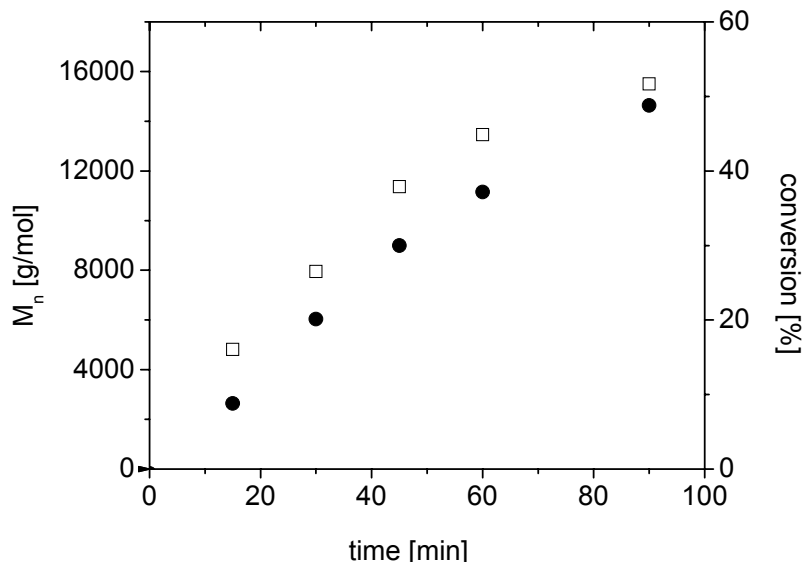


Figure 2-12: Evolution of molecular weight (□) and conversion (●) with time for nitroxide-mediated controlled polymerization of vTPA **22** to PvTPA **23**. Composition: 6 mmol vTPA **22**, 0.03 mmol **21**, 0.0015 mmol **7**, 600 μ l anisole; $T = 125\text{ }^{\circ}\text{C}$.

The homopolymers PPerAcr **25** were prepared in a similar fashion. This homopolymer was used as macroinitiator for the polymerization of vTPA **22**. As it is described in literature⁴⁹ that poly(*n*-butyl acrylate) terminated with an alkoxyamine could be used as macroinitiator for the polymerization of styrene, but a polystyrene macroinitiator is not suitable for the polymerization of *n*-butyl acrylate, the perylene bisimide substituted acrylate polymer PPerAcr **25** was used as macroinitiator. But the resulting block copolymer had a low

molecular shoulder in the GPC which could be attributed to remaining macroinitiator **25**. So PvTPA **23** was used as macroinitiator for the polymerization of PerAcr **20**. Here the resulting block copolymers show monomodal distributions. The reason that it is advantageous to use PvTPA as macroinitiator is its better solubility. This is probably the same reason why poly(*n*-butyl acrylate) can be used as macroinitiator for the polymerization of styrene and not the other way round.

In table 2-3 some of the prepared homo and block copolymers are listed. The composition of the block copolymers and the molecular weight can be varied by using different polymerization conditions. The same PvTPA macroinitiator can be used and the length of the second block is varied (see appendix A3). Another possibility is to use different PvTPA macroinitiators, keeping the ratio of the two blocks nearly constant, resulting in block copolymers with different molecular weights (see appendix A4). Thus the influence of individual parameters like the ratio of the blocks or the molecular weight can be studied.

2.4.2 Results and Discussion

In this chapter the thermal, optical and electrochemical properties as well as the morphology of the block copolymers will be discussed. In table 2-3 the thermal properties of the homopolymers and the block copolymers are given. PvTPA **23** is an amorphous polymer which has therefore only a glass transition temperature (T_g). The T_g depends on the molecular weight, ranging from 111 °C to 145 °C. The PPerAcr **25** on the other hand is semi-crystalline with a melting peak at 190 °C. The block copolymers **24** consisting of a both a PvTPA and a PPerAcr part which are covalently linked, exhibit both the T_g of the PvTPA and the melting peak of PPerAcr. These are in the same range as in the homopolymers. This indicates that the block copolymers are phase separated into two domains. The thermal stability was measured by determining the thermal weight loss by TGA. The onsets of the thermal loss of the block copolymers are above 300°C.

	macro-initiator	M _n [g/mol] ^a	PDI ^a	wt% of PPerAcr ^b	T _g [°C] ^c	T _m [°C] ^c	TGA-5% [°C]
23A	-	2440	1.21	-	111	-	311
23B	-	11440	1.11	-	138	-	362
23C	-	15830	1.22	-	144	-	378
23D	-	23210	1.19	-	145	-	376
24A	23A	9220	1.43	73	139	168	390
24B	23B	27850	1.47	64	136	194	389
24C	23C	26900	1.50	86	-	198	400
24D	23C	17610	1.37	14	142	181	380
24E	23C	24170	1.47	40	138	188	391
24F	23C	37710	1.97	79	150	198	396
25	-	19900	1.65	100	-	190	404

Table 2-3: Overview of the prepared homopolymers and block copolymers. ^a Measured with GPC using THF + 0.25 wt% TBAB as solvent and polystyrene standards. ^b Calculated from ¹H NMR spectra. ^c heating rate 10 K/min, values taken from second heating curve of the DSC experiments.

The ratio of the blocks is determined by ¹H NMR spectroscopy. These values are in close agreement with the ratio that is determined with UV/vis absorption coefficients. The UV/vis absorption spectra of the block copolymers **24D-24F** which were all prepared from the same macroinitiator **23C** are shown together with the PPerAcr homopolymer **25** in figure 2-13. The block copolymers have different lengths of the perylene bisimide block. All samples were measured using a concentration of 0.02 mg/ml THF. The PPerAcr absorbs from 400 to 600 nm and the PvTPA in the ultraviolet part of the spectra.

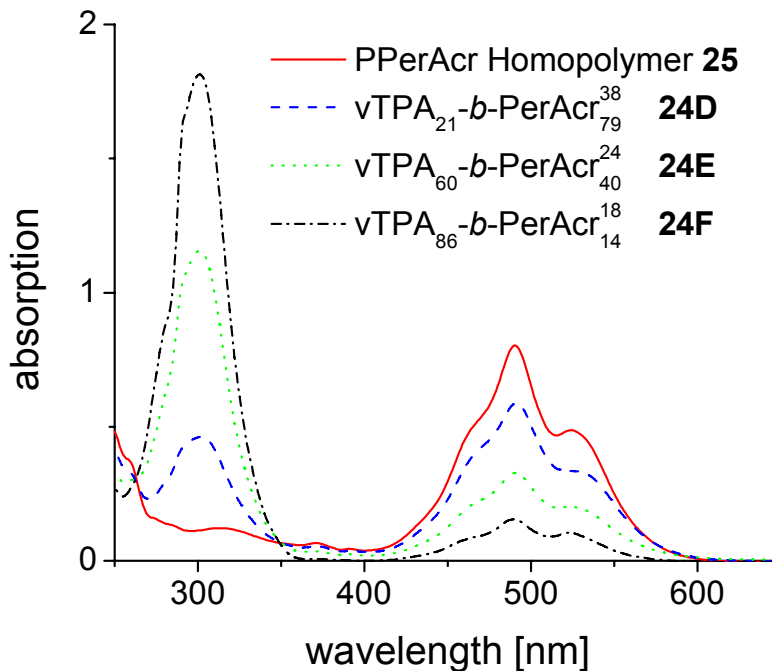


Figure 2-13: UV/vis spectra of the block copolymers **24D-24F** and the homopolymer **25** measured in THF (concentration: 0.02 mg/ml).

The UV/vis absorption spectra of the perylene bisimide part is very broad in solution. This is an indication for aggregation of the perylene bisimide moieties in the polymer. In contrast to that, the PerAcr monomer shows a typical spectrum for isolated perylene bisimides. The absorption peaks as well as the fluorescence peaks are red-shifted (figure 2-14). The UV/vis spectra of films of the block copolymers are even more red-shifted and the absorption gets broader. This behavior is analogous to the interchain coupling in conjugated polymers and oligomers⁸¹. But here it is an intramolecular effect in solution.

The aggregation of perylene bisimides⁷⁰ can be described by the quotient of the vibronic transitions. The quotient of the absorption at the second and the first vibronic transition is introduced to describe the degree of aggregation. This quotient changes from 0.61 for monomer **20** to 1.63 for the polymer **25** in THF solution. The aggregation is also dependant on the solvent. For polymer **25** with the same concentration in chloroform the quotient is 1.07.

⁸¹ J. Cornil, A. J. Heeger, J. L. Bredas *Chem. Phys. Lett.* **1997**, 272, 463-470.

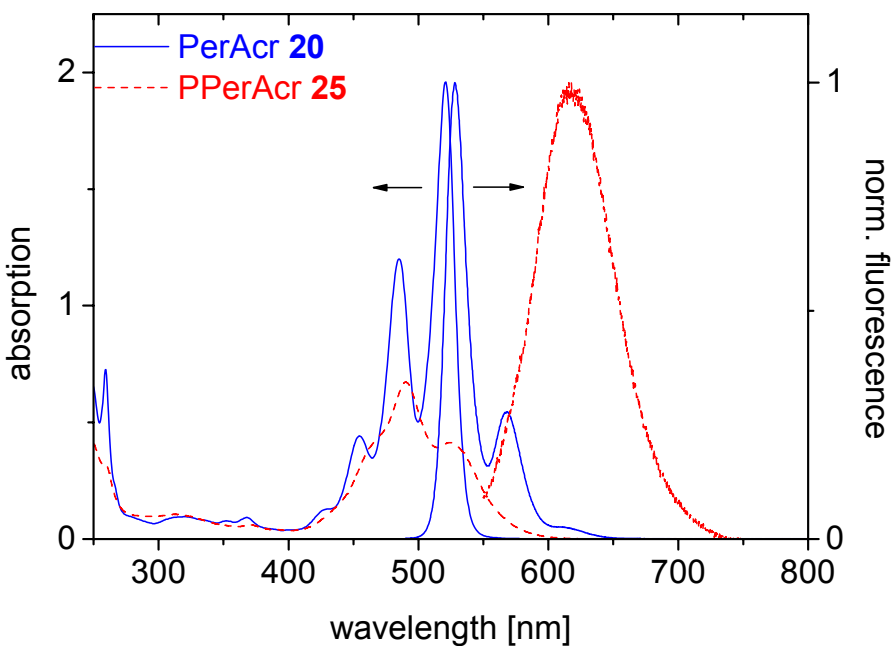


Figure 2-14: UV/vis and fluorescence spectra of the PerAcr monomer **20** and the corresponding homopolymer PPerAcr **25** (concentration: 0.02 mg/ml THF)

The strong aggregation behavior is due to the π - π stacking of the perylene bisimide units. This is a very characteristic behavior of perylene bisimides. The overlap of the perylene bisimide units in the crystal determines the color of the dye. The color of perylene bisimide dyes varies from red to black depending on the substitution at the imide group⁸².

The stacking properties were examined with wide angle X-ray scattering (WAXS) of the polymer powders. In figure 2-15 the WAXS spectra of the PerAcr monomer **20** and the block copolymer **24C** are shown. Beside the amorphous halo, both spectra have a crystalline peak at 25.8° .

⁸² F. Graser, E. Hädicke *Liebigs Ann. Chem.* **1984**, 483-494.

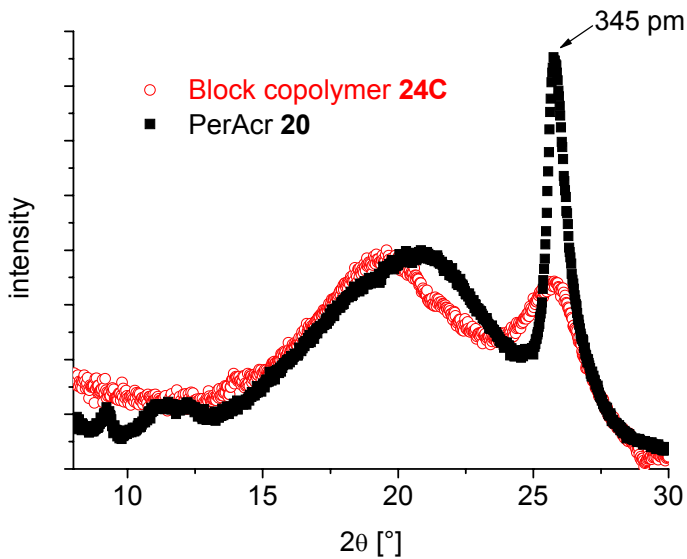


Figure 2-15: Wide angle X-ray scattering (WAXS) of the monomer **20** and the block copolymer **24C**.

The distance between the perylene bisimides units can be calculated using Bragg's law. It is 3.45 Å, only 0.1 Å larger than the layer distance in graphite (3.35 Å). It is in the same range as in insoluble perylene bisimides^{83,84} or perylene itself. This is a very important point as not only the absorption spectra are influenced by the packing but also the charge carrier mobility in organic semiconductors³⁵.

The distance between the perylene bisimide moieties is not increased by the swallow-tail substituent which is needed for the solubility. This is astonishing as normally the solubility is connected with the distance between the perylene bisimides⁸⁵. The distance for the soluble perylene bisimide derivate which is symmetrically substituted with 2,6-diisopropylbenzene is 6.65 Å. But the swallow-tail substituents provide solubility without increasing the perylene to perylene distance.

In the last paragraph the optical properties of the homopolymers were correlated with the π - π stacking of the perylene bisimide units. In this section the effect of the electron donating PvTPA on the optical properties will be investigated. The fluorescence of an electron acceptor like perylene bisimide is quenched if an electron is injected from the triphenylamine HOMO into the HOMO of the perylene bisimide. Therefore the fluorescence quenching of the block copolymer **24F** and a blend with the same ratio of the blocks were compared

⁸³ E. Hädicke, F. Graser *Acta Cryst. C* **1986**, 42, 189-195.

⁸⁴ E. Hädicke, F. Graser *Acta Cryst. C* **1986**, 42, 195-198.

⁸⁵ F. Graser, E. Hädicke *Liebigs Ann. Chem.* **1980**, 1994-2011.

(PPerAcr **25**/PvTPA **23C** = 80/20) to study the effect in block copolymers. The films were spin-coated onto a glass substrate. The films of the block copolymer and the corresponding blend had nearly the same optical density (figure 2-16). After excitation with 470 nm the fluorescence was measured. As the samples have the same optical density, the same number of excitons are generated. The exciton can either reach the interface between the electron acceptor and the electron donor, or recombine, resulting in fluorescence. The fluorescence quenching of the block copolymer is significantly stronger than that of the corresponding blend. This is an indication that in the block copolymer more excitons reach the interface leading to reduced fluorescence. This is supported by the fact that the block copolymers exhibit microphase separation whereas blends show macrophase separation (see 2.4.2)

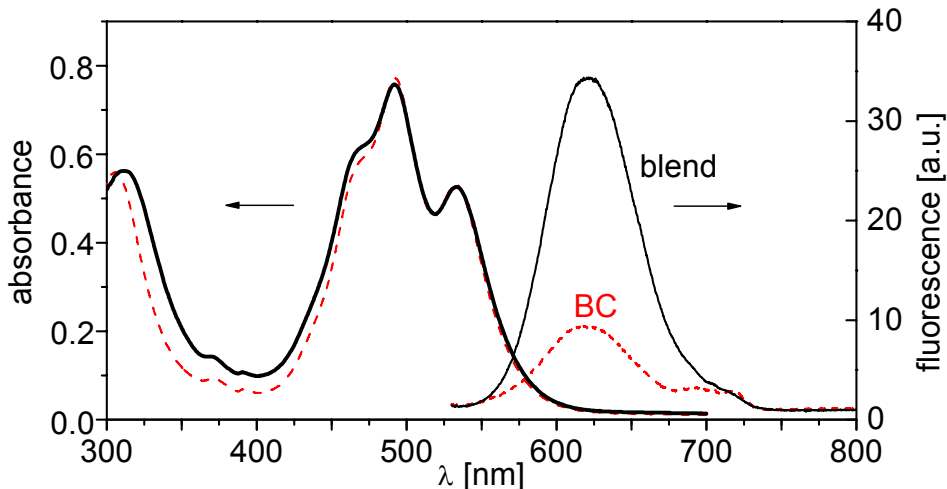


Figure 2-16: Absorption spectra of both blend (solid line) and block copolymer **24F** (dashed line) with the same ratio (weight fractions: $\phi_{\text{PvTPA}} = 0.2$, $\phi_{\text{PPerAcr}} = 0.8$). Photoluminescence spectra of blend and block copolymer films under an excitation wavelength of 470 nm.

The electrochemical properties were studied using cyclic voltammetry. The measurements were conducted in THF containing 0.1 M tetrabutylammonium hexafluorophosphate as solvent. The HOMO (Highest Occupied Molecular Orbital) and LUMO (Lowest Unoccupied Molecular Orbital) values were calculated with respect to ferrocene (HOMO: -4.8 eV). The perylene bisimides have two reversible reduction peaks and one oxidation peak. From the first reduction peak the LUMO can be calculated as -3.72 eV for the monomer PerAcr **20**, -3.66 eV for the homopolymer **25** and -3.65 eV for the block copolymer **24F**. The HOMO value of the PvTPAs **23** is -5.23 eV.

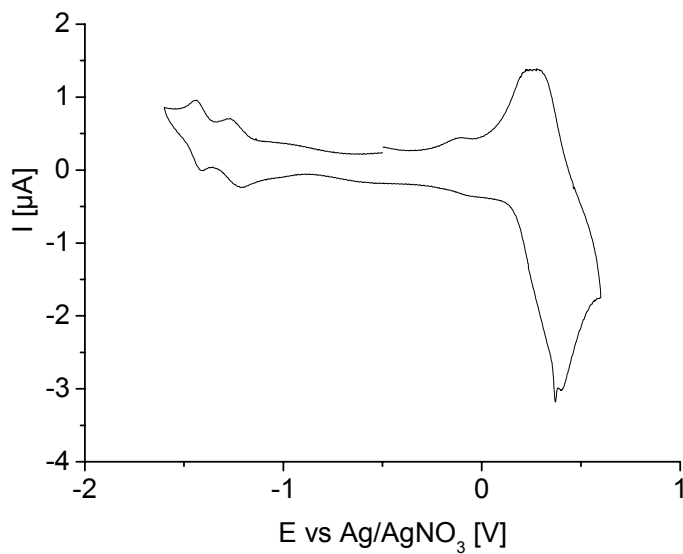


Figure 2-17: Example of a cyclic voltammogram for block copolymer **24F** with two reversible reduction peaks for the perylene bisimide unit and one oxidation for the triphenylamine unit. The spectrum was measured in THF containing 0.1 M tetrabutylammonium hexafluorophosphate.

The block polymers **24** or the homopolymer **25** are not soluble enough in CH_2Cl_2 to enable the study of the oxidation behavior of perylene units which take place at higher potentials at which THF is not stable. For this reason a highly soluble symmetrical N,N'-di(1-heptyloctyl)perylene-3,4:9,10-tetracarboxylic bisimide **18** was used as a model and it was measured in CH_2Cl_2 containing 0.1 M tetrabutylammonium hexafluorophosphate. For this compound the LUMO could be calculated as -3.71 eV (very similar to those of block copolymer **24** and perylene bisimide homopolymer **25**) and the HOMO as -6.03 eV. The HOMO/LUMO gap is 2.32 eV.

In the case of block copolymers both the reduction peaks due to the perylene bisimide and the oxidation peak of the triphenylamine can be seen in THF (see figure 2-17). The LUMO and HOMO values were determined as -3.65eV and -5.23eV respectively.

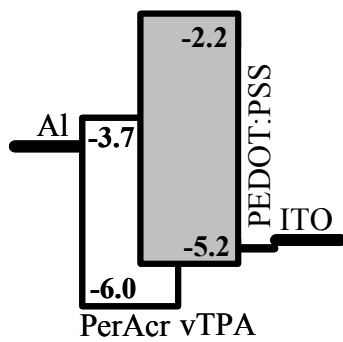


Figure 2-18: Schematic representation of energy levels in a PvTPA-*b*-PPerAcr block copolymer solar cell.

The maximum built-in potential and theoretically achievable photovoltage (V_{oc}) is determined by this electrical gap between the LUMO of PPerAcr and the HOMO of PvTPA, which is 1.58 eV for the block copolymers. The energetic level diagram is shown in figure 2-18 which explains the energetical offsets in the device structure used for the solar cells.

As the optical and electric properties of the block copolymers are suitable for organic solar cells, the investigation of the morphology is the next requirement for the realization of “nanostructured bulk heterojunction” solar cells. For this purpose the morphology of the block copolymers **24D-24F** were examined. They were prepared with the same macroinitiator **23C**, thus only varying in the length of the PPerAcr block. From the DSC experiments it could already been shown that they exhibit the T_g from the amorphous PvTPA block and the melting point from the semi-crystalline PPerAcr block which shows that they are phase separated into two different domains.

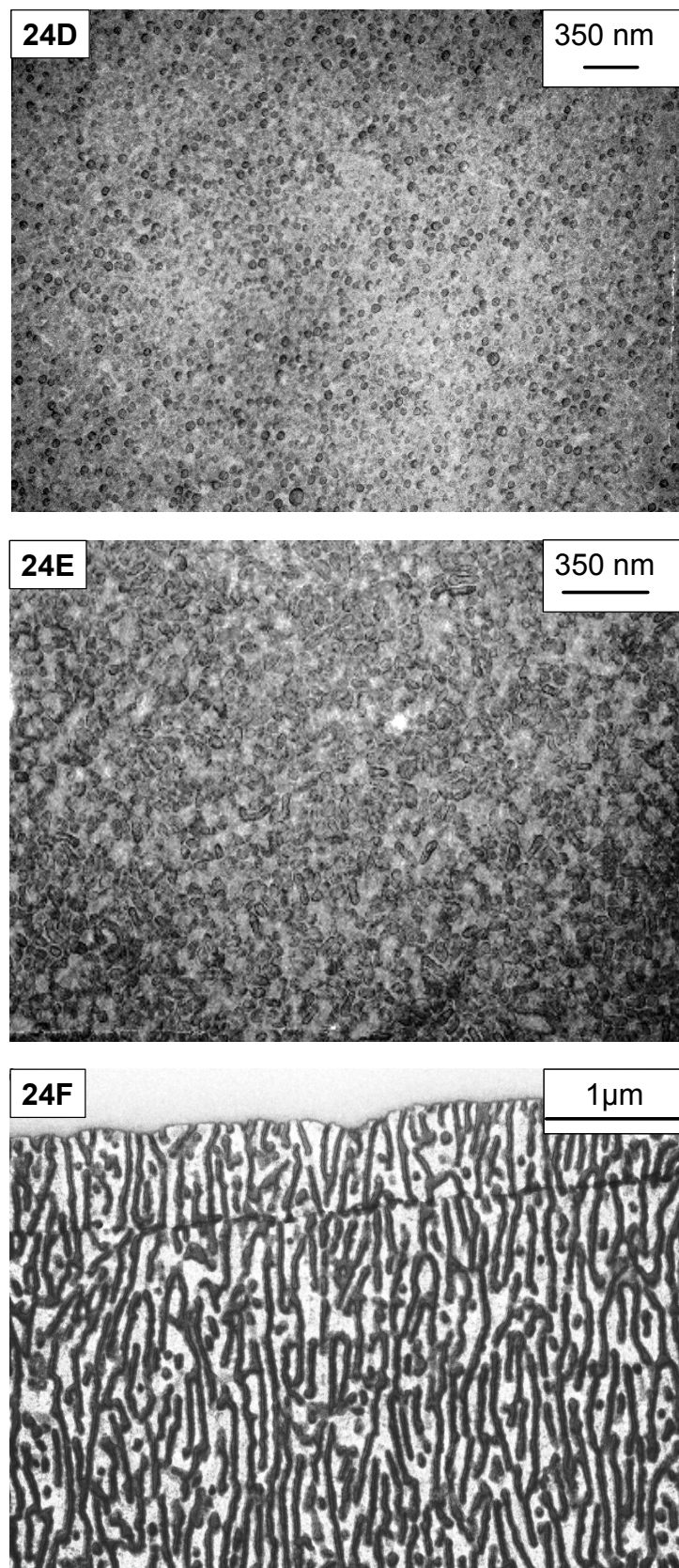


Figure 2-19: TEMs of the cross-sections of block copolymers 24D ($PvTPA_{86}-b-PPerAcr_{14}$), 24E ($PvTPA_{40}-b-PPerAcr_{60}$), 24F ($PvTPA_{21}-b-PPerAcr_{79}$), which were made with the same macroinitiator, thus varying only in the content of PPerAcr. The samples were stained with RuO_4 .

Depending on the perylene bisimide content the morphology changes from spherical (**24D**) to elongated structures (**24E**) and finally for high perylene bisimide contents to a nanowire like structure (**24F**). This is the first block copolymer consisting of an electron transport and a hole transport block that shows microphase separation on a nanometer scale.

Especially the structures of block copolymer **24F** are very promising for solar cell applications. These elongated, nanowire like structures do not only increase the interface between the electron acceptor and the electron donor dramatically, they also function as percolation ways for the electrons.

A series of block copolymers was prepared with different PPerAcr content. Block copolymers with high PPerAcr content (64 wt% - 86 wt%) show similar nanostructures. Only the block copolymer **24A** with a very short PvTPA block ($M_n = 2440$ g/mol) shows no structure although it has a PPerAcr content of 73 wt%.

All the other samples have a very similar structure. The TEM of **24B** shows the parallel alignment of the domains (figure 2-20). Some parts are disturbed and some of the nanodomains seem to be orientated perpendicular to the surface. If the TEM pictures of **24B** and **24C** are compared with a high magnification they reveal the same structural sizes. The thickness of these domains is about 13 nm over the whole length of the domain which is several micrometers. This result is very interesting as the domain size of the block copolymers is usually influenced by the chain length and the polydispersity⁸⁶.

These structures have to be induced by self-assembly via π - π stacking of the perylene bisimides. There are examples^{87,88} that perylene bisimides together with melamine form hexagonal structures.

⁸⁶ A. Noro, D. Cho, A. Takano, Y. Matsushita *Macromolecules* **2005**, *38*, 4371-4376.

⁸⁷ J. A. Theobald, N. S. Oxtoby, M. A. Philips, N. R. Champness, P. H. Beton *Nature* **2003**, *424*, 1029-1031.

⁸⁸ L. E. Sinks, B. Rybtchinski, M. Iimura, B. A. Jones, A. J. Goshe, X. Zuo, D. M. Tiede, X. Li, M. R. Wasielewski *Chem. Mater.* **2005**, *17*, 6295-6303.

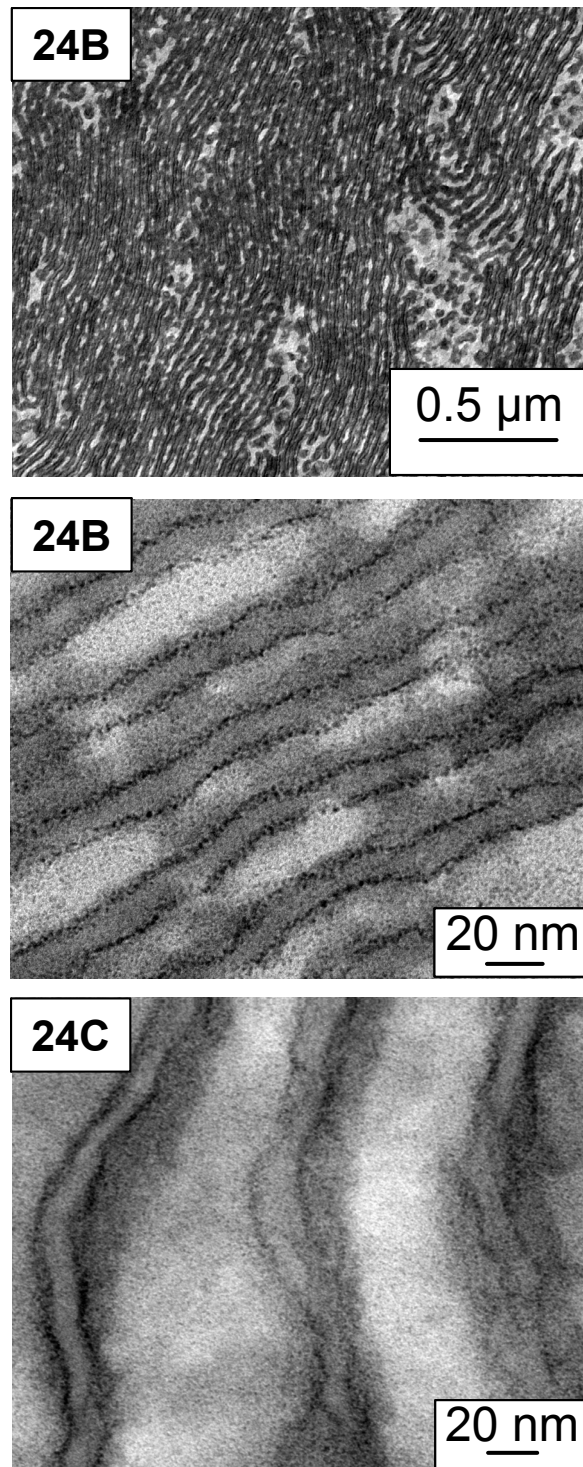


Figure 2-20: TEMs of the cross-sections of block copolymers **24B** ($PvTPA_{36}-b-PPerAcr_{64}$) and **24C** ($PvTPA_{14}-b-PPerAcr_{86}$). The samples were stained with RuO_4 .

2.5 Photovoltaic Devices

2.5.1 Methods

The device structure used for the determination of the photovoltaic characteristics is shown in figure 2-21.

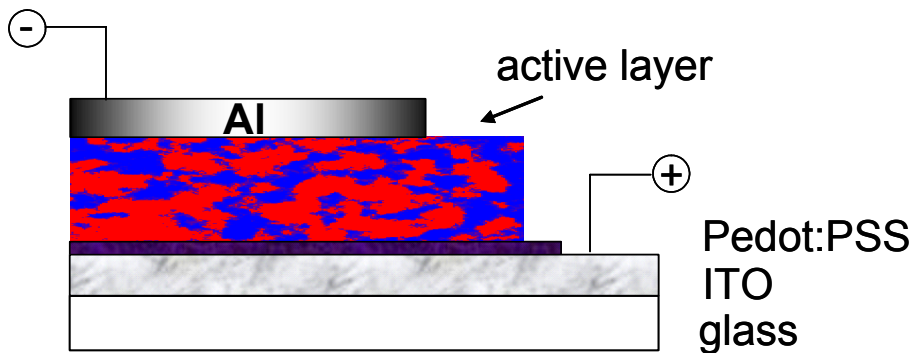


Figure 2-21: Schematic representation of device structure of a polymer solar cell.

ITO (indium tin oxide) is used as electrode. As it is transparent, the active layer is illuminated through this electrode. The ITO substrates were patterned by acid etching, cleaned and treated with oxygen plasma.

To avoid short-circuits between the active layer and the ITO electrode, a layer of PEDOT:PSS was spin-coated and afterwards annealed. PEDOT:PSS is a dispersion in water, therefore it is not removed by organic solvents used for the preparation of the organic layers. The use of orthogonal solvents allows the preparation of two stacked layers. The active layer was deposited by spin-coating. The aluminum electrode (100 nm) was deposited by thermal vacuum evaporation with a BOC Edwards Auto 306 vacuum deposition chamber. The active area of the cell is 0.18 cm^2 .

The performance of the photovoltaic devices was tested by IPCE (incident photon to current conversion efficiency) and current-voltage measurements at the chair of macromolecular chemistry I.

Current-voltage measurements were done with a constant intensity of 76.7 mW/cm^2 light under standard AM 1.5 G spectral conditions (Oriel set up with 150 W Xenon arc lamp and suitable filters). AM 1.5 G is a simulated sun spectrum for 48.2° above the horizon. This set up is calibrated using a reference Si-cell from ISE Freiburg at the sample position and height.

2. Overview of Thesis

The fill factor (FF) can be determined as:

$$FF = \frac{V_{MPP} \times I_{MPP}}{V_{OC} \times I_{SC}}$$

The subscript MPP denotes the maximal power point, V_{OC} is the open circuit voltage and I_{SC} is the short circuit current.

Incident photon to current conversion efficiency (IPCE) determines the percentage of electrons that are obtained from the incident photons at a distinct wavelength. It is measured using a monochromator (Spex, Model 1681 B) with holographic grid (Lamp: 300 W Xenon arc lamp Model: 6259 Oriel) creating homogeneous illumination of a circular spot of 3.5 cm diameter (Power: <1 mW) for the wavelength range from 280 nm to 1000 nm.

2.5.2 Solar Cell Results

The opportunities of nanostructured solar cells can finally only be shown with the photovoltaic device characteristics. Therefore the blend of the two homopolymers PPerAcr **25** and PvTPA **23C** and the block copolymer **24F** with the same weight ratio of the blocks (weight fractions: $\phi_{PvTPA} = 0.2$, $\phi_{PPerAcr} = 0.8$) were compared.

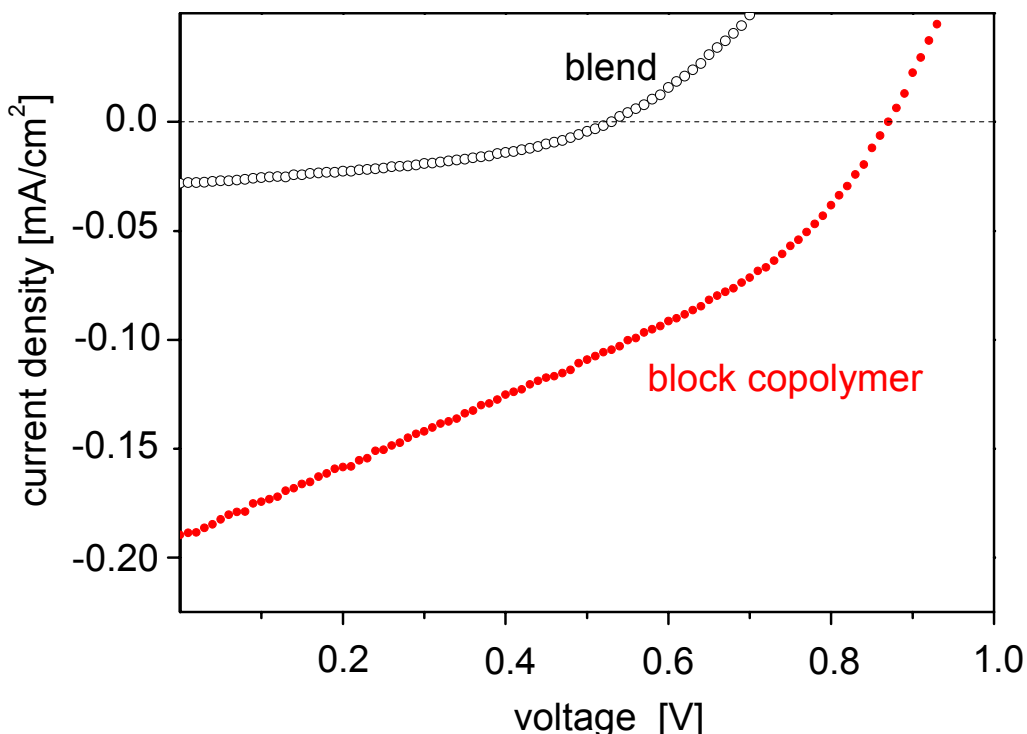


Figure 2-22: Current-voltage characteristics of a photovoltaic device using a polymer blend (\circ) and the block copolymer **24F** (\bullet) with the same ratios.

The devices were prepared under the same conditions. As the optical density in both devices is the same, the number of photons absorbed is also comparable. The thickness of the active layer is 250 nm. But the photovoltaic characteristics show an enormous improvement for the block copolymer solar cell.

The short circuit current (I_{sc}) increases from 0.028 mA/cm² for the blend device to 0.190 mA/cm² for the block copolymer device. Also the open circuit voltage (V_{oc}) is improved from 0.525 V to 0.865 V for the block copolymer system. Altogether the power conversion efficiency was improved by one order of magnitude from 0.007% in the polymer blend to 0.07% in the block copolymer device.

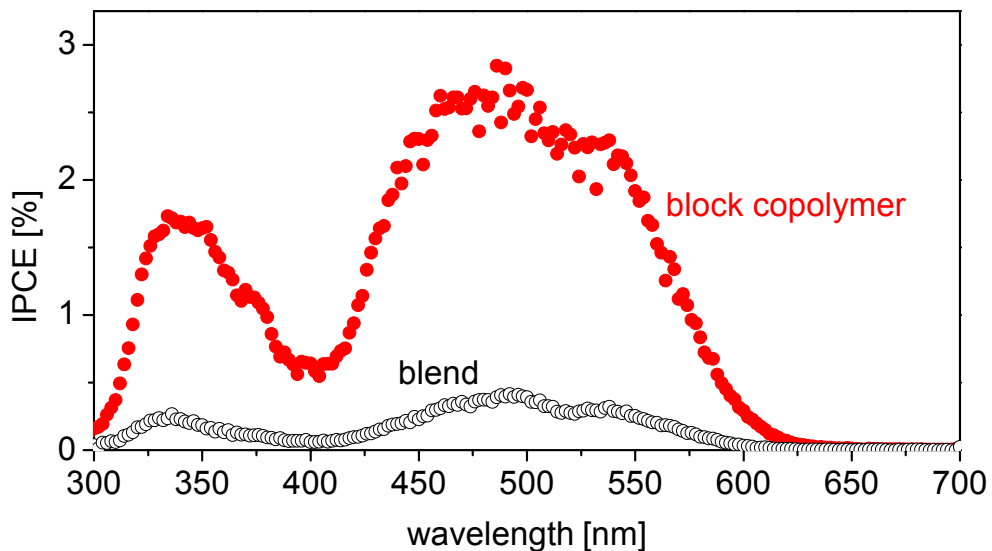


Figure 2-23: IPCE curves of the blend (\circ) and the block copolymer 24F (\bullet) device with a 250 nm thick layer are compared.

With the same cells the external quantum efficiency (IPCE) was determined. The IPCE spectrum (figure 2-23) correlates with the UV/vis absorption spectrum, indicating that the whole absorption of the molecule is used for current generation. Also the IPCE is higher for the block copolymer than for the blend device. The improved efficiency by one order of magnitude and the increased quantum efficiency are an unambiguous proof-of-principle for nanostructured photovoltaic devices using block copolymers.

As it could be shown that the device characteristics are clearly improved by using block copolymers, the question is whether these findings could be related to the morphology in thin films. Therefore the active layer of the photovoltaic device was investigated with TEM. The active layer could be floated onto water as the PEDOT:PSS layer is soluble in water. The active layer was then embedded into epoxy resin and cut vertically to get a cross-section of the solar cell (figure 2-24).

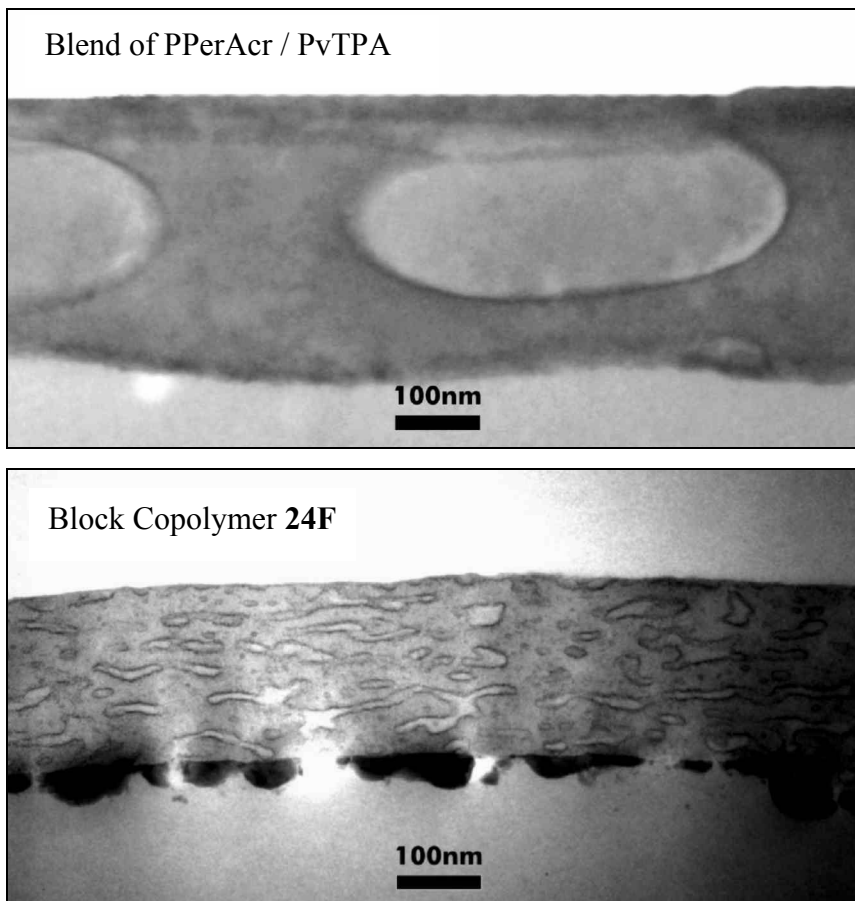


Figure 2-24: TEM cross-sections of a polymer blend solar cell with 20 wt% of PvTPA and 80 wt% of PPerAcr and of a block copolymer solar cell ($\text{PvTPA}_{21}\text{-}b\text{-PPerAcr}_{79}$, **24F**). The samples were stained with RuO_4 .

The cross-section of the block copolymer **24F** solar cell reveals a nanostructured morphology whereas the blend solar cell with the same ratio shows macrophase separation. These findings explain the better efficiency of the block copolymer devices. The number of absorbed photons is in both devices similar, but in the nanostructured block copolymer device more of the created excitons can reach the interface between the acceptor and the donor where the excitons are dissociated into an electron and hole. Then the charge carriers have to drift to the electrodes. These results correspond with the stronger fluorescence of the blend film as described in chapter 2.4.2. As the numbers of excitons which reach the donor / acceptor interface is lower in the blend, more excitons recombine by a radiative decay in the blend. The alignment of the domains of the block copolymer in figure 2-24 is far from ideal. These nanostructures should ideally be perpendicular to the electrodes as the charge carriers can then

2. Overview of Thesis

be easily transported through the domains to the corresponding electrodes. The orientation of the domains can be achieved by electric fields^{89,90,91} or by solvent induced alignment⁹².

The increase in the interfacial area of the donor / acceptor block copolymer results in an enhancement of one order of magnitude in the device performance. This demonstrates the opportunities for nanostructured bulk heterojunction solar cells.

⁸⁹ T. Thurn-Albrecht, J. DeRouchey, T. P. Russell, H. M. Jaeger *Macromolecules* **2000**, *33*, 3250-3253.

⁹⁰ A. Böker, H. Elbs, H. Hänsel, A. Knoll, S. Ludwigs, H. Zettl, V. Urban, V. Abetz, A. H. E. Müller, G. Krausch *Phys. Rev. Lett.* **2002**, *89*, 135502.

⁹¹ T. Xu, A. V. Zvelindovsky, G. J. A. Sevink, K. S. Lyakhova, H. Jinnai, T. P. Russel *Macromolecules* **2005**, *38*, 10788-10798.

⁹² S. H. Kim, M. J. Misner, T. P. Russell *Advanced Materials* **2004**, *16*, 2119-2123.

2.5.3 Additional Results

In addition to the photovoltaic studies in the previous chapter some supplementary results are given in the following. The device setup used for the determination of the photovoltaic characteristics is illustrated in figure 2-21. A PEDOT:PSS layer was introduced between the ITO electrode and the active layer. The PEDOT:PSS layer is smoothening the surface but is also preventing charge recombination of the active layer with the ITO electrode. Without this electron blocking layer the open circuit voltage is drastically reduced (figure 2-25), whereas the short circuit current I_{SC} is nearly constant.

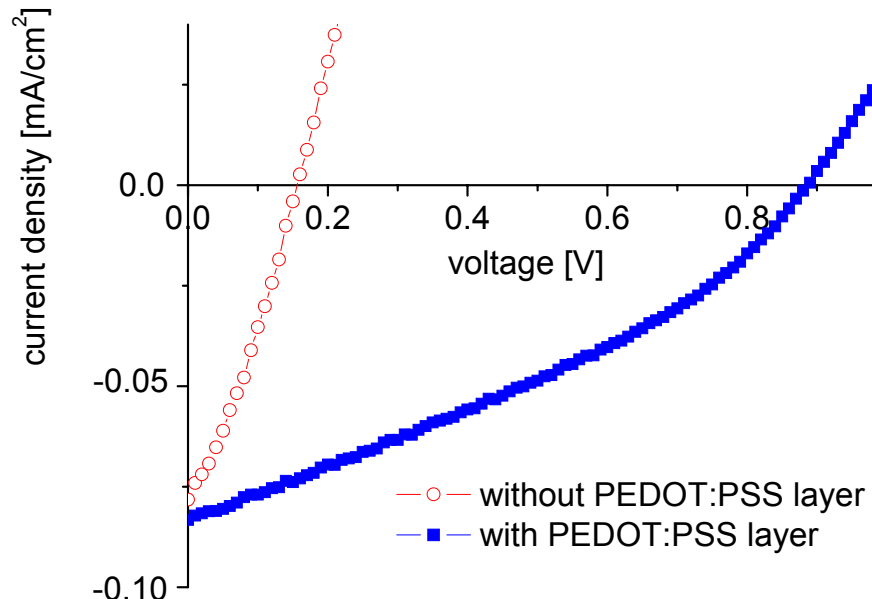


Figure 2-25: Current-voltage characteristics of photovoltaic device with and without an additional PEDOT:PSS layer between the ITO electrode and the active layer (**24C**). Al is used as top electrode.

This device setup is possible by the use of orthogonal solvents for the different layers. The PEDOT:PSS layer is not removed by organic solvents like chloroform or chlorobenzene. The influence of the hole conductor was studied by blending the homopolymer PPerAcr **25** with different low molecular weight hole conductors. A constant weight ratio of PPerAcr **25** to the low molecular weight hole transport material of 80:20 was used. The layers were prepared by spin-coating 0.8 wt% **25** and 0.2 wt% hole transport material from a chloroform solution. As hole transport materials, tri(p-tolyl)amine (TMTPA) which is comparable to the

TPA moieties in the block copolymers, and 4,4'-DMeOTPD and 1-NPD which are hole conductors with a higher mobility, were compared.

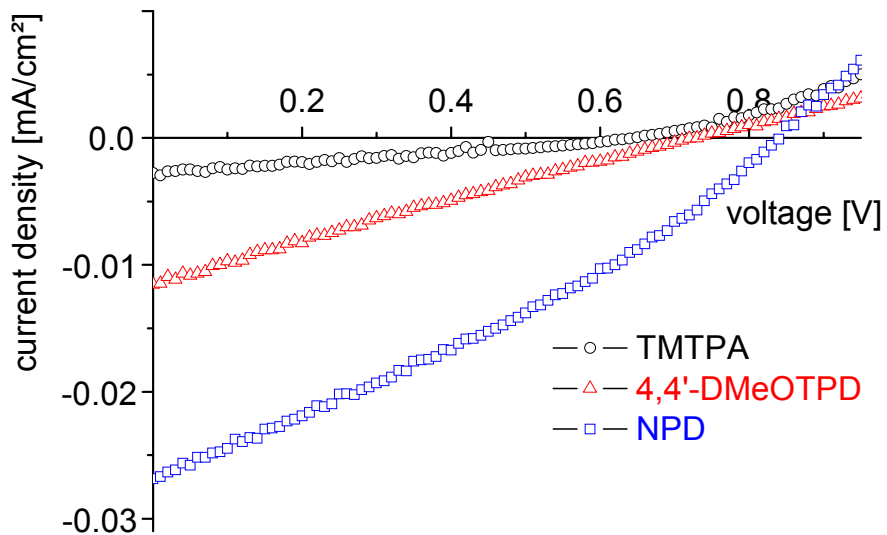


Figure 2-27: Current-voltage characteristics of photovoltaic blend devices with different hole transport materials. Blend ratio: PPerAcr **25** / HTM = 80 / 20. (device setup: ITO/PEDOT:PSSblend/Al).

The I_{SC} is clearly improved by the use of 1-NPD or 4,4'-DMeOTPD instead of TMTPA (figure 2-27). But still the current density in blend devices consisting of PPerAcr **25** and low molecular weight hole conductors were significantly lower than in the block copolymer solar cells. This demonstrates the beneficial effects of nanostructured bulk heterojunctions with block copolymers in organic solar cells.

2.6 Statement

The results presented in this thesis were obtained in parts in collaboration with other workers and published or submitted as indicated in the appendix. In the following, my own contributions to the different publications or manuscripts are specified.

A1

Fluorescent Acceptor Labeled Polymers carrying Hole Transport Pendant Groups

Stefan M. Lindner, Mukundan Thelakkat

manuscript

I synthesized and characterized (GPC, NMR, DSC, TGA, UV/vis, fluorescence, cyclic voltammetry) all the investigated acceptor labeled polymers. I wrote the first draft of the manuscript, which was finalized jointly with my thesis advisor PD Dr. Mukundan Thelakkat.

A2

Synthesis, Photophysical and Electrochemical Characterization of Novel Soluble Perylene Bisimide - Fullerene Dyads

Stefan M. Lindner, Michaela Ruppert, Andreas Hirsch and Mukundan Thelakkat

manuscript

The synthesis of the perylene bisimide precursor **5** was done by me. The final conversions to perylene bisimide – fullerene dyads were done by Michaela Ruppert (Prof. Dr. Hirsch, Universität Erlangen-Nürnberg) as part of her diploma thesis in a joint research project. I made the photophysical and electrochemical characterization. I wrote the first draft of the manuscript, which was finalized jointly with my thesis advisor PD Dr. Mukundan Thelakkat.

A3

Nanostructures of n-Type Organic Semiconductor in a p-Type Matrix via Self-Assembly of Block Copolymers

Stefan M. Lindner, Mukundan Thelakkat

Macromolecules 2004, 37, 8832-8835.

I synthesized and characterized (GPC, NMR, DSC, TGA, UV/vis, fluorescence) all investigated monomers, homopolymers and block copolymers. I wrote the first draft of the manuscript, which was finalized jointly with my thesis advisor PD Dr. Mukundan Thelakkat.

A4

Nanostructured Semiconductor Block Copolymers: π - π Stacking, Optical and Electrochemical Properties

Stefan M. Lindner, Nadine Kaufmann, Mukundan Thelakkat

manuscript

I synthesized the compounds with the support of N. Kaufmann who worked on this topic during her advanced lab course in our group. The characterization was done by me (GPC, NMR, DSC, TGA, UV/vis, fluorescence, cyclic voltammetry, WAXS). I wrote the first draft of the manuscript, which was finalized jointly with my thesis advisor PD Dr. Mukundan Thelakkat.

A5

Charge Separation at Self-Assembled Nanostructured Bulk Interfaces in Block Copolymers

Stefan M. Lindner, Sven Hüttner, Arnaud Chiche, Mukundan Thelakkat, Georg Krausch

Angewandte Chemie International Edition, **2006**, *45*, 3364-3368.

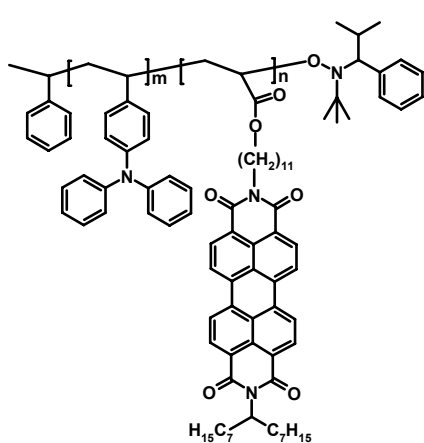
I synthesized all the compounds in this paper and I performed the optical experiments (UV/vis, fluorescence). The preparation and characterization of the solar cells was done together with S. Hüttner. The morphology of the solar cells was investigated by S. Hüttner and Dr. A. Chiche.

3. Summary

The motivation for this thesis was the synthesis and characterization of novel materials exhibiting nanstructured interfaces for electro-optical studies. Therefore a series of functionalized block copolymers, acceptor labeled polymers and low molecular weight model compounds were synthesized in which hole transport (donor), electron transport (acceptor) and light absorbing functionalities were incorporated. In this chapter the concept and the outstanding results are briefly summarized.

The morphology in organic solar cells is one of the key factors for obtaining efficient devices. This is due to the excitonic charge carrier generation process present in organic materials. After illumination an exciton (bound electron-hole pair) is formed, which has to reach the donor / acceptor interface where it is dissociated into an electron and a hole. As the exciton diffusion length is only in the range of some nanometers, the domain sizes in an organic solar cell have to be in the same nanometer range. This principle was realized efficiently in dye sensitized nanocrystalline TiO₂ solar cells and also by blending π -conjugated polymers with the fullerene derivative PCBM.

My approach was to use functionalized block copolymers. Block copolymers exhibit microphase separation with domain sizes on a nanometer scale by the interplay between immiscibility and molecular connectivity. I used a controlled radical polymerization technique, the nitroxide mediated radical polymerization (NMRP), to get block copolymers with one block consisting of an electron transport material and the other one of a hole transport material (figure 3-1).



block copolymer	macro-initiator used	M _n [g/mol]
24A	23A	9220
24B	23B	27850
24C	23C	26900
24D	23C	17610
24E	23C	24170
24F	23C	37710

Figure 3-1: Chemical structures of the block copolymers **24** consisting of an electron transport perylene bisimide block and a hole transport triphenylamine segment and the various block copolymers obtained.

3. Summary

Triphenylamine was used as hole conductor in combination with perylene bisimide as dye and electron conductor. First, a soluble perylene bisimide monomer had to be synthesized. This was achieved by an unsymmetrical synthesis starting from the perylene-3,4:9,10-tetracarboxylic bisanhydride. For the solubility a swallow-tail substituent was introduced and the other imide group was functionalized with an acrylate to get the monomer.

Starting the polymerization with 4-vinyltriphenylamine, different PvTPA **23** macroinitiators were synthesized. A series of block copolymers **24C-24F** were prepared using the same PvTPA macroinitiator **23C**, thus only varying the perylene bisimide block. Furthermore, a series of block copolymers **24A-24C** were synthesized using different PvTPA macroinitiators **23A-23C**. Thus block copolymers with different molecular weights, but similar ratios of the blocks could be prepared. The controlled nature of NMRP allowed the architecture of these block copolymers with low polydispersities and controlled molecular weight.

The block copolymers exhibited microphase separation, revealing elongated nanowire like structures (figure 3-2) for those with high perylene bisimide content. Most of these block copolymers exhibit a constant width of 13 nm for the nanowire like structure of the perylene bisimides. This was the first examples of microphase separation of block copolymers carrying electron transport and hole transport blocks.

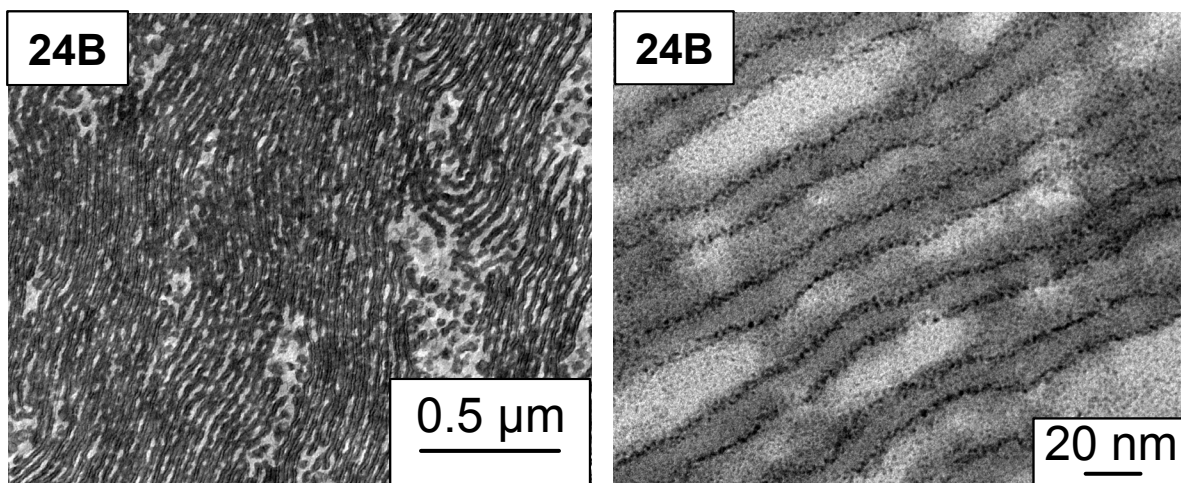


Figure 3-2: Example of a TEM cross-section of block copolymer **24B** with different magnifications. The sample was stained with RuO_4 .

The optical properties of the block copolymers were compared with that of the blend containing the same weight ratio of the electron and hole transport materials. It could be shown that the fluorescence is more efficiently quenched in the block copolymers as the

3. Summary

domain sizes are smaller and therefore more excitons reach the donor / acceptor interface in the block copolymer.

The electrochemical properties of the block copolymers were studied using cyclic voltammetry. The LUMO of the perylene bisimide block is -3.65 eV and the HOMO of the triphenylamine block is -5.23 eV. Therefore the maximum built-in potential and theoretically achievable photovoltage V_{OC} is 1.58V.

In order to proof the concept of nanostructured bulk heterojunction solar cells, the block copolymer and a blend with the same weight composition were compared in photovoltaic devices.

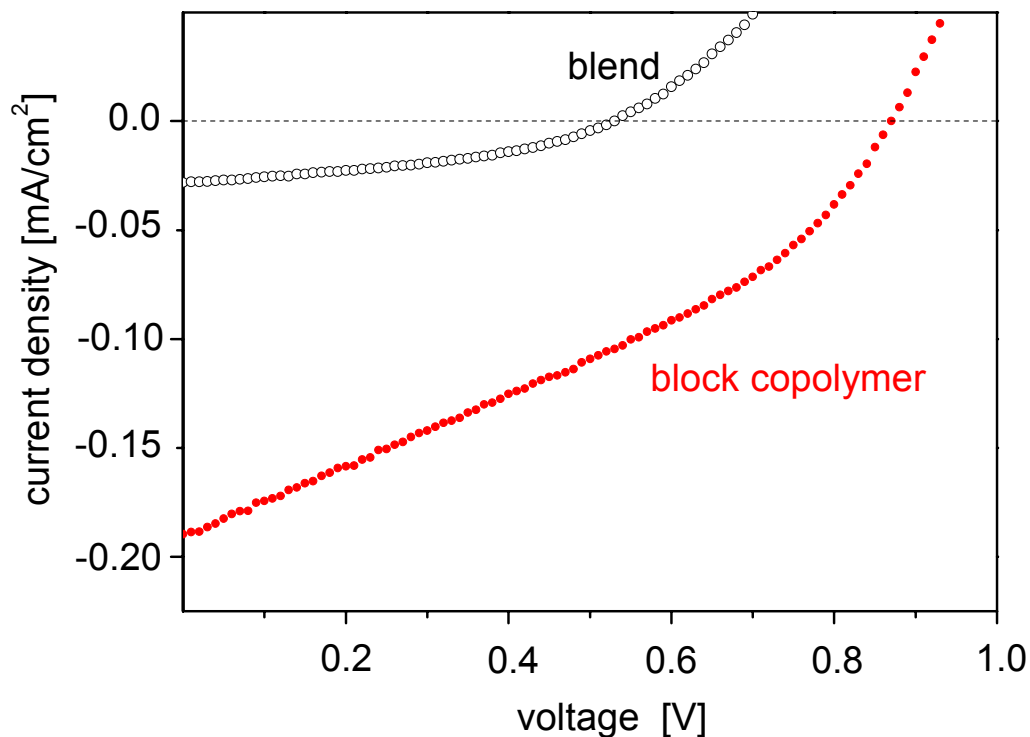


Figure 3-3: Current-voltage characteristics of photovoltaic devices using the blend of the homopolymers (○) or the block copolymer 24F (●) with the same weight ratios.

The efficiency of the block copolymer solar cells is one order of magnitude higher than that of the comparable blend device (figure 3-3). It could also be shown that the block copolymer in the solar cell is microphase separated, revealing domain sizes from 10 to 50 nm, whereas the blend on the other hand is macrophase separated. This is the first report of charge separation at a nanostructured bulk interface in a block copolymer consisting of an electron transport and

3. Summary

a hole transport material exhibiting microphase separation. These results are thus proof-of-principle for the nanostructured bulk heterojunction solar cells using block copolymers.

Furthermore, fluorescent acceptor labeled polymers were synthesized using a series of monomers in order to obtain a single dye unit attached to various polymer chains. These polymers were prepared by nitroxide mediated radical polymerization with an alkoxyamine initiator that is covalently bound to a perylene bisimide moiety. It could be shown with MALDI-TOF mass spectrometry that a single perylene bisimide unit is incorporated in each polymer chain. By using 4-vinyltriphenylamine monomers bifunctional polymers (**8**) containing electron donating moieties and a single electron acceptor unit were obtained. The polymerization of standard monomers such as styrene and acrylates, gave polymers (**9-12**) with only a single electron acceptor unit (figure 3-4).

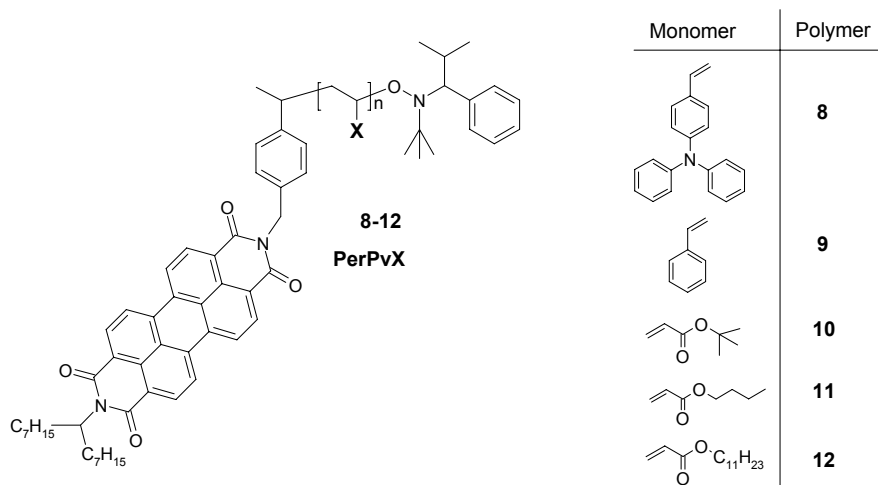


Figure 3-4: Chemical structures of the acceptor labeled polymers **8-12** having a single perylene bisimide moiety.

The polymerization is controlled for styrene, 4-vinyltriphenylamine as well as for different acrylates. The polymers **9-12** exhibited a strong fluorescence, whereas the fluorescence in polymer **8** with the triphenylamine moieties is completely quenched, most probably due to electron transfer. The optical properties and the aggregation behavior depend on the polymer chain length and the monomers used. Thus, the thermal and optical properties of the perylene bisimide labeled polymers can be tailored varying the monomers used.

3. Summary

Also novel electron acceptors consisting of perylene bisimide and fullerene moieties **15** and **17** (figure 3-5) were prepared and characterized.

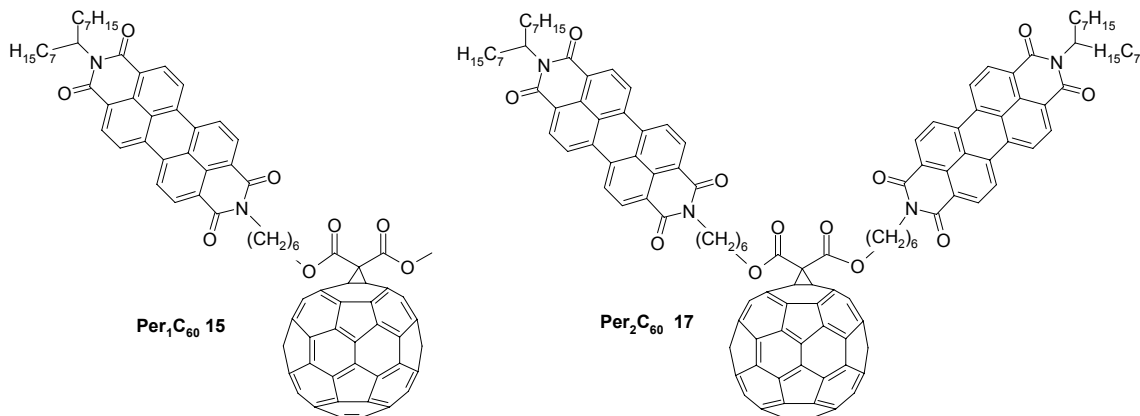


Figure 3-5: Chemical structures of the perylene bisimide – fullerene dyads $\text{Per}_1\text{C}_{60}$ (**15**) and $\text{Per}_2\text{C}_{60}$ (**17**).

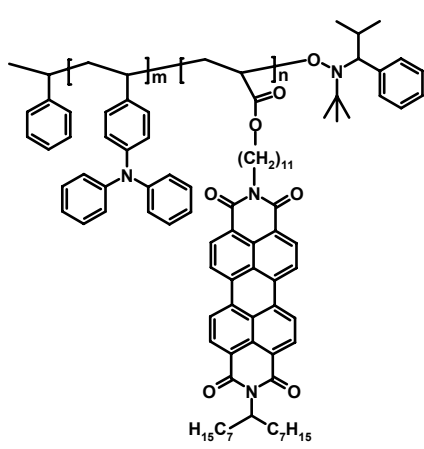
Although these dyads do not exhibit any ground state electronic coupling between the individual moieties, the emissive properties of the perylene bisimide units are strongly influenced by the covalently bound fullerene. The fluorescence of the perylene bisimide moiety is quenched by 99 % due to energy and electron transfer between the fullerene and the perylene bisimide. Beside the use as a model system these dyads are also capable of being used in organic solar cells. PCBM, the fullerene derivative which is usually used in polymer solar cells, is barely absorbing light and therefore perylene bisimide functionalized fullerenes may be an alternative as they strongly absorb light in the visible region.

4. Zusammenfassung

Ziel dieser Dissertation war die Synthese und Charakterisierung von neuen Materialen mit nanostrukturierten Grenzflächen für elektro-optische Untersuchungen. Dafür wurden verschiedene funktionalisierte Blockcopolymere, Akzeptor funktionalisierte Polymere und niedermolekulare Modellverbindungen synthetisiert, die aus Lochtransport-, Elektronentransport- und Farbstoffeinheiten bestehen. In diesem Kapitel werden das Konzept und die herausragenden Ergebnisse zusammengefasst.

Die Morphologie in organischen Solarzellen ist einer wichtigsten Faktoren für effiziente Solarzellen. Dies beruht auf der exzitonischen Ladungsträgererzeugung in organischen Materialien. Nach der Belichtung bildet sich ein Exziton (gebundenes Elektronen-Loch Paar), das, um in ein Elektron und ein Loch zu zerfallen, die Grenzfläche zwischen dem Elektronen- und dem Lochtransportmaterial erreichen muß. Da die Exzitonendiffusionslänge nur einige Nanometer beträgt, muß die Domänengröße in der gleichen Größenordnung sein. Dies konnte bisher mit farbstoffsensibilisierten, nanokristallinen TiO₂ Solarzellen und Mischungen aus leitfähigen Polymeren mit PCBM, einem Fullerenderivat, verwirklicht werden.

Mein Ansatz war die Verwendung von funktionalisierten Blockcopolymeren. Diese zeigen durch das Wechselspiel von Unlöslichkeit und kovalenter Verknüpfung der Blöcke eine Mikrophasenseparation mit Domänengrößen im Nanometerbereich. Ich verwendete die Nitroxid vermittelte kontrollierte radikalische Polymerisation (NMRP), um Blockcopolymere zu erhalten, die aus einem Elektronen- und einem Lochtransportmaterial bestehen (Abbildung 4-1).



Block-copolymer	Verwendeter Makro-initiator	M _n [g/mol]
24A	23A	9220
24B	23B	27850
24C	23C	26900
24D	23C	17610
24E	23C	24170
24F	23C	37710

Abbildung 3-1: Strukturformel des Blockcopolymers **24** das aus einem elektronenleitenden Perylenbisimidblock und einem lochleitenden Triphenylaminblock besteht und die verschiedenen, hergestellten Blockcopolymere.

Dabei wurde Triphenylamin als Lochtransportmaterial zusammen mit Perylenbisimid als Farbstoff und Elektronentransportmaterial verwendet. Zuerst mußte dafür ein lösliches Perylenbisimidmonomer hergestellt werden. Dies wurde durch eine unsymmetrische Synthese, ausgehend von Perylen-3,4:9,10-tetracarbonsäurebisanhidrid, erreicht. Ein sogenannter Schwalbenschwanzsubstituent wurde für eine gute Löslichkeit verwendet. Die andere Imidgruppe wurde mit einem Acrylat funktionalisiert, um das entsprechende Monomer zu erhalten.

Zuerst wurde 4-Vinyltriphenylamin polymerisiert, um die verschiedenen PvTPA Makroinitiatoren **23** herzustellen. Eine Reihe von Blockcopolymeren **24C-24F** wurde aus demselben PvTPA Makroinitiator **23C** hergestellt. Daher unterscheiden sich diese Blockcopolymere nur durch die Perylenbisimidblöcke. Außerdem wurde eine Reihe von Blockcopolymeren **24A-24C** aus verschiedenen PvTPA Makroinitiatoren **23A-23C** hergestellt. Diese Blockcopolymere haben ein ähnliches Verhältnis der Blöcke zueinander, aber verschiedene Molekulargewichte. Durch die kontrollierte Polymerisation mittels NMRP konnten diese Blockcopolymerarchitekturen mit geringen Polydispersitäten und kontrollierten Molekulargewichten hergestellt werden.

Die Blockcopolymere zeigen eine Mikrophasenseparation mit langen, drahtähnlichen Strukturen im Nanometerbereich bei einem hohen Perylenbisimidanteil. Diese Blockcopolymerstrukturen haben eine konstante Breite von etwa 13 nm. Dies war das erste Beispiel mikrophasenseparierter Blockcopolymere, die aus einem Elektronen- und Lochtransportblock bestehen.

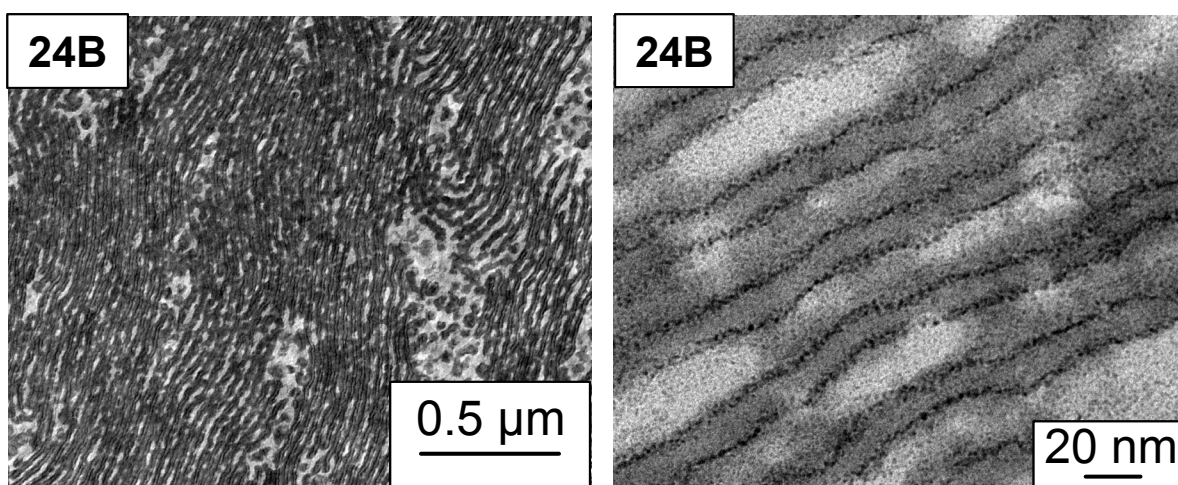


Abbildung 3-2: Beispiel für ein TEM des Blockcopolymers **24B** mit verschiedenen Vergrößerungen. Die Probe wurde mit RuO_4 bedampft.

Die optischen Eigenschaften der Blockcopolymere wurden mit denen der Mischung aus den beiden Homopolymeren im gleichen Gewichtsverhältnis verglichen. Es konnte gezeigt werden, daß die Fluoreszenz im Blockcopolymer schwächer als in der Mischung ist. Dies beruht auf den kleineren Domänengrößen des Blockcopolymers, da die Exzitonen an der Grenzfläche zerfallen und daher nicht zur Fluoreszenz beitragen.

Die elektrochemischen Eigenschaften der Blockcopolymere wurde mit Cyclovoltammetrie untersucht. Das LUMO des Perylenbisimidblocks liegt bei -3,65 eV und das HOMO des PvTPA blocks bei -5,23 eV. Daher ergibt sich theoretisch eine maximal Spannung V_{OC} von 1,58 V.

Um das Konzept der nanostrukturierten Blockcopolymersolarzellen zu beweisen, wurde das Blockcopolymer mit der Mischung der entsprechenden Homopolymeren im gleichen Gewichtsverhältnis, in Solarzellen verglichen.

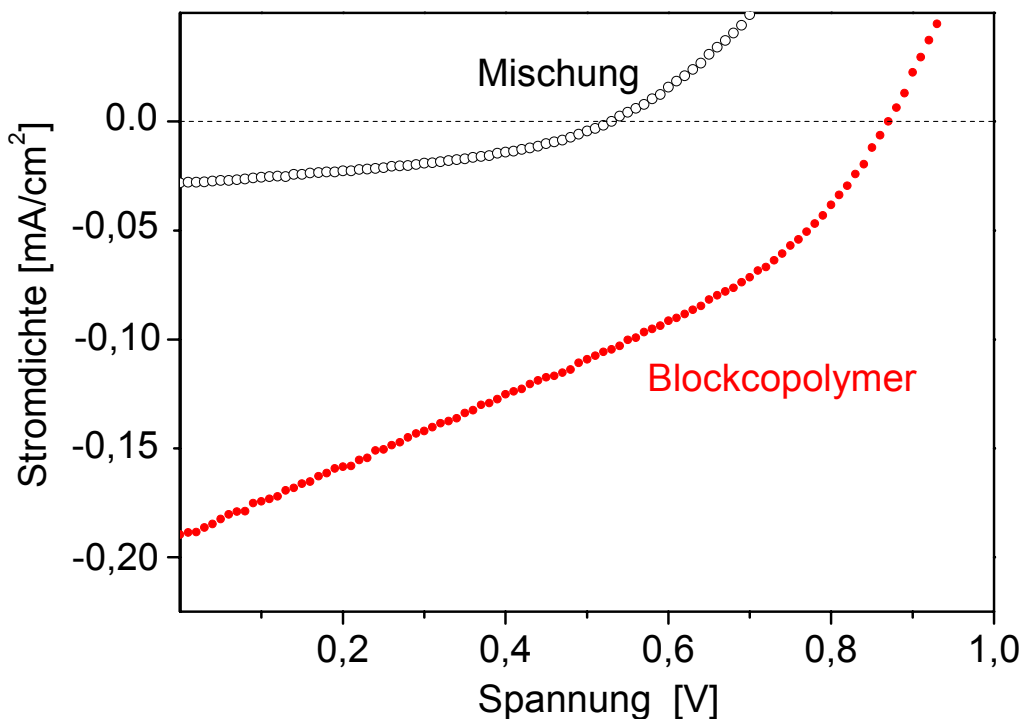


Abbildung 3-3: Strom-Spannungs-Kennlinien der Solarzellen, die aus der Mischung der Homopolymeren (○) oder dem Blockcopolymer 24F (●) im gleichen Verhältnis bestehen.

Der Wirkungsgrad der Blockcopolymersolarzelle ist um eine Größenordnung besser als die der entsprechenden Solarzellen, die aus einer Mischung der beiden Homopolymeren hergestellt wurde (Abbildung 3-3). Es konnte auch gezeigt werden, daß das Blockcopolymer mikrophasensepariert ist und Domänengrößen zwischen 10 und 50 nm aufweist. Die

Mischung ist im Gegensatz dazu makrophasensepariert. Dies war der erste Bericht von Ladungstrennung an nanostrukturierten Grenzflächen in Blockcopolymeren, die aus einem Elektronen- und Lochtransportblock bestehen und mikrophasensepariert sind. Diese Ergebnisse sind ein eindeutiger Beweis für die Wirksamkeit des Konzept der nanostrukturierten Blockcopolymersolarzellen.

Weiterhin wurden Polymere hergestellt, die genau einen fluoreszierenden Farbstoff in jeder Polymerkette enthalten. Es wurden mittels NMRP verschiedene Monomere polymerisiert, um die unterschiedlichen Polymere zu untersuchen und zu vergleichen. Mit MALDI-TOF Massenspektrometrie konnte gezeigt werden, daß genau eine Perylenbisimideinheit in jede Polymerkette eingebaut wurde. Wird 4-Vinyltriphenylamin als Monomer verwendet, entsteht ein bifunktionelles Polymer (**8**), das aus einer Elektronentransporteinheit und lochleitenden Wiederholungseinheiten besteht. Werden hingegen Styrol oder verschiedene Acrylate polymerisiert, entsteht ein Polymer (**9-12**), das nur eine Elektronentransporteinheit enthält (Abbildung 3-4).

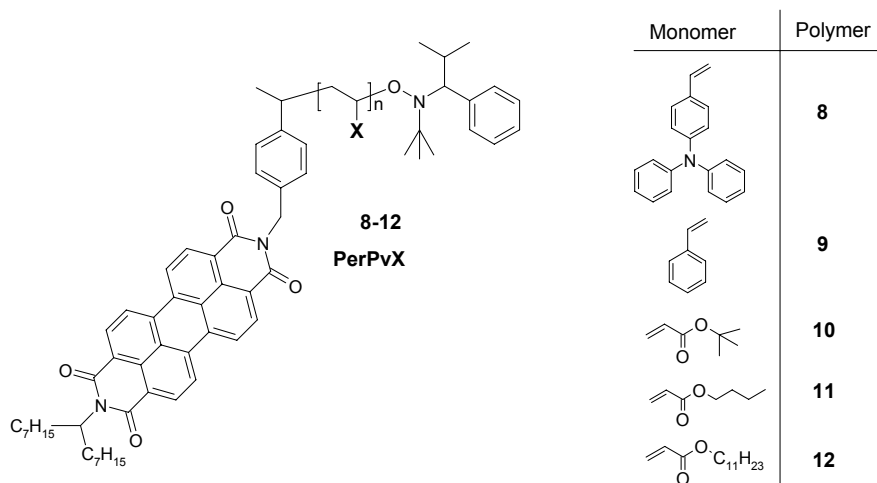


Abbildung 3-4: Strukturformel der Polymere **8-12**, die jeweils eine Perylenbisimideinheit in jeder Kette enthalten.

Die Polymerisation verläuft für Styrol, 4-Vinyltriphenylamin und verschiedene Acrylate kontrolliert. Die Polymere **9-12** fluoreszieren stark, wohingegen die Fluoreszenz der Polymere **8**, die die Triphenylamingruppen tragen, gelöscht wurde. Die optischen Eigenschaften und die Aggregation der Perylenbisimidgruppen wird von den verwendeten Monomeren und dem Molekulargewicht bestimmt. Daher können die thermischen und optischen Eigenschaften dieser Polymere gezielt beeinflußt werden.

Außerdem wurden die neuen Elektronentransportmaterialien **15** und **17**, die aus Perylenbisimid und Fullerenen bestehen (Abbildung 3-5), hergestellt und charakterisiert.

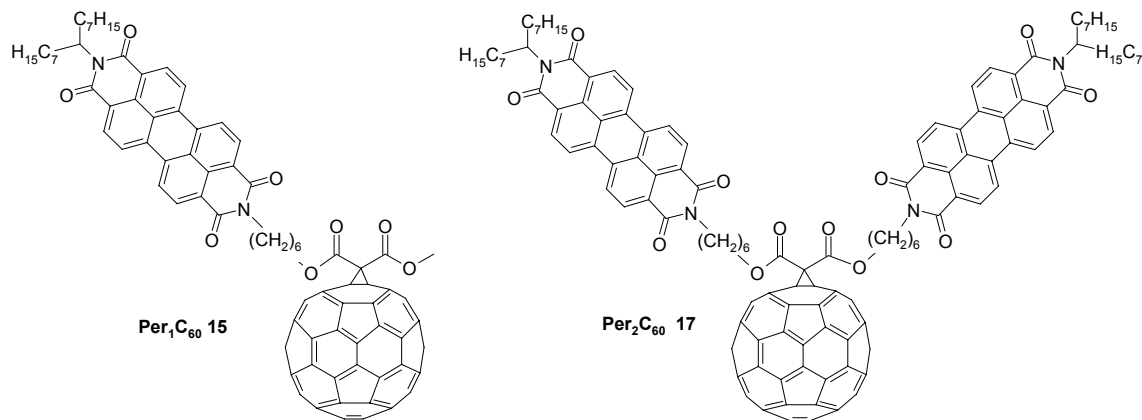


Abbildung 3-5: Strukturen der Perylenbisimid – Fulleren Dyaden Per₁C₆₀ (**15**) und Per₂C₆₀ (**17**).

Obwohl diese Dyaden keine elektronische Kopplung zwischen den einzelnen Einheiten im Grundzustand zeigen, wird die Fluoreszenz der Perylenbisimideinheit sehr deutlich verändert. Aufgrund von Energie- und Elektronenübertragung wird sie zu etwa 99% gelöscht. Neben der Verwendung als Modellsystem können diese Dyaden in Polymersolarzellen eingesetzt werden. PCBM, das Fullerenderivat, das üblicherweise eingesetzt wird, absorbiert kaum Licht im sichtbaren Bereich. Daher können diese perylenbisimidhaltigen Fullerene alternativ zu PCBM eingesetzt werden, um die Lichtabsorption in Solarzellen zu erhöhen.

Fluorescent Acceptor Dye Labeled Polymers carrying Hole Transport Pendant Groups

manuscript

*Stefan M. Lindner and Mukundan Thelakkat**

Makromolekulare Chemie I, Universität Bayreuth, Universitätsstrasse 30, 95440 Bayreuth, Germany

* Corresponding author: e-mail mukundan.thelakkat@uni-bayreuth.de

ABSTRACT

A perylene bisimide labeled alkoxyamine initiator suitable for the nitroxide mediated controlled radical polymerization of different monomers was synthesized. The synthesis, characterization and properties of a series of polymers obtained from monomers such as 4-vinyltriphenylamine, styrene and different acrylates using this initiator are described. The controlled nature of the polymerization was demonstrated by time-dependent measurements of the conversion and the molecular weight. The incorporation of the single fluorescent unit to the polymer chain end was verified by MALDI-TOF mass spectrometry. The perylene bisimide acts as an electron acceptor with a strong fluorescence. Since 4-vinyltriphenylamine is a donor monomer, the resulting polymers exhibit photoluminescence quenching due to electron transfer between the donor polymer chain and the acceptor moiety. The perylene bisimide moiety shows aggregation via π - π stacking which was studied using UV/vis and fluorescence spectroscopy. By controlling the polymer chain length, the stacking of the perylene bisimide can be controlled. The LUMO and HOMO levels of the perylene bisimide initiator and the dye labeled polymer were determined by cyclic voltammetry as -3.7 eV and -6.0 eV respectively. With this approach tailor-made fluorescent dye labeled polymers with desired architecture, low polydispersity and controlled molecular weight can be obtained as model systems for electron and energy transfer studies.

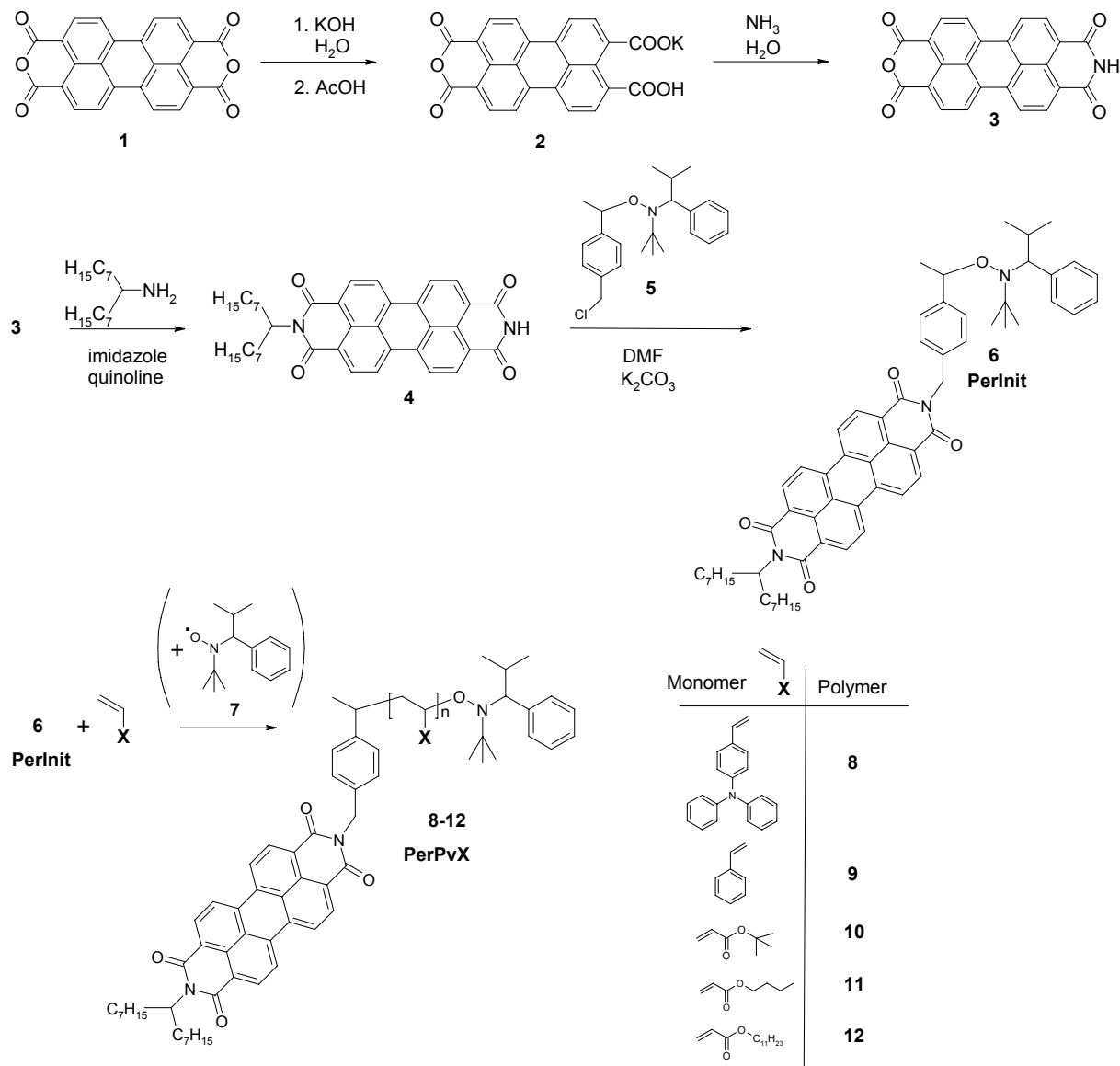
Introduction

The control of the molecular structure of the polymer chain is an important topic for all aspects of materials science. Especially for creating structures on a nanometer scale, well-defined polymer synthesis is essential. Factors like molecular weight, the polydispersity, the chain ends, and the architecture are important for the performance of the materials. To achieve these goals, living polymerization techniques are required. Living (controlled) radical polymerization has not only the advantage of the controlled character of the polymerization, but also the versatility and compatibility with a wide variety of functional groups. We used the nitroxide-mediated controlled radical polymerization (NMRP)¹ as it is metal free method, which is of advantage for preparing materials for opto-electronic applications.

In this paper we present an alkoxyamine initiator with a covalently attached perylene bisimide, which is an electron acceptor fluorescent dye to be used in NMRP. Perylene bisimides were used due to their outstanding thermal, chemical and photochemical stability. Besides the conventional use of perylene derivates as important dyes and pigments, they are used as optical switches², for single molecule spectroscopy³, in organic field-effect transistors⁴, in lasers⁵, in solar cells⁶ and as interesting markers/labels for the study of polymer diffusion⁷ and imaging⁸. These outstanding electro-optical properties are combined with the fact that they easily crystallize via π - π stacking to form supramolecular architectures⁹. As monomers we used triphenylamines which act as electron donors to get an electron donating polymer chain with one covalently attached electron acceptor. We also used monomers that are electronically inactive such as styrene or acrylates, to study and compare the different photophysical properties of the resulting polymers. Perylene dye labeled polymers containing such electronically inactive monomers for the purpose of single-molecule imaging have been reported in literature⁸. These polymers carrying fluorescent dye unit at the polymer chain end and hole transport pendant groups can be used as model systems to study energy or electron transfer which are fundamental processes in OLED and organic solar cells.

Results and Discussion

The initiator used here is a second-generation alkoxyamine initiator for NMRP that can not only polymerize styrene, but also acrylates and dienes. This initiator is covalently attached to a perylene bisimide as shown in scheme 1. The first step of the synthesis is the opening of one of the anhydride groups in the perylene-3,4:9,10-tetracarboxylic dianhydride **1** to form the mono potassium salt **2**^{10,11}.



Scheme 1. Synthesis of perylene bisimide labeled polymers **8-12** via nitroxide-mediated controlled radical polymerization.

With ammonia the ring is closed again to get a monoanhydride monoimide **3**. This imide group is stable against basic and acidic reactions. Due to this stability of the imide group only the anhydride group reacts in the next step with 8-aminopentadecane, which builds together a so called swallow-tail substituent. Swallow-tail substituted perylene bisimides are in contrast to most of the well-known perylene bisimides highly soluble in organic solvents¹². The initiator **6 (PerInit)** was prepared by coupling of a chloromethyl functionalized initiator **5**¹³ with the unsymmetrical perylene bisimide **4**.

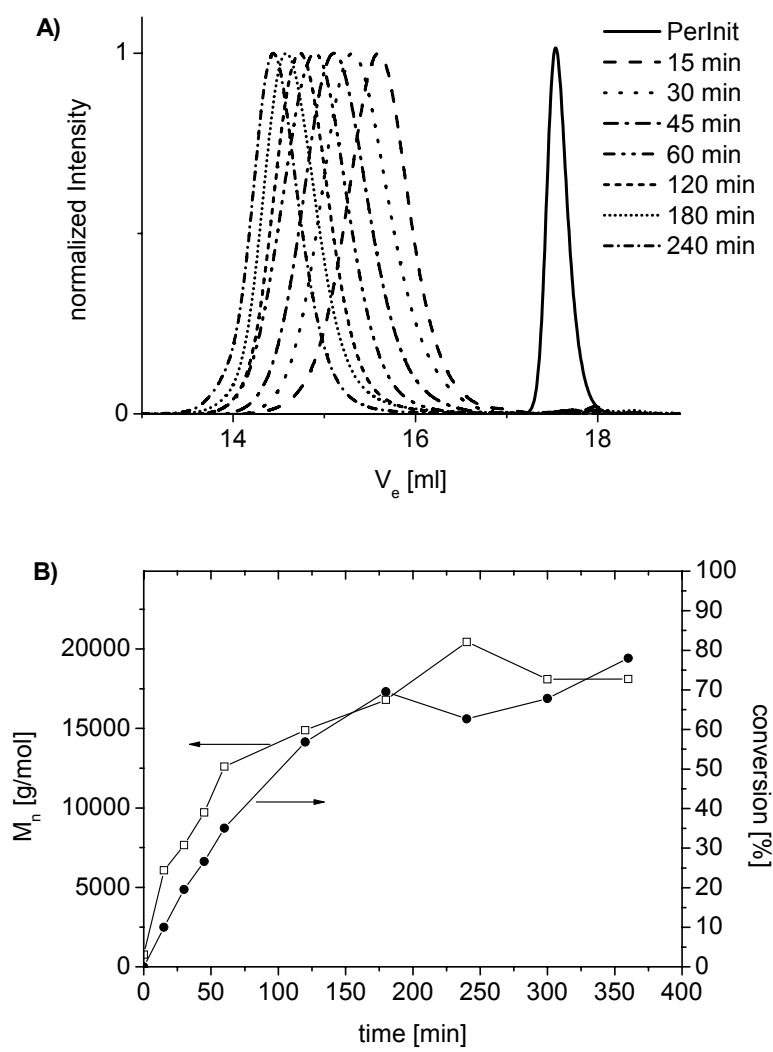


Figure 1. A) Evolution of GPC elution curves for the polymerization of styrene (molar ratio [M]: [I] = 250:1) with initiator **6** at 125 °C. B) Evolution of M_n (□) and conversion (●) for the same polymerization reaction as in Figure 1A.

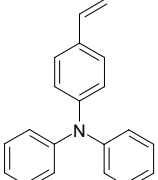
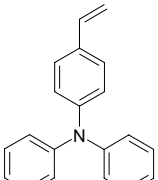
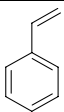
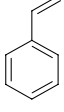
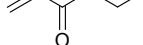
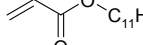
Polymer	monomer	mol% 7	reaction time	M _n [g/mol]	PDI	T _g [°C]	TGA _{-5%} [°C]
8a		0.05	30 min	3050	1.10	114	331
8b		0.05	60 min	7510	1.23	133	355
9a		---	1 h	9560	1.15	97	344
9b		---	4 h	17950	1.10	99	352
10		0.05	18 h	25740	1.30	46	241
11		0.05	18 h	21950	1.19	-48	309
12		0.05	18 h	8300	1.19	-*	336

Table 1. Polymerization conditions of different monomers, polymer data and thermal properties (from DSC and TGA) of the dye labeled polymers; polydispersity and M_n were determined by GPC with polystyrene standards using THF as solvent.*only the melting point at -17 °C could be detected.

With this initiator 4-vinyltriphenylamine as well as different acrylates and styrene monomers were polymerized (see table 1). The controlled character of the bulk polymerization of styrene was studied using gel permeation chromatography (GPC). Styrene was polymerized with **PerInit 6** (monomer: initiator = 250: 1 molar ratio) at 125 °C. At different time intervals samples were taken from the reaction mixture and the conversion, the molecular weight and the polydispersity were determined (see figure1). At the beginning the molecular weight of the polymer increases linearly with time. But after approximately one hour, the increase of the molecular weight became significantly lower and later the molecular weight remained nearly constant. This behavior can be explained as due to the lower concentration of the monomer and the higher viscosity towards the end of polymerization. The polydispersity in all samples was below 1.2.

Different batches of perylene bisimide labeled polystyrene were prepared by varying the reaction time. For example after 1h of polymerization we obtained a dye labeled polymer **9a** with number average molecular weight M_n of 9560 g/mol and polydispersity PDI of 1.15, whereas after 4h a polymer (**9b**) resulted with a M_n of 17950 g/mol and a PDI of 1.10.

It is of interest to analyze the end group fidelity of these polymers as the insertion of the initiator is a clear sign for controlled nature of the polymerization and it is important to get defined polymers with exact one electron acceptor in the polymer chain. The insertion of initiators into the polymer chain can be for example investigated by UV/vis spectroscopy for dyes¹⁴ or by potentiometric titration for amino terminated polymers¹⁵. We used MALDI-TOF mass spectrometry as it is a very straightforward method and shows the complete composition of the polymer. With this high resolution mass spectrometry, measured in the reflectron mode, one can see the isotopic peaks of each polymer chain up to a molecular weight of approximately 20000 g/mol. As can be seen in figure 2A the MALDI-TOF-MS spectrum for the polymer consists of discrete peaks only. The peak separation corresponds exactly to one repeating unit (here: styrene) and no other peaks can be seen. In figure 2B the magnified measured spectrum and the calculated spectrum of the polymer (25mer and 26mer) are shown. As the isotopic resolution fits very well with the calculated spectrum of the complete polymer including the initiator, it is obvious that both the perylene bisimide and the terminating fragment of the initiator are incorporated.

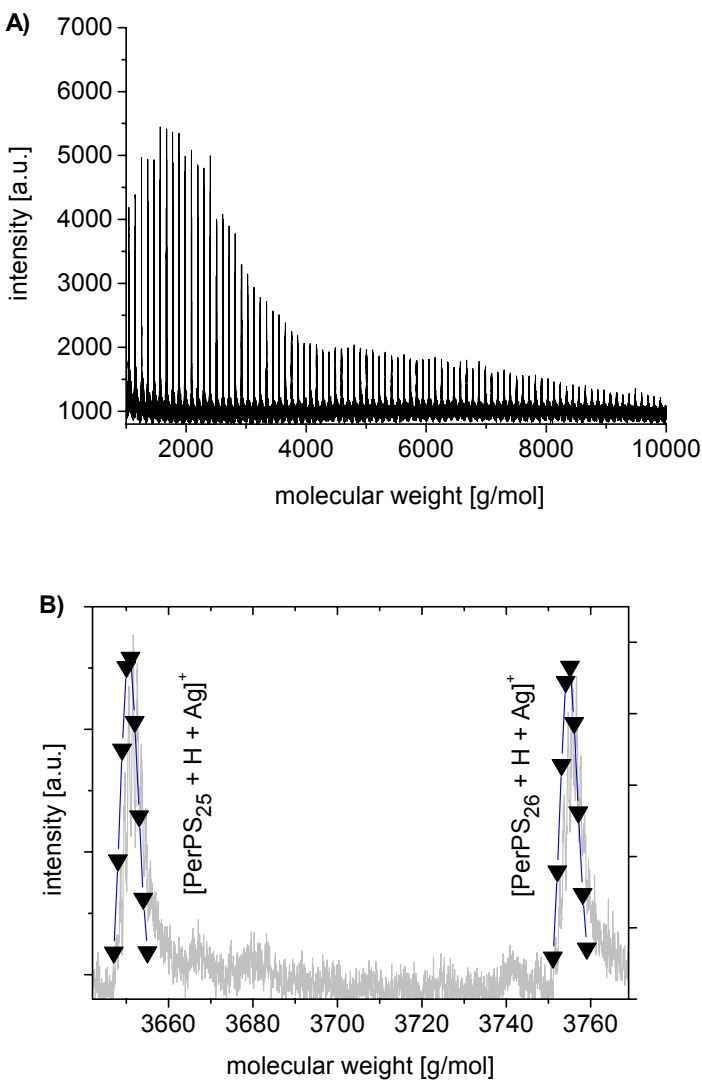


Figure 2. A) MALDI-TOF-mass spectra of a low molecular perylene bisimide labeled polystyrene sample measured in reflectron mode. B) Magnification of two measured peaks of the polymers, 25mer and the 26mer and the corresponding simulated spectra (\blacktriangledown) of $PerPS_{25}$ and $PerPS_{26}$. Recorded with DTCB as matrix and silver triflate.

Since with styrene the controlled insertion of the electron acceptor could be shown, the electron donating 4-vinyltriphenylamines were then used as monomers to get the polymers **8a** and **8b**. In the case of the polymerization of the 4-vinyltriphenylamines as well as later for the acrylates, 5 mol% of the free nitroxide **7** was added to get well-defined polymers¹³. The chain length of the polymers and thereby the ratio of electron acceptor to electron donor can be varied by varying the time of polymerization or by changing the ratio of initiator to monomer.

From $^1\text{H-NMR}$ spectroscopy the average number of the triphenylamine repeating units can be calculated as 14 for **8a** and 44 for **8b**. Also the thermal properties like the glass transition temperature T_g can be varied by controlling the polymer chain length. Here the T_g increases by 19°C from **8a** to **8b**.

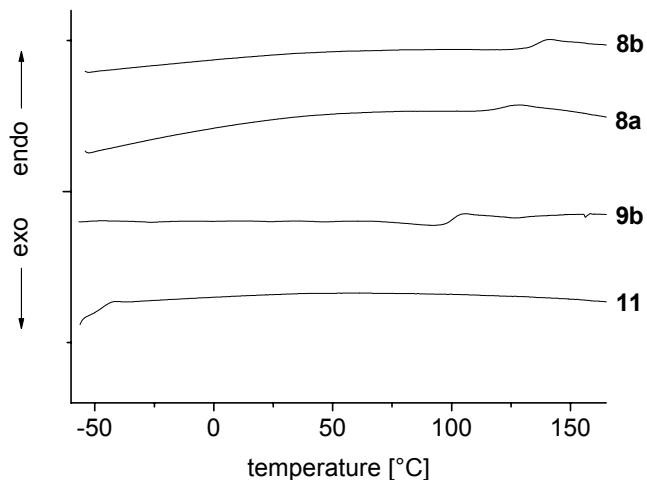


Figure 3. DSC curves of different dye labeled polymers **8a**, **8b**, **9b** and **11** (second heating curves at 10 K/min).

To compare the effects of the electron donating vinyltriphenylamine repeating units, a series of electronically non-active alkyl acrylates was also used as monomers to get polyacrylates carrying one single dye unit. The polarity and the thermal properties of the resulting polymers can be thus varied over a wide range (table 1). The DSC curves of different polymer chains with perylene bisimide as electron acceptor (for the second heating cycle at 10 K/min) are given in fig. 3. The T_g varies from -48 °C for the n-butyl acrylate polymer **11** to 133 °C for the 4-vinyltriphenylamine polymer **8b**. For the polymerization of *tert*-butyl acrylate and *n*-butyl acrylate reasonably high molecular weights of 25740 g/mol and 21950 g/mol were achieved after 18 hours of polymerization at 125 °C. But for the polymerization of *n*-undecyl acrylate with the same reaction conditions the obtained molecular weight was significantly lower. This can be explained as due to a dilution of the active acrylate group with the long alkyl chain. All the above results are summarized in table 1.

The UV-vis spectroscopy is an important method to determine the aggregation of perylene bisimide dyes. The incorporation of the dye in all the polymers can be clearly observed in

UV/vis spectra. As an example figure 4A shows UV/vis absorption spectra of **PerInit 6** and the polymer **8a** as measured in films. In **8a** both the absorptions due to triarylamine and perylene bisimide can be observed. In order to compare peak shifts of perylene bisimides, the absorption for the vibronic fine structure of the electronic S₀-S₁ transition which is in the range of 400 to 600 nm for **6**, **8a** and **8b** are depicted in figure 4B. The first vibronic transition is shifted from 544 nm in **6** to 529 nm for the polymer **8b** and the second vibronic transition from 498 nm in **6** to 493 nm in polymer **8b**. The corresponding peak shifts in **8a** are less pronounced.

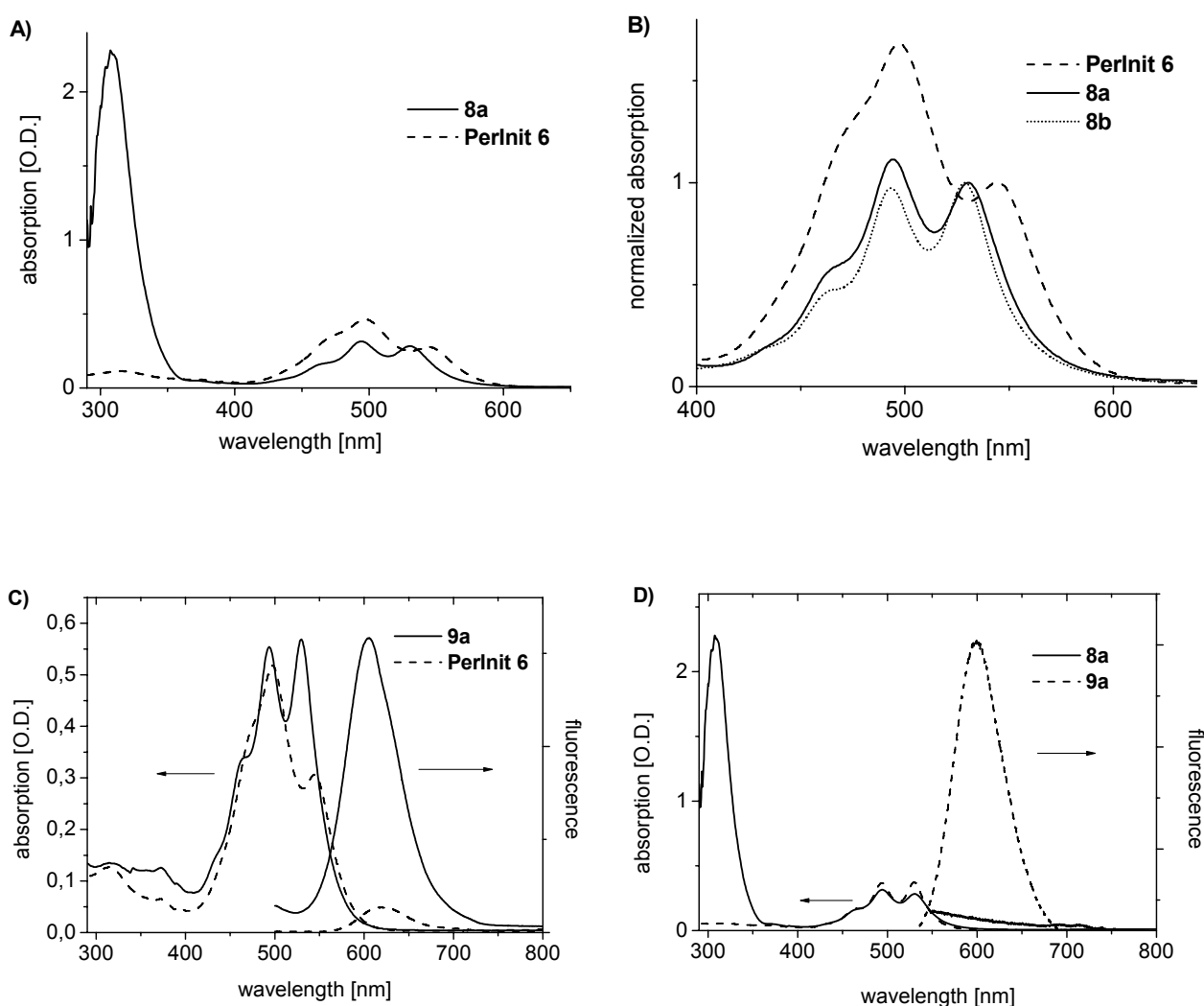


Figure 4. A) UV/vis absorption spectra of **PerInit 6** and the polymer **8a** in films. B) UV/vis spectra of **PerInit 6** and the polymers **8a** and **8b** in films. The UV/vis spectra are normalized. C) UV/vis and fluorescence spectra of **PerInit 6** and the polymer **9a**. D) UV/vis and fluorescence spectra of the **8a** and **9a**.

Also the fluorescence of the dye labeled polystyrene polymer is influenced by the stacking of the perylene bisimides. As an example in fig 4C, the UV/vis and fluorescence spectra of **6** and **9a** are compared. Unlike **8a** and **8b**, **9a** does not have the strong absorption at 300 nm due to the triphenylamine. The fluorescence peak is shifted from 605 nm for **9a** to 619 nm for the perylene labeled initiator **6** indicating strong aggregation in **6**. The same behavior is observed for the polymers **10-12**.

Another possibility to monitor the aggregation of perylene bisimide dyes is the change of the intensity of the transitions¹⁶. The quotient of the absorption at the second and first vibronic transition is introduced as a parameter for the degree of order. If one compares the absorption maxima for the first two vibronic transition, the quotient changes from 1.68 for the **PerInit 6** to 1.11 for **8a** and 0.97 for **8b**. Thus the stacking order of the dye moieties decrease from **PerInit 6** with a very high dye content to **8a** with 14 repeating units and to **8b** with 44 repeating units. Therefore the stacking properties of the perylene bisimide can be tailored by varying the length of the polymer chain. Similar aggregation behavior of the dye units is observed in the other dye labeled polymers **9-12**.

All the polymers except **8a** and **8b** exhibit strong fluorescence also in the solid state corresponding to the emission of the dye. This can be well understood if we take into consideration the fact that among these polymers, only poly(4-vinyltriphenylamine)s **8a** and **8b** are capable of exhibiting any energy or electron transfer processes with the acceptor dye unit. As an example, in figure 4D the UV/vis and fluorescence spectra of the dye labeled poly(4-vinyltriphenylamine) **8a** and polystyrene **9a** are compared. By excitation of the dye with a wavelength of 490 nm, where both films have the same optical density, the fluorescence was determined. For the polystyrene sample **9a** an intense red fluorescence can be seen, whereas for the poly(4-vinyltriphenylamine) **8a** the fluorescence is quenched completely. This quenching can be explained as due to electron transfer from the HOMO of the electron donor to fill the hole created in the electron acceptor due to excitation. This electron transfer is an important step for photovoltaic cells. Recently it could be shown that block copolymers with similar donor and acceptor units could be used as novel materials for organic photovoltaics¹⁷.

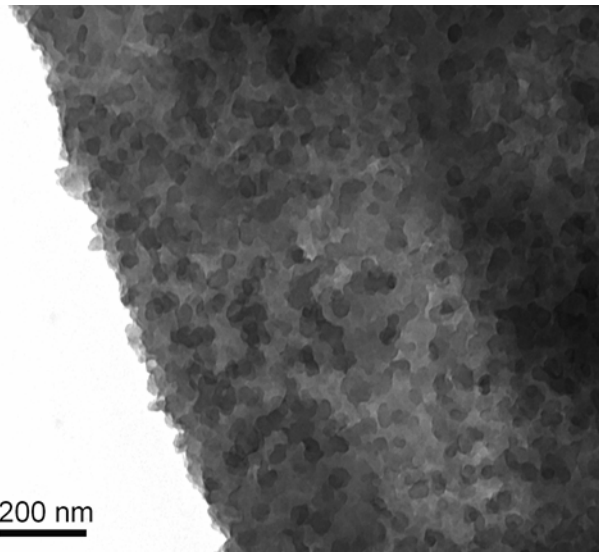


Figure 5. TEM of cross-section of **8b**. The sample was tempered for 1h at 150 °C and stained with RuO₄.

In order to elucidate the electronic energy levels which determine the energy and electron transfer processes, the electronic properties were studied. The perylene bisimide labeled initiator **6** and the perylene bisimide labeled polymer poly(*n*-undecyl acrylate) **12** as an example were studied by cyclic voltammetry. The measurement was conducted on a glassy carbon electrode coupled with a Ag/AgNO₃ reference electrode in a three-electrode assembly system. CH₂Cl₂ containing 0.1 M tetrabutylammonium hexafluorophosphate was used as a solvent. It could be seen that the perylene bisimide exhibits two reversible reduction peaks and one oxidation peak (figure 6). From the data for **6** the LUMO (Lowest Unoccupied Molecular Orbital) value could be calculated as -3.74 eV and the HOMO (Highest Occupied Molecular Orbital) as -6.01 eV with respect to the zero energy level. For the perylene bisimide labeled acrylate polymer **12** the LUMO could be determined as -3.75 eV the HOMO as -6.02 eV, showing that the electrochemical properties are preserved in the polymer. The HOMO of poly(4-vinyltriphenylamine)s is at about -5.2 eV¹⁸. This allows an electron transfer between the excited state of dye and the ground state of the poly(4-vinyltriphenylamine) resulting in quenching of the dye emission as observed in polymers **8a** and **8b**. To further investigate the bulk structure and morphology of these films, TEM measurements from annealed films were carried out. It seems that these films show microphase separation. As an example, the TEM cross section of **8b** after tempering for 1h at 150 °C and staining with RuO₄ is shown in figure 5. The precise morphology of these polymers is not clear. There

could be no crystallinity detected with polarized optical microscopy and DSC (fig. 3) probably due to the small amount of dye content in these polymers.

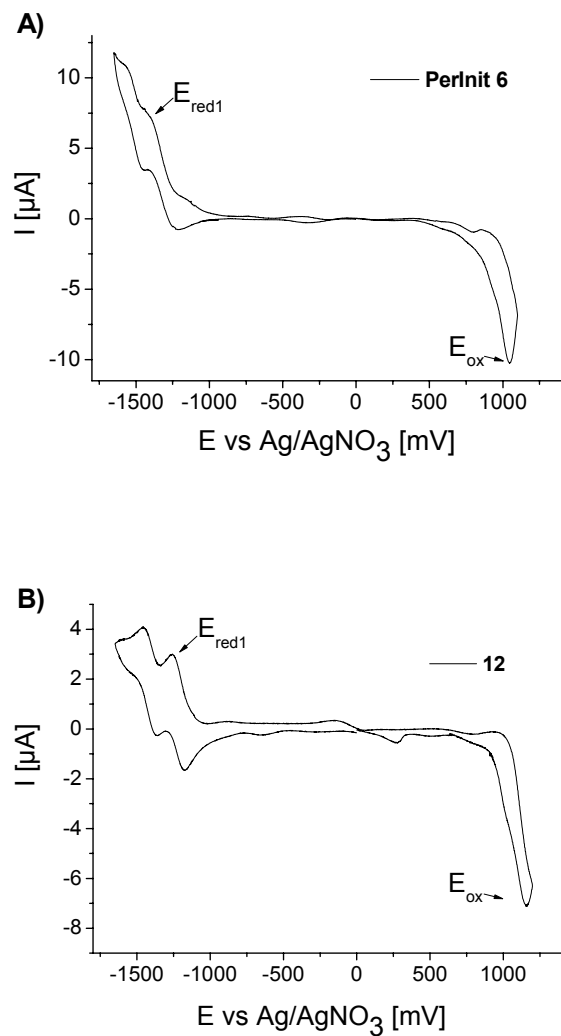


Figure 6. Cyclic voltammogram of A) **PerInit 6** and B) the dye labeled polymer **12** in CH_2Cl_2 containing 0.1 M tetrabutylammonium hexafluorophosphate as a salt.

Conclusion

A new perylene bisimide labeled alkoxyamine initiator for the nitroxide-mediated controlled radical polymerization was utilized to synthesize different polymers. The resulting dye labeled polymers were obtained with well-defined molecular weights and narrow polydispersities. Using hole transport monomers the electron transfer in this system could be studied whereas with electronically non-active monomers such as styrene and acrylates an intense red fluorescence due to perylene bisimide could be seen. Therefore these strong fluorescent polymers can be used for single-molecule investigations like imaging, spectroscopy or diffusion experiments¹⁹. Furthermore, these polymers show an interesting aggregation behavior. The aggregation of these polymers via π - π stacking can be tailored via tuning the length of the polymer chain and the bulk of the polymer seems to be nanostructured. As perylene bisimides can be monitored using absorption and emission spectroscopy, the insertion of functional monomers such as 4-vinyltriphenylamine open up new concepts for model donor – acceptor systems for ensemble and single molecule studies. Moreover, the flexibility of this synthetic strategy allows to tailor the opto-electronic properties of the acceptor labeled polymers by using other hole transport monomers or non-active monomers.

Experimental Section

Materials. All solvents were distilled prior to use. Styrene and the acrylates were distilled over CaH₂ under vacuum. The chloromethyl substituted initiator **5** and the free nitroxide **7** were prepared according to literature procedure¹³, the 4-vinyltriphenylamine according to literature²⁰ and **3** according to literature¹⁰.

Instrumentation. ¹H NMR and ¹³C NMR spectra were acquired on a Bruker AC 250 spectrometer (250 MHz). The conversion was determined by using ¹H NMR. Gel permeation chromatography (GPC) was performed with two Polymer Labs Mixed-C columns, a Waters 410 differential refractometer (used for the determination of M_n and PDI) and a Waters 486 UV absorbance detector employing THF as the mobile phase with a flow rate of 0.5 ml/min. Polystyrene standards were used for calibration. UV/vis spectra were recorded using a Hitachi U-3000 spectrometer and fluorescence spectra were recorded using a Shimadzu RF-5301 PC Spectrofluorophotometer. IR spectroscopy was carried out in thin films on silicon wafers with a BioRad Digilab FTS-40 (FTIR). The thermal degradation of polymers was studied using a Mettler Toledo TGA/SDTA 851^e with a heating rate of 10 K/min under N₂ atmosphere and the differential scanning calorimetry was carried out with a Perkin Elmer Diamond DSC with a heating rate of 10 K/min under N₂ atmosphere. MALDI-TOF mass spectrometry was performed on a Bruker Daltonics Reflex 3 with an N₂ laser (337 nm) with a 20 kV acceleration voltage. The spectra were measured in reflectron mode with the matrix 2-[(2E)-3-[4-(tert-butyl)phenyl]-2-methylprop-2-enylidine]malononitrile (DTCB) and silver triflate as additive. For the cyclic voltammetry experiments a three-electrode assembly with a Ag/AgNO₃ electrode was used. CH₂Cl₂ containing 0.1 M tetrabutylammonium hexafluorophosphate was used as a solvent and each measurement was calibrated with ferrocene as internal standard.

Synthesis. N-(1-Heptyloctyl)-perylene-3,4:9,10-tetracarboxylic bisimide (**4**)

Perylene-3,4:9,10-tetracarboxylic monoanhydride monoimide (**3**) (3.13 g, 8 mmol), 8-aminopentadecane (2.91 g, 12.8 mg), imidazole (30 g) and quinoline (5 ml) were stirred under argon (160 °C, 2h). After cooling down, the mixture was dissolved in THF and precipitated in 400 ml of a mixture of ethanol and 2N HCl (1:1). The precipitate was collected by vacuum filtration, treated with boiling aqueous K₂CO₃ solution (100 ml, 10%, 1h), washed with

distilled water and dried under vacuum. The dye was purified by extractive recrystallization²¹. Traces of N,N'-di(1-heptyloctyl)-perylene-3,4:9,10-tetracarboxylic bisimide were removed by extraction with hexane to yield a red solid (3.64 g, 77%). ¹H NMR (CDCl₃, 250 MHz) δ: 8.56 (m, 8H), 5.16 (m, 1H), 2.21 (m, 2H), 1.87 (m, 2H), 1.28 (m, 16H), 0.81 (m, 6H) ppm. IR (Si, v, cm⁻¹): 3067w, 2958m, 2927m, 2855m, 1698s, 1659s, 1594s, 1432m, 1403m, 1343s, 1269m, 1179w, 810w, 741w, 655m. MS (EI) m/z: 600 [M⁺-1].

PerInit (6)

N-(1-Heptyloctyl)-perylene-3,4:9,10-tetracarboxylic bisimide (**4**) (1.40 g, 3.75 mmol), 2,2,5-trimethyl-3-(1-(4'-chloromethyl)phenylethoxy)-4-phenyl-3-azahexane (**5**) (1.80 g, 3 mmol), K₂CO₃ (0.75 g, 5.4 mmol) and some crystals of NaI were stirred in 30 ml DMF at 40 °C over night. The reaction mixture was poured into a mixture of 300 ml of methanol and 100 ml water. The precipitate was collected by vacuum filtration, dried and purified by column chromatography (silica gel, hexane/THF = 5/1) to yield **6** (2.31 g, 82%). ¹H NMR (CDCl₃, 250 MHz) δ: 8.6-8.0 (m, 8H+8H, both diastereomeres), 7.6-7.0 (m, 9H+9H, both diastereomeres), 5.27 (m, 2H+2H, both diastereomeres), 5.12 (m, 1H+1H, both diastereomeres), 4.81 (m, 1H+1H, both diastereomeres), 3.30 (d, 1H, minor diastereomer), 3.19 (d, 1H, major diastereomer), 2.21 (m, 5H), 1.85 (m, 5H), 1.49 (d, 3H, minor diastereomer), 1.41 (d, 3H, major diastereomer), 1.35-1.0 (m, 40H), 0.88 (s, 9H, major diastereomer), 0.8-0.5 (m, 18H), 0.67 (d, 9H, minor diastereomer), 0.43 (d, 3H, major diastereomer), 0.08 (d, 3H, major diastereomer) ppm. ¹³C NMR (CDCl₃, 62.5 MHz) δ: 162.93, 145.25, 144.42, 142.16, 134.23, 133.81, 131.07, 130.92, 130.82, 129.27, 129.15, 129.04, 128.93, 127.82, 127.12, 127.03, 126.27, 126.18, 126.06, 125.90, 122.81, 122.57, 82.14, 72.11, 60.46, 60.40, 54.85, 32.36, 31.79, 31.65, 29.52, 29.20, 28.34, 28.19, 27.02, 24.74, 23.04, 22.58, 22.11, 21.85, 21.04, 14.04 ppm. IR (Si, v, cm⁻¹): 2958m, 2927m, 2859m, 1699s, 1660s, 1596s, 1435m, 1405m, 1356w, 1337m, 1254w, 1214w, 1171w, 1059w, 853m, 810s, 743s.

Procedure for the Polymerization of 4-Vinyltriphenylamine **8a**, **8b**

A mixture of the **PerInit 6** (46.9 mg, 0.05 mmol), the nitroxide **7** (2.5 μmol as a stock solution from o-dichlorobenzene) and 4-vinyltriphenylamine (678 mg, 2.5 mmol) in 100μl o-dichlorobenzene was degassed by three freeze/pump/thaw cycles, sealed under argon, and heated at 125 °C for 30 min and 60 min for **8a** and **8b** respectively. The solidified mixture

was dissolved in THF and precipitated twice in hexane. The polymers were collected by vacuum filtration and dried (**8a**: 89 mg, yield 12%; **8b** 465 mg, yield 64%).

8a: ^1H NMR (CDCl_3 , 250 MHz) δ : 8.62 (m, 0.68H), 6.90 (m, 15.45H), 6.58 (m, 2.00H), 5.28 (m, 0.25), 1.99 (m, 1.81H), 1.60 (m, 2.19H), 1.19 (m, 1.99H), 0.80 (m, 0.83H). **8b:** ^1H NMR (CDCl_3 , 250 MHz) δ : 8.63 (m, 0.18H), 6.87 (m, 12.64H), 6.54 (m, 2.00H), 5.28 (m, 0.09), 1.98 (m, 1.23H), 1.60 (m, 1.82H), 1.19 (m, 0.71H), 0.80 (m, 0.29H) ppm. IR (Si, v, cm^{-1}): 3058, 3027, 2926, 2857, 1698, 1659, 1593, 1508, 1493, 1451, 1314, 1278, 1177, 1073, 1030.

Procedure for Styrene Polymerization **9a**, **9b**

A mixture of the **PerInit 6** (46.9 mg, 0.05 mmol) and styrene (1302 mg, 12.5 mmol) was degassed by three freeze/pump/thaw cycles, sealed under argon, and heated at 125 °C. (1h for **9a** and 4h for **9b**). The solidified mixture was dissolved in CHCl_3 and precipitated three times in isopropanol. The polymers **9a** and **9b** were collected by vacuum filtration and dried (**9a**: 351 mg, yield 26%; **9b**: 1.03 g, yield 76%).

9a: ^1H NMR (CDCl_3 , 250 MHz) δ : 8.61 (m, 0.10H), 7.03 (m, 3.10H), 6.56 (m, 2.00H), 1.83 (m, 1.04H), 1.41 (m, 2.33H), 0.81 (m, 0.15H). **9b:** ^1H NMR (CDCl_3 , 250 MHz) δ : 8.62 (m, 0.05H), 7.06 (m, 3.03H), 6.57 (m, 2.00H), 1.83 (m, 1.00H), 1.42 (m, 2.14H), 0.81 (m, 0.08H) ppm. IR (Si, v, cm^{-1}): 3028, 2927, 2855, 1698, 1659, 1597, 1494, 1449, 1154, 1026, 764.

Procedure for the Polymerization of Acrylates **10**, **11**,**12**

A mixture of the **PerInit 6** (46.9 mg, 0.05 mmol), the nitroxide **7** (2.5 μmol as a stock solution from the corresponding acrylate), the acrylate (t-butyl acrylate: 1602 mg, 12.5 mmol; n-butylacrylate: 1602 mg, 12.5 mmol and undecylacrylate: 2830 mg, 12.5 mmol) were degassed by three freeze/pump/thaw cycles, sealed under argon, and heated at 125 °C for 18h. The viscous mixture was dissolved in THF and precipitated in methanol. The polymers **10**, **11** and **12** were collected and dried (**10**: 1.02 g, yield 62%, **11**: 633 mg, yield 38% and **12**: 945 mg, yield 39%).

10: ^1H NMR (CDCl_3 , 250 MHz) δ : 8.64 (m, 0.05H), 2.20 (m, 1.00H), 1.79 (m, 0.44H), 1.45 (m, 9.96H) ppm. IR (Si, v, cm^{-1}): 2978, 2933, 1731, 1659, 1594, 1481, 1459, 1447, 1394, 1369, 1259, 1152, 847.

11: ^1H NMR (CDCl_3 , 250 MHz) δ : 8.62 (m, 0.06H), 4.01 (m, 2.00H), 2.25 (m, 1.01H), 1.87 (m, 0.51H), 1.58 (m, 3.23H), 1.36 (m, 2.60H), 0.91 (m, 3.18H) ppm. IR (Si, v, cm^{-1}): 2960, 2875, 1737, 1696, 1659, 1594, 1457, 1403, 1262, 1174, 1121.

12: ^1H NMR (CDCl_3 , 250 MHz) δ : 8.62 (m, 0.20H), 7.45 (m, 0.09H), 7.05 (m, 0.11H), 5.34 (m, 0.06H), 3.98 (m, 2.00H), 2.25 (m, 1.05H), 1.86 (m, 0.59H), 1.57 (m, 3.33H), 1.24 (m, 17.17H), 0.86 (m, 3.60H) ppm. IR (Si, v, cm^{-1}): 2928, 2857, 1738, 1702, 1696, 1653, 1596, 1470, 1170.

Acknowledgement. The financial support for this research work from the German Research Council (DFG/SFB 481) is kindly acknowledged. We also thank Astrid Göpfert, University of Bayreuth, for the TEM measurement and Markus Bäte, University of Bayreuth, for the MALDI-TOF MS analysis.

¹ Hawker, C. J.; Bosman, A. W.; Harth, E. *Chem. Rev.* **2001**, *101*, 3661-3688.

² O'Neil, M. P.; Niemczyk, M. P.; Svec, W. A.; Gosztola, D.; Gaines III, G. L.; Wasielewski, M. R. *Science* **1992**, *257*, 63-65.

³ Lang, E; Würthner, F; Köhler, J. *ChemPhysChem* **2005**, *6*, 935-941.

⁴ Malenfant, P. R. L.; Dimitrakopoulos, C. D.; Gelorme, J. D.; Kosbar, L.L.; Graham, T. O.; Curioni, A.; Andreoni, W. *Appl. Phys. Lett.* **2002**, *80*, 2517-2519.

⁵ Gvishi, R.; Reisfeld, R.; Burshtein, Z. *Chem. Phys. Lett.* **1993**, *213*, 338-344.

⁶ For example Tang, C. W. *Appl. Phys. Lett.* **1986**, *48*, 183-185; Gregg, B. A. *J. Phys. Chem. B* **2003**, *107*, 4688-4698.

⁷ Hejtmanek, V.; Schneider, P. *J. Chem. Eng. Data* **1993**, *38*, 407-409.

⁸ Bowden, N. B.; Willets, K. A.; Moerner, W. E.; Waymouth, R. M. *Macromolecules* **2002**, *35*, 8122-8125.

⁹ Wüthner, F. *Chem. Comm.* **2004**, *14*, 1564-1579.

¹⁰ Kaiser, H.; Lindner, J.; Langhals, H. *Chem. Ber.* **1991**, *124*, 529-535.

¹¹ Langhals, H.; Saulich, S. *Chem. Eur. J.* **2002**, *8*, 5630-5643.

¹² Langhals, H.; Demmig, S.; Potrawa, T. *Journal f. prakt. Chemie* **1991**, *333*, 733-748.

¹³ Benoit, D.; Chaplinski, V.; Braslau, R. Hawker, C. J. *J. Am. Chem. Soc.* **1999**, *121*, 3904-3920.

¹⁴ Rodlert, M.; Harth, E.; Rees, I.; Hawker, C. J. *J Polym Sci Part A: Polym Chem* **2000**, *38*, 4749-4763.

¹⁵ Hawker, C. J.; Hedrick, J. L. *Macromolecules* **1995**, *28*, 2993-2995.

¹⁶ Gregg, B. A. *J. Phys. Chem.* **1996**, *100*, 852-859.

¹⁷ Lindner, S. M.; Hüttner, S.; Chiche, A.; Thelakkat, M.; Krausch, G. *Angew. Chem., Int. Ed.* in print.

¹⁸ Lindner, S. M.; Kaufmann, N.; Thelakkat, M., *Organic Electronics* submitted.

¹⁹ Zettl, H.; Häfner, W.; Böker, A.; Schmalz, H.; Lanzendörfer, M.; Müller, A. H. E.; Krausch, G., *Macromolecules* **2004**, *37*, 1917-1920.

²⁰ Lindner, S. M.; Thelakkat, M. *Macromolecules* **2004**, *37*, 8832-8835.

²¹ Langhals, H. *Chem. Ber.* **1985**, *118*, 4641-4645.

Synthesis, Photophysical and Electrochemical Characterization of Novel Soluble Perylene Bisimide - Fullerene Dyads

manuscript

Stefan M. Lindner,^a Michaela Ruppert,^b Andreas Hirsch^b and Mukundan Thelakkat*^a

^a Makromolekulare Chemie I, Universität Bayreuth, Universitätsstrasse 30, 95440 Bayreuth, Germany *corresponding author. e-mail address: mukundan.thelakkat@uni-bayreuth.de

^b Organische Chemie II, Friedrich-Alexander-Universität Erlangen-Nürnberg, Henkestrasse 42, 91054 Erlangen, Germany

ABSTRACT

Two novel fullerene dyads containing one ($\text{Per}_1\text{C}_{60}$) and two ($\text{Per}_2\text{C}_{60}$) perylene bisimide units were prepared by coupling C_{60} with the corresponding malonate derivatives. The presence of swallow-tail substituents and a flexible hexyl spacer at the perylene bisimide moiety allows the synthesis of soluble dyads without the need of bay substituents at the perylene core. The electrochemical and photophysical properties were determined with cyclic voltammetry, UV/vis absorption and fluorescence spectroscopy and compared to those of PCBM ([6,6]phenyl- C_{61} -butyric acid methyl ester) and N,N'-di(1-heptyloctyl)perylene-3,4:9,10-tetracarboxylic bisimide. The dyads reveal no strong electronic interaction in the ground-state between the fullerene and the perylene bisimide units. The absorption spectra of the dyads are simply an overlay of the absorptions of the individual moieties. Thus the absorption of fullerene is extended to the visible range of up to 600 nm in the dyads. Moreover, the dyads exhibit high extinction coefficients similar to perylene bisimides. But the fluorescence is strongly quenched in the dyads due to energy and electron transfer in these systems. In contrast, a mixture of PCBM and perylene bisimide exhibits no photoluminescence quenching in solution. These fullerene dyads containing dye moieties are very interesting for the application in organic solar cells.

Introduction

The development of highly efficient organic solar cells¹ with efficiencies of up to 5.1 % has attracted great attention. Since the discovery of photoinduced electron transfer from a conjugated polymer to fullerene², the performance of solar cells could be gradually improved. The bulk heterojunction concept was realized by blending a π -conjugated polymer with the fullerene derivative PCBM ([6,6]phenyl-C₆₁-butyric acid methyl ester)³. Most of the early work is based on soluble poly(*para*-phenylenevinylene) (PPV) derivates as electron donor and PCBM as electron acceptor. The performance of the photovoltaic devices is dependant on the ratio between PCBM and PPV which determines the morphology of the blend films. The power conversion efficiency is optimum for high amounts of PCBM (80%) although it is barely absorbing in the visible range of the solar spectrum. But for an appropriate morphology⁴ which is fundamental for efficient devices, these high amounts of PCBM are necessary⁵. The devices consisting of 80 % PCBM have to be rather thick to get sufficient absorption which requires very high charge carrier mobilities for efficient charge collection. Polymeric materials were functionalized with fullerenes in order to get a defined morphology. The so-called double-cable polymers⁶ consist of a polythiophene backbone with covalently grafted fullerenes or block copolymers with a PPV block and a fullerene functionalized block⁷. At present, the most efficient polymer solar cells¹ consist of poly(3-hexylthiophene) (P3HT) blended with PCBM. The ratio of P3HT to PCBM could be reduced to 1 to 0.8 which is advantageous for a good absorption in thin films. But the optical density of the most efficient photovoltaic devices is still low. This is a limitation for the performance as even for the peak maximum absorption of the P3HT a notable amount of the sun light is not absorbed and therefore not available for the photovoltaic process.

One possibility to increase the absorption in the photovoltaic device is to use strongly absorbing fullerene derivatives by attaching an electron transporting dye onto it. As reported, most of these dyads⁸ are fullerenes in combination with a low molecular weight electron donor like porphyrins⁹ or Ru-complexes¹⁰. We synthesized a fullerene dyad with perylene bisimide as second electron acceptor moiety. Perylene bisimides are known for their chemical, photochemical and thermal stability as well as for good electron mobilities¹¹, the formation of supramolecular assemblies¹² and their strong light absorption. This combination is very interesting for the application in organic solar cells, since these dyads can be used as electron transport moieties in combination with hole transport materials. In order to enable the aggregation of the perylene bisimides, we used a flexible hexyl spacer in contrast to rigid

5. Appendix A2

bound fullerene - perylene bisimide dyads, that are also reported in literature¹³. A possibility to get soluble perylene bisimides is to use derivatives which are substituted at the 1,6,7,12 position (bay-position) of the perylene core. But the LUMO values of bay substituted perylene bisimides and fullerenes do not match very well^{14,15}. Thus, dyads containing both moieties can act as traps for electrons. So it is necessary to tune the structure of dyads in such a way, that the first reduction peaks overlay very well. Here, we describe the synthesis and the electrochemical and photophysical properties of tailored fullerene-perylene bisimide dyads in which the perylene units do not carry any substituents at bay-positions. For the solubility, we used swallow-tail substituted perylene bisimides¹⁶. Moreover, these perylene bisimides exhibit strong face-to-face π - π stacking and the stacking distance is very small¹⁷ which can favor an enhanced electron transport.

Experimental

UV/vis spectra were recorded using a Hitachi U-3000 spectrometer and fluorescence spectra were recorded using a Shimadzu RF-5301 PC Spectrofluorophotometer (concentration: 10^{-6} mol/L). IR spectroscopy was carried out in thin films on silicon wafers with a BioRad Digilab FTS-40 (FTIR). ^1H NMR and ^{13}C NMR spectra were acquired on a Bruker AC 250 (250 MHz) and a Bruker Avance 300 (300 MHz). For the cyclic voltammetry experiments a three-electrode assembly with a Ag/AgNO₃ electrode was used. CH₂Cl₂ containing 0.1 M tetrabutylammonium hexafluorophosphate was used as a solvent and each measurement was calibrated with ferrocene as internal standard. Compounds **2**, **3** and **10** were prepared according to literature^{18,19}. PCBM was purchased from ADS Inc. All reagents and solvents were of analytical grade or purified using standard methods.

Synthesis of (1-Heptyloctyl)-perylene-3,4:9,10-tetracarboxylic bisimide (**4**)

Perylene-3,4:9,10-tetracarboxylic monoanhydride monoimide (**3**) (3.13 g, 8 mmol) and 8-aminopentadecane (2.91 g, 12.8 mg) were stirred in imidazole (30 g) and quinoline (5 ml) under argon (160 °C, 2h). The mixture was dissolved in THF and precipitated in 400 ml of a mixture of ethanol and 2N HCl (1:1). The precipitate was collected by vacuum filtration, treated with boiling aqueous K₂CO₃ solution (100 ml, 10%), washed with distilled water and dried under vacuum. The compound was purified by extractive recrystallization²⁰ and traces

5. Appendix A2

of N,N'-di(1-heptyloctyl)-perylene-3,4:9,10-tetracarboxylic bisimide were removed by extraction with hexane to yield a red solid (3.64 g, 77%). ^1H NMR (CDCl_3 , 250 MHz) δ : 0.81 (t, $^3\text{J} = 6.95$ Hz, 6H), 1.28 (m, 16H), 1.87 (m, 2H), 2.21 (m, 2H), 5.16 (m, 1H), 8.56 (m, 8H). MS (EI) m/z: 600 [$\text{M}^+ - 1$]. IR (Si) v: 3067, 2958, 2927, 2855, 1698, 1659, 1594, 1432, 1403, 1343, 1269, 1179, 810, 741, 655 cm^{-1} .

Synthesis of 5

1202 mg (2 mmol) **4**, 743 mg (2.8 mmol) 1-bromo-6-tetrahydropyranloxyhexane and 498 mg (3.6 mmol) K_2CO_3 were stirred in a mixture of 30 ml DMF and 10 ml THF under argon at 60 °C for 24 h. The mixture was precipitated in 200 ml methanol, collected by vacuum filtration and dried in vacuum. The precipitate was dissolved in 20 ml THF and 50 mg (0.2 mmol) pyridinium para-toluenesulfonate (PPTS) and three drops of hydrochloric acid in 10 ml ethanol were added and stirred at 55 °C for 3 hours. The product was precipitated in 200 ml cold methanol, collected by vacuum filtration and dried in vacuum. It was purified by column chromatography (silica gel, hexanes/THF = 4/1) to yield 823 mg (1.17 mmol, 59%).

$^1\text{H-NMR}$ (CDCl_3 , 250 MHz) δ : 0.80 (t, $^3\text{J} = 6.56$ Hz, 6H), 1.20 (m, 20H), 1.46 (m, 4H), 1.64 (m, 2H), 1.84 (m, 4H), 2.20 (m, 2H), 3.35 (s, 2H), 4.10 (m, 4H), 5.10 (m, 1H), 8.20 (m, 8H) ppm. MS (EI) m/z: 701 [M^+]. IR (Si) v: 2954, 2925, 2856, 1698, 1648, 1596, 1578, 1405, 1346, 1255, 1179, 1082, 810, 746 cm^{-1} .

Synthesis of the unsymmetrical malonate **6**

100 mg (0.14 mmol) **5** was dissolved in 50 ml CH_2Cl_2 and 14 μl (0.17 mmol) pyridine was added under protecting gas. The mixture was cooled on an ice bath and 18 μl (0.17 mmol) methyl malonyl chloride in 10 ml CH_2Cl_2 was added dropwise. The mixture was stirred for 12h at room temperature. Compound **6** was purified by column chromatography (silica gel, $\text{CH}_2\text{Cl}_2/\text{ethyl acetate} = 80/20$) to yield 110 mg (0.14 mmol, 98%).

$^1\text{H-NMR}$ (CDCl_3 , 300 MHz) δ : 0.83 (t, $^3\text{J} = 6.61$ Hz, 6H), 1.20 (m, 20H), 1.45 (m, 4H), 1.65 (m, 4H), 1.85 (m, 2H), 2.20 (m, 2H), 3.35 (s, 2H), 3.57 (s, 3H), 4.10 (m, 4H), 5.10 (m, 1H), 8.20 (m, 8H) ppm. $^{13}\text{C-NMR}$ (CDCl_3 , 75MHz) δ : 14.00, 22.60, 25.50, 26.60, 27.00, 27.95, 28.15, 29.40, 29.50, 31.80, 32.20, 40.20, 41.20, 52.50, 54.80, 65.45, 122.60, 122.70, 122.80,

5. Appendix A2

125.60, 125.70, 129.00, 129.10, 130.80, 133.90, 134.10, 160.60, 166.50, 167.00 ppm. MS (FAB) m/z: 801 [M⁺].

Synthesis of the symmetrical substituted malonate **8**

100 mg (0.14 mmol) **5** was dissolved in 50 ml CH₂Cl₂ and 14 µl (0.17 mmol) pyridine was added under protecting gas. The mixture was cooled on an ice bath and 10 µl (0.11 mmol) malonyl dichloride in 10 ml CH₂Cl₂ was added dropwise. The mixture was stirred for 12h at room temperature. Compound **8** was purified by column chromatography (silica gel, CH₂Cl₂/ethyl acetate = 80/20) to yield 104 mg (0.07 mmol, 99%).

¹H-NMR (CDCl₃, 300 MHz) δ: 0.83 (t, ³J = 6.57 Hz, 12H), 1.30 (m, 40H), 1.50 (m, 8H), 1.75 (m, 8H), 1.90 (m, 4H), 2.20 (m, 4H), 3.40 (s, 2H), 4.15 (m, 8H), 5.10 (m, 2H), 8.10 (d, ³J = 8.15 Hz, 4H), 8.20 (d, ³J = 8.15 Hz, 4H), 8.30 (d, ³J = 7.98 Hz, 4H), 8.40 (d, ³J = 7.55 Hz, 4H) ppm. ¹³C-NMR (CDCl₃, 75MHz) δ: 14.10, 22.60, 25.50, 26.70, 27.00, 27.80, 28.25, 29.20, 29.60, 31.80, 32.20, 42.00, 44.00, 55.00, 65.50, 122.60, 125.80, 129.00, 131.00, 134.10, 162.80, 166.60 ppm. MS (FAB) m/z: 1469 [M⁺].

Synthesis of Per₁C₆₀ (**7**)

33 mg (0.13 mmol) iodine were added to a solution of 140 mg (0.20 mmol) C₆₀ in 150 ml toluene. The malonate **6** which is dissolved in toluene was added and the mixture was degassed with argon for 30 minutes. 40 µl (0.26 mmol) 1,8-diazabicyclo[5.4.0]undec-7-ene (DBU) in 30 ml toluene was added dropwise within one hour and the reaction was stirred over night. The Per₁C₆₀ (**7**) was purified with column chromatography (silica gel, toluene/ethyl acetate = 98/2) to yield 112 mg (0.08 mmol, 57%).

¹H-NMR (CDCl₃, 300 MHz) δ: 0.82 (t, ³J = 6.78 Hz, 6H), 1.20 (m, 20H), 1.50 (m, 4H), 1.75 (m, 4H), 1.85 (m, 2H), 2.25 (m, 2H), 4.05 (s, 3H), 4.15 (t, ³J = 7.32 Hz, 2H), 4.50 (t, ³J = 6.32 Hz, 2H), 5.15 (m, 1H), 8.40 (m, 8 H) ppm. ¹³C-NMR (CDCl₃, 75MHz) δ: 14.00, 22.60, 25.50, 26.60, 27.00, 27.95, 28.15, 29.20, 29.50, 31.80, 32.20, 40.5, 52.50, 54.80, 55.00, 67.45, 71.40, 122.60, 122.70, 122.80, 125.60, 125.70, 129.00, 129.10, 130.80, 133.90, 134.10, 140.85, 141.80, 141.85, 142.50, 142.10, 142.82, 142.86, 142.90, 143.00, 143.70, 143.82, 144.48, 144.52, 144.54, 144.58, 144.6, 144.80, 145.04, 145.07, 145.10, 145.20, 145.30, 163.20,

5. Appendix A2

163.60, 164.10 ppm. MS (FAB) m/z: 720 [C₆₀⁺], 1519 [M⁺]. IR (Si) v: 2954, 2927, 2855, 1746, 1697, 1658, 1594, 1578, 1435, 1405, 1341, 1254, 1242, 810, 745, 528 cm⁻¹.

Synthesis of Per₂C₆₀ (**9**)

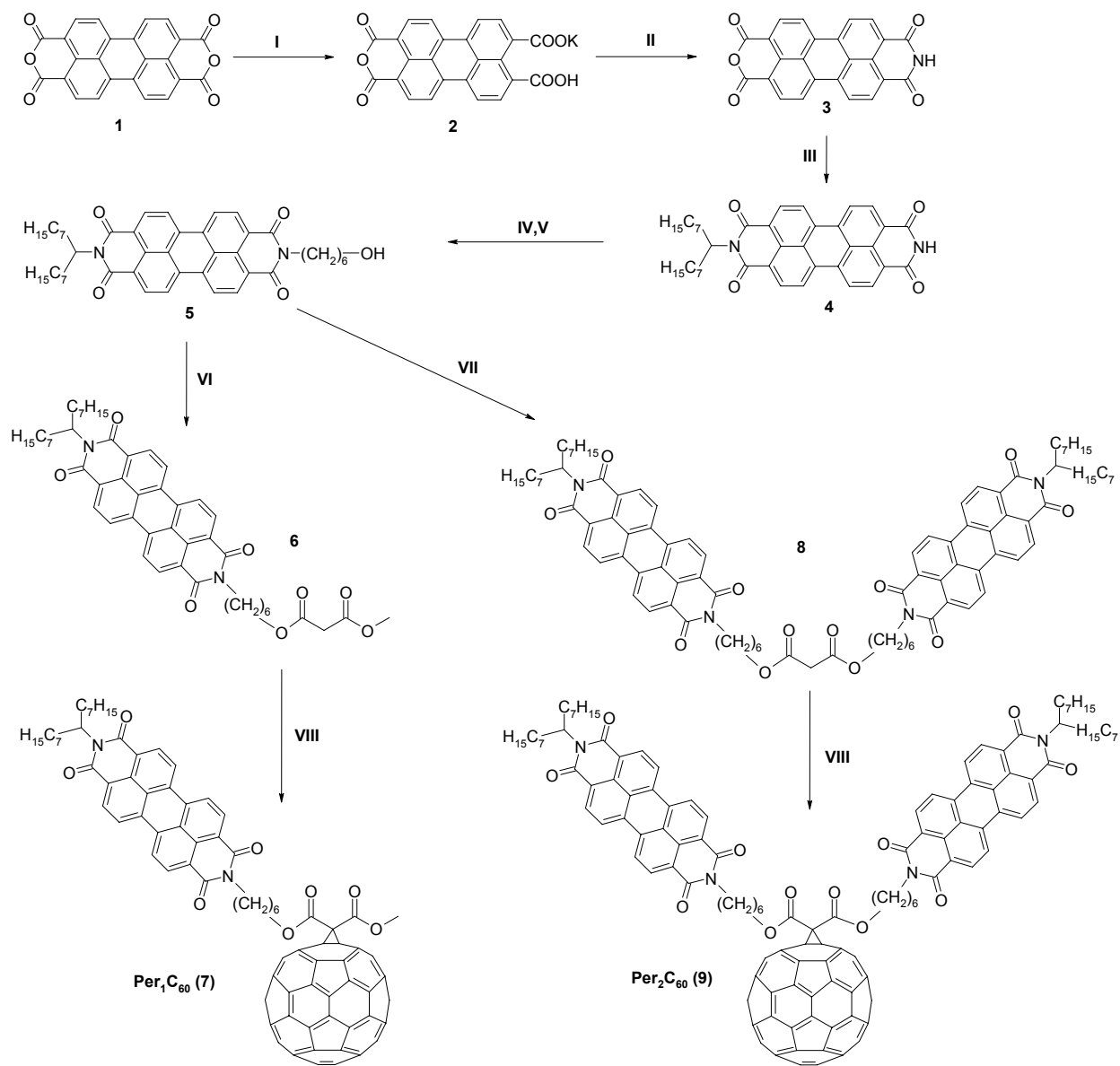
18 mg (0.07 mmol) iodine were added to a solution of 74 mg (0.10 mmol) C₆₀ in 150 ml toluene. The malonate **8** which is dissolved in toluene was added and the mixture was degassed with argon for 30 minutes. 20 µl (0.14 mmol) 1,8-diazabicyclo[5.4.0]undec-7-ene (DBU) in 15 ml toluene was added dropwise within one hour and the reaction was stirred over night. The Per₂C₆₀ (**9**) was purified with column chromatography (silica gel, toluene/ethyl acetate = 90/10) to yield 70 mg (0.03 mmol, 47%).

¹H-NMR (CDCl₃, 300 MHz) δ: 0.83 (t, ³J = 6.53 Hz, 12H), 1.30 (m, 40H), 1.60 (m, 8H), 1.90 (m, 8H), 2.20 (m, 4H), 4.30 (m, 4H), 4.53 (t, ³J = 6.22 Hz, 2H), 5.10 (m, 2H), 8.20 (m, 8H), 8.40 (m, 8H) ppm. ¹³C-NMR (CDCl₃, 75MHz) δ: 14.10, 22.60, 25.50, 26.70, 27.00, 27.80, 28.25, 29.20, 29.60, 31.80, 32.20, 42.00, 52.00, 55.00, 65.50, 71.60, 122.60, 122.80, 123.00, 125.80, 129.30, 131.00, 134.10, 140.85, 141.90, 142.10, 142.90, 142.95, 143.00, 143.20, 143.80, 144.50, 144.60, 144.80, 145.10, 145.20, 145.40, 163.10, 163.90 ppm. MS (FAB) m/z: 720 [C₆₀⁺], 2188 [M⁺]. IR (Si) v: 2952, 2925, 2855, 1746, 1732, 1698, 1658, 1594, 1578, 1457, 1435, 1405, 1343, 1254, 1096, 810, 745, 528 cm⁻¹.

Results and discussion

The synthetic route for the preparation of fullerenes with covalently linked perylene bisimide is shown in scheme 1. Two different dyads, Per₁C₆₀ (**7**) and Per₂C₆₀ (**9**) with one and two perylene bisimide moieties attached to a C₆₀ unit were prepared. The synthesis starts with the opening of one of the anhydride groups in the perylene-3,4:9,10-tetracarboxylic dianhydride **1** to form the mono potassium salt **2**. The ring is closed again to get the unsymmetrical monoanhydride monoimide **3**¹⁸. As the imide group is stable against basic and acidic reactions, only the anhydride group reacts with 8-aminopentadecane, forming a swallow-tail substituted product **4**. In contrast to most perylene bisimide derivatives these swallow-tail substituted perylene bisimides are highly soluble in organic solvents¹⁹. The unsymmetrical perylene bisimide **4** was coupled with 1-bromo-6-tetrahydropyranloxyhexane and afterwards

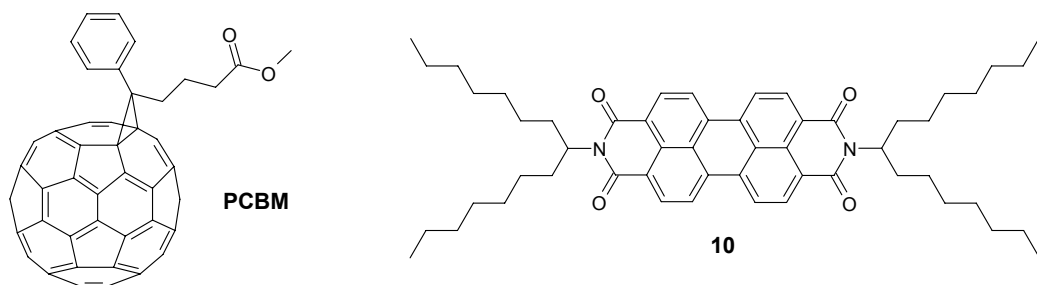
the free hydroxyl group was obtained by removing the THP protecting group under acidic conditions.



Scheme 1. Synthesis of the perylene bisimide – fullerene dyad **7** and chemical structure of **9**. *Reagents and conditions:* (I) KOH, H₂O; AcOH; (II) NH₃, H₂O; (III) 8-aminodecane, imidazole, quinoline, 160 °C; (IV) Br-(CH₂)₆-OTHP, K₂CO₃, DMF, THF, 60 °C; (V) PPTS, HCl, THF, ethanol, 55°C; (VI) methyl malonyl chloride, pyridine, CH₂Cl₂; (VII) malonyl dichloride, pyridine, CH₂Cl₂; (VIII) C₆₀, I₂, DBU, toluene.

5. Appendix A2

The hydroxyl functionalized perylene bisimide was coupled with methyl malonyl chloride or malonyl dichloride to get the mono (**6**) and disubstituted (**8**) malonates. The cyclopropanation of C₆₀ was carried out by a modified Bingel reaction²¹ of the malonate **6** or **8** with iodine and 1,8-diazabicyclo[5.4.0]undec-7-ene (DBU) in toluene²². These coupling reactions were performed with good yields (57% for **7**; 47% for **9**). The resulting fullerenes Per₁C₆₀ (**7**) and Per₂C₆₀ (**9**) have one and two covalently linked perylene bisimide units, respectively.



Scheme 2. Chemical structures of the model compounds PCBM ([6,6]phenyl-C₆₁-butyric acid methyl ester) and the N,N'-di(1-heptyloctyl)perylene-3,4:9,10-tetracarboxylic bisimide **10**.

Both the dyads **7** and **9** were thoroughly characterized using spectroscopic methods (see experimental section). The electrochemical properties of Per₁C₆₀ and Per₂C₆₀ were determined by cyclic voltammetry and compared with those of model compounds PCBM and the symmetrically substituted N,N'-di(1-heptyloctyl)perylene-3,4:9,10-tetracarboxylic bisimide **10** (scheme 2). The measurements were conducted on a glassy carbon working electrode coupled with a Ag/AgNO₃ reference electrode and a Pt counter electrode in a three-electrode assembly system using CH₂Cl₂ containing 0.1 M tetrabutylammonium hexafluorophosphate as solvent. The HOMO (highest occupied molecular orbital) and LUMO (lowest unoccupied molecular orbital) values were calculated with respect to ferrocene (HOMO: -4.8 eV). The results are summarized in table 1.

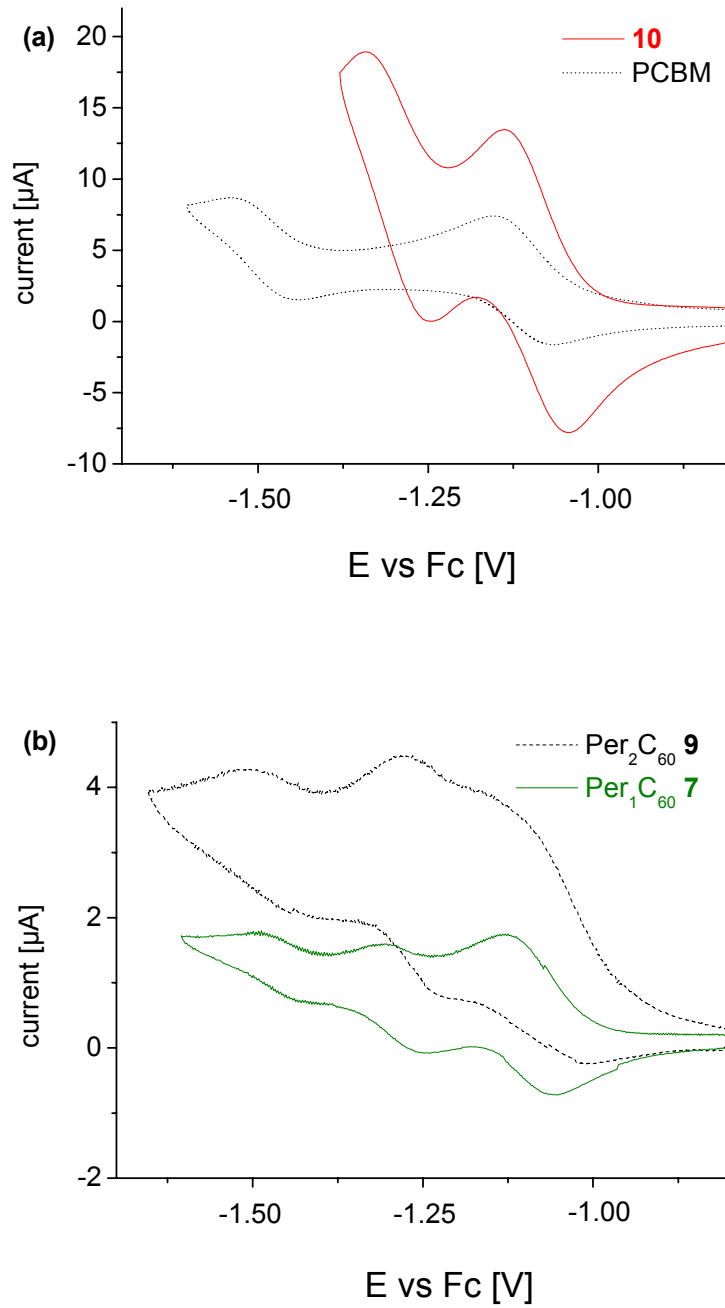


Fig. 1 (a) Cyclic voltammogramm of the perylene bisimide **10** and PCBM. (b) Cyclic voltammogramm of $\text{Per}_1\text{C}_{60}$ (**7**) and $\text{Per}_2\text{C}_{60}$ (**9**). The measurements were conducted in CH_2Cl_2 containing 0.1 M tetrabutylammonium hexafluorophosphate with respect to ferrocene (Fc) at a scan rate of 50 mV s⁻¹.

5. Appendix A2

It could be shown that the perylene bisimide **10** exhibits two reversible reduction peaks and one oxidation peak (Fig. 1a). The LUMO value could be calculated from the first reduction E_{red1} as -3.71 eV and the HOMO from the first oxidation peak E_{ox1} as -6.03 eV with respect to the zero energy level. PCBM also shows two reversible reduction peaks. The LUMO of PCBM is with -3.69 eV comparable to the value of the perylene bisimide **10**. Therefore the LUMOs of the dyads Per_1C_{60} (**7**) and Per_2C_{60} (**9**) are also similar with -3.71 eV and -3.72 eV respectively. But the second reduction peaks of the fullerene derivative PCBM and the perylene bisimide occur at different potentials. The E_{red2} of PCBM is at -1.49 V and that for **10** is at -1.29 V with respect to ferrocene. Therefore three reduction peaks occur for the dyads Per_1C_{60} (**7**) and Per_2C_{60} (**9**), in which the first reduction peak is an overlap of the first reduction peaks of the fullerene and perylene bisimide units. The reduction potentials of the dyads and the model compounds are similar. The second reduction peaks corresponding to fullerene and perylene bisimide are unaffected in the dyads and occur at similar potential values as for the individual moieties. This suggests that no strong interaction between the fullerene and the perylene bisimide units occur in the ground state.

Compound	E_{red1} vs Fc / V	E_{red2} vs Fc / V	E_{red3} vs Fc / V	LUMO / eV
Per_1C_{60} 7	-1.09	-1.28	-1.45	-3.71
Per_2C_{60} 9	-1.08	-1.25	-1.46	-3.72
PCBM	-1.11	-1.49	-	-3.69
10	-1.09	-1.29	-	-3.71

Table 1. CV data for the model compounds **10** and PCBM and the dyads **7** and **9**. The measurement was conducted in CH_2Cl_2 containing 0.1 M tetrabutylammonium hexafluorophosphate in a three electrode assembly using $Ag/AgNO_3$ as a reference electrode. The reduction potentials are given with respect to ferrocene.

5. Appendix A2

The absorption spectra of the dyads **7** and **9** and the model systems **10** and PCBM are shown in figure 2a. It can be seen that the fullerene derivative PCBM barely absorbs light in the range between 400 and 600 nm. The main absorption is in the ultraviolet part of the spectra with a characteristic peak at 327 nm.

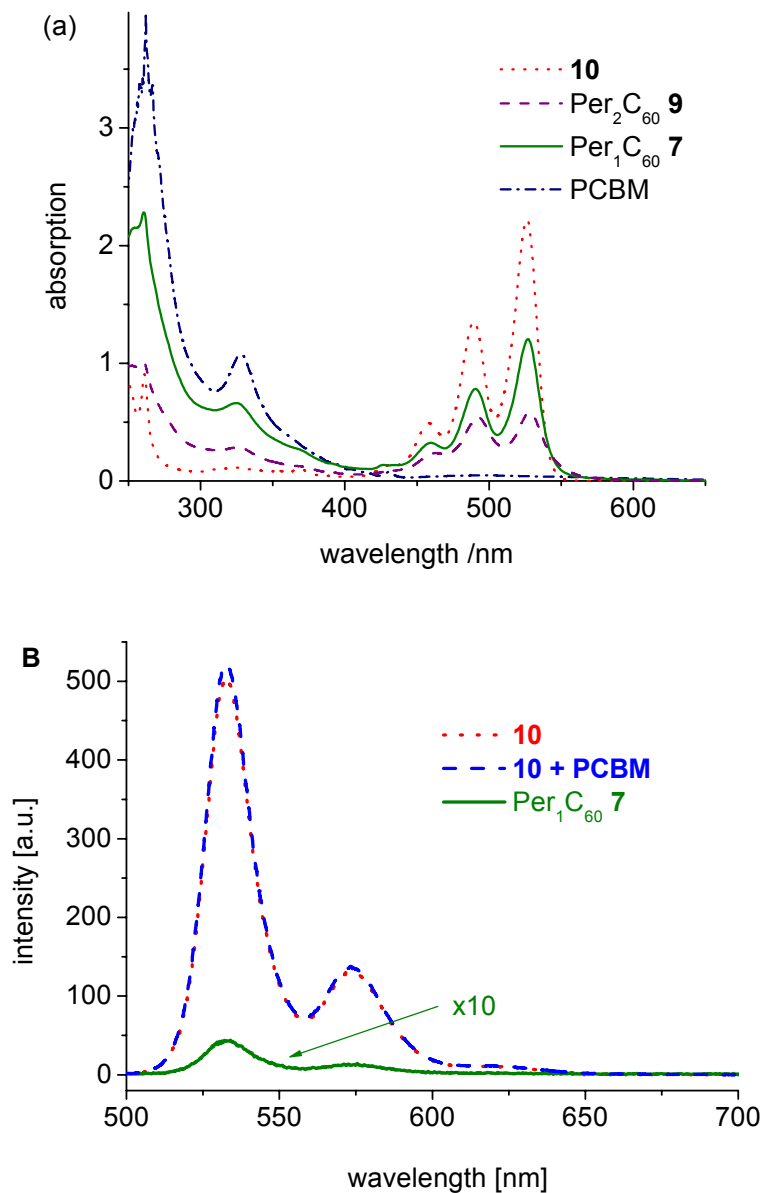


Fig. 2 (a) UV/vis spectra of the perylene bisimide **10**, PCBM, $\text{Per}_1\text{C}_{60}$ (**7**) and $\text{Per}_2\text{C}_{60}$ (**9**) measured in CHCl_3 (0.02 mg/ml). (b) Fluorescence spectra of **10**, the dyad **7** (magnification: 10x) and a mixture of **10** and PCBM in CHCl_3 .

5. Appendix A2

The dyads on the other hand have a strong absorption between 400 and 600 nm due to the perylene bisimide moieties. The characteristic peaks for the first (527 nm), the second (491 nm) and the third (459 nm) vibronic transition of the electronic S₀-S₁ transition can be observed. The extinction coefficient for the dyads **7** and **9** are 91600 and 63900 1 mol⁻¹ cm⁻¹, respectively. Interestingly the molar extinction coefficient for Per₁C₆₀ (**7**) is remarkably higher than that for Per₂C₆₀ (**9**). This behavior can be attributed to π-π stacking which is also observed for polymers¹⁷ in solution. This effect is not observed for rigid bound perylene bisimides on a fullerene core¹³. But with the flexible hexyl-bridge the perylene bisimide units interact strongly in **9** in solution. This can be also seen from the quotient of the absorption at the second and first vibronic transition. Such quotients express the degree of aggregation²³. The quotient changes from 0.65 for Per₁C₆₀ (**7**) to 0.93 for Per₂C₆₀ (**9**) and is virtually independent of the concentration in dilute solution. Thus in **9** the aggregation observed is of intramolecular nature, Per₁C₆₀ (**7**) and Per₂C₆₀ (**9**) both exhibit fluorescence quenching, which can be attributed to electron and energy transfer between the fullerene and the perylene bisimide. In figure 2b the UV/vis and fluorescence spectra of the perylene bisimide **10**, the dyad **7** and 1:1 molar mixture of **10** and PCBM in solutions with the same molar concentrations were compared. The perylene bisimide **10** shows a very strong fluorescence with three distinct transitions. The same three transitions are observed for the dyad **7** but the fluorescence is quenched by about 99%. This quenching is caused by electron and energy transfer²⁴. This transfer is strongly influenced by the distance of the donor and acceptor. For example, the fluorescence of the mixture of **10** and PCBM which has the same molar concentration as **7**, is not notably quenched. As the individual moieties are covalently linked, the transfer reactions are considerably favored. This paves the way to tune the opto-electronic properties in such dyads by using different bridges connecting the two units. Thus with this concept not only the absorption in the solar spectrum can be enhanced, but also the energetic processes between the fullerene and the perylene bisimide moiety can be manipulated.

Summary

Two new fullerene dyads containing one and two perylene bisimides moieties covalently linked to the fullerene moiety were synthesized. The electronic and optical properties of these two electron transport materials were compared with the corresponding perylene bisimide and PCBM. The electrochemical and optical studies reveal no strong electronic coupling in the ground-state between the perylene bisimide and the fullerene unit. It could be shown that the fluorescence in the dyads is strongly quenched due to energy and electron transfer. This makes these systems interesting as model systems for energy transfer using various linkers between the moieties. The change of the linker units can therefore vary the interactions. The UV/vis absorption of the two dyads was compared and it reveals interesting aggregation behavior of the two perylene bisimide groups in $\text{Per}_2\text{C}_{60}$. Especially, the dyad $\text{Per}_1\text{C}_{60}$ exhibits very promising properties for organic electronics. The strong absorption within the solar spectrum of the dye-linked fullerene enables the use as light absorbing electron acceptor in organic solar cells.

Acknowledgement. The financial support for this research work from German Research Council (DFG/SFB 481) is gratefully acknowledged.

5. Appendix A2

- ¹ W. Ma, C. Yang, X. Gong, K. Lee, A. J. Heeger, *Adv. Funct. Mater.*, 2005, **15**, 1617-1622.
- ² N. S. Sariciftci, L. Smilowitz, A. J. Heeger, F. Wudl, *Science*, 1992, **258**, 1474-1476.
- ³ G. Yu, J. Gao, J. C. Hummelen, F. Wudl, A. J. Heeger, *Science*, 1995, **270**, 1789-1791.
- ⁴ H. Hoppe, N. S. Sariciftci, *J. Mater. Chem.*, 2006, **16**, 45-61.
- ⁵ J. K. J. van Duren, X. Yang, J. Loos, C. W. T. Bulle-Lieuwma, A. B. Sieval, J. C. Hummelen, R. A. J. Janssen *Adv. Funct. Mater.*, 2004, **14**, 425-434.
- ⁶ A. Cravino, N. S. Sariciftci *J. Mater. Chem.*, 2002, **12**, 1931-1943.
- ⁷ U. Stalmach, B. de Boer, C. Videlot, P. F. van Hutten, G. Hadzioannou, *J. Am. Chem. Soc.*, 2000, **122**, 5464-5472.
- ⁸ N. Martin, L. Sanchez, B. Illescas, I. Perez, *Chem. Rev.*, 1998, **98**, 2527-2547.
- ⁹ P. A. Liddell, J. P. Sumida, A. N. MacPherson, L. Noss, G. R. Seely, K. N. Clark, A. L. Moore, T. A. Moore, D. Gust, *Photochem. Photobiol.*, 1994, **60**, 537-541.
- ¹⁰ N. S. Sariciftci, F. Wudl, A. J. Heeger, M. Maggini, G. Scorrano, M. Prato, J. Bourassa, P. C. Ford, *Chem. Phys. Lett.*, 1995, **247**, 510-514.
- ¹¹ E. H. Magin, P.M. Borsenberger, *J. Appl. Phys.*, 1993, **73**, 787-791.
- ¹² F. Würthner, *Chem Commun.*, 2004, **14**, 1564-1579.
- ¹³ R. Gomez, J. Segura, N. Martin, *Org. Lett.*, 2005, **7**, 717-720.
- ¹⁴ J. Baffreau, L. Perrin, S. Leroy-Lhez, P. Hudhomme, *Tetrahedron Lett.*, 2005, **46**, 4599-4603.
- ¹⁵ J. Hua, F. Meng, F. Ding, F. Li, H. Tian, *J. Mater. Chem.*, 2005, **14**, 1849-1853.
- ¹⁶ H. Langhals, S. Demmig, T. Potrawa, *Journal f. prakt. Chemie*, 1991, **333**, 733-748.
- ¹⁷ S. M. Lindner, N. Kaufmann, M. Thelakkat, *Organic Electronics*, submitted.
- ¹⁸ H. Kaiser, J. Lindner, H. Langhals, *Chem. Ber.*, 1991, **124**, 529-535.
- ¹⁹ H. Langhals, S. Demmig, T. Potrawa, *Journal f. prakt. Chemie*, 1991, **333**, 733-748.
- ²⁰ H. Langhals, *Chem. Ber.* 1985, **118**, 4641-4645.
- ²¹ C. Bingel, *Chem. Ber.*, 1993, **126**, 1957-1959.
- ²² J.-F. Nierengarten, V. Gramlich, F. Cardullo, F. Diederich, *Angew. Chem., Int. Ed.*, 1996, **35**, 2101-2103.
- ²³ B. A. Gregg, *J. Phys. Chem.*, 1996, **100**, 852-859.
- ²⁴ I. B. Martini, B. Ma, T. Da Ros, R. Helgeson, F. Wudl, B. J. Schwartz, *Chem. Phys. Lett.*, 2000, **327**, 253-262.

**Nanostructures of n-Type Organic Semiconductor in a p-Type Matrix via
Self-Assembly of Block Copolymers**

Macromolecules **2004**, *37*, 8832-8835

*Stefan M. Lindner and Mukundan Thelakkat**

Makromolekulare Chemie I, Universität Bayreuth, Universitätsstrasse 30, 95440 Bayreuth,
Germany

* Corresponding author: e-mail mukundan.thelakkat@uni-bayreuth.de

Received September 7, 2004

Revised Manuscript Received October 18, 2004

ABSTRACT

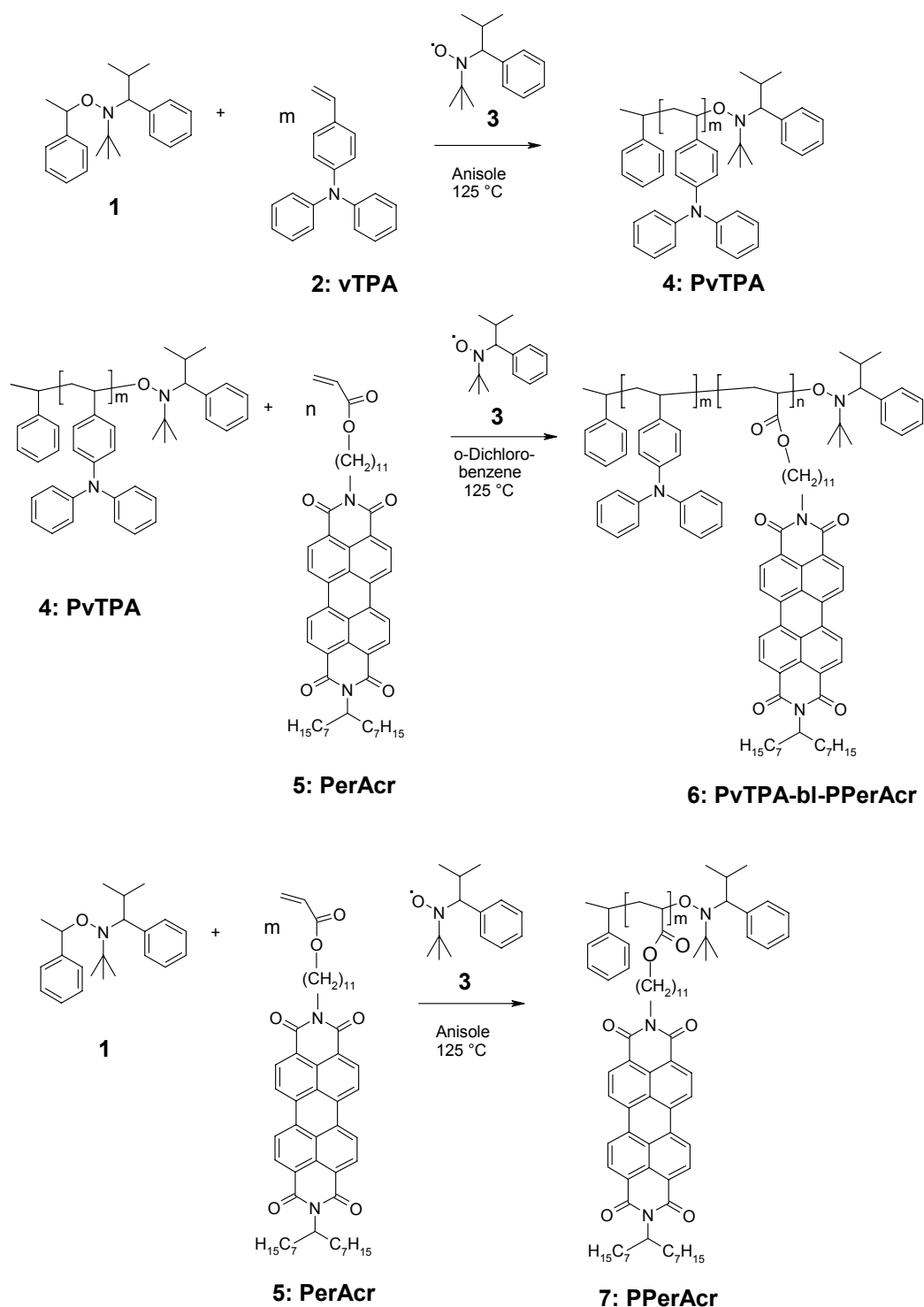
The synthesis, characterization and properties of fully functionalized diblock copolymers are described in which one block acts as a hole transport material and the other block as an electron transport material and dye. The block copolymers were prepared by nitroxide-mediated living radical polymerization. First 4-vinyl-triphenylamine was polymerized and used as a macroinitiator for the sequential polymerization of the second monomer, a functionalized perylene bisimide with an acrylate group. The block copolymers were obtained with well-defined molecular weights in the range of 18 to 40 kg/mol and with appreciably low polydispersities. All the polymers were characterized and analyzed using NMR, SEC, DSC, TGA and TEM. It is shown that such fully functionalized diblock copolymers exhibit phase separation on nanometer scale and form nanostructures of perylene bisimide moieties in a polymeric hole conductor matrix. Initial UV/vis and fluorescence spectrometry experiments show charge transfer between the two domains.

There has been an increasing interest in the morphology of organic semiconductors^{1,2,3} in film because of its strong influence on the performance of devices using these materials. Especially for electro-optical applications like light emitting diodes and solar cells an increase in the interface area between the electron (ETM) and the hole transport material (HTM) could enhance the performance since the interface is the active area for charge recombination or separation. This phenomenon was studied experimentally⁴ and by numerical simulations⁵. In photovoltaic devices the light is absorbed by the dye and the generated exciton (electron-hole pair) has to diffuse to the interface between ETM and HTM where they are separated. The exciton diffusion length is only in the order of a few nanometers, which is at least 10 times smaller than the optical absorption depth. This limits the efficiency for simple two layer devices⁶. To overcome this problem the active organic layer has to be structured on a nanometer scale. Such microphase separation can be realized using block copolymers. Synthetic attempts for obtaining functionalized block copolymers have been successfully tried out by Hadzioannou et al.⁷ using p-phenylenevinylene and a partially fullerene functionalized block, by Zentel et al⁸ using triphenylamines and NLO-functionalized triphenylamines, by Stupp et al.⁹ using functional triblock copolymers and in our group by using metal centred bifunctional polymers¹⁰. In this work, we use poly(vinyltriphenylamine) as HTM, which is known to be a stable and good hole conductor. The other block is made up of perylene bisimide¹¹ acrylate which has high electron mobility and high light fastness so that it can also be used as a dye as it strongly absorbs light between 400 and 600 nm. The perylene-3,4:9,10-tetracarboxylic bisimide monomer **5** (PerAcr) was designed unsymmetrically with a swallow-tail substituent¹² for good solubility and an acrylate group at the other end for the polymerization. Thus in this concept, all the three functions of light absorption, hole transport and electron transport are taken care of in a self-assembling system with the challenging task of creating nanostructures with large amount of interface suitable for solar cell applications.

In order to get well-defined block copolymers we used the nitroxide-mediated living radical polymerization¹³. This controlled radical polymerization technique tolerates a wide range of functional groups and is a metal-free method. The initiator **1** is a second generation initiator which was first reported by Hawker et al¹⁴. With this initiator styrene and acrylate derivates could be polymerized. As a first step 4-vinyl-triphenylamine **2** was polymerized via nitroxide-mediated controlled radical polymerization (scheme1). In Figure 2a the linear dependence between the reaction time and the conversion for conversions up to 50 % is shown, which is consistent with the controlled nature of the polymerization. The polydispersities are in the range of 1.20 to 1.26. With longer reaction time the polydispersity increases to 1.43 for 80 %

conversion. A small excess (5 mol%) of the free nitroxide **3** was added to optimize the control of the polymerization. The free nitroxide is necessary so that it can act as an artificial persistent radical functioning similar to the persistent radical effect¹⁵. Initial experiments without the free nitroxide resulted in poorer control of the reaction and therefore higher polydispersities. Two macroinitiators, PvTPA1 **4A** and PvTPA2 **4B** were synthesized using the same technique. The polymer properties are listed in table 1. Even for high molecular weights the polydispersities are low. These homopolymers are amorphous with glass transition temperatures of about 144-145 °C and are thermally stable.

The perylene bisimide monomer **5** was also homopolymerized to get the polymer PPerAcr **7**. This perylene containing homopolymer **7** has a melting point of 190 °C, but no glass transition temperature could be detected down to -50 °C. For the polymerization of the perylene bisimide substituted acrylates longer reaction times were necessary and the polydispersity of the homopolymer **7** was higher than those of the homopolymers **4**. This may be due to the dilution of the acrylate group in the monomer **5**, which mainly consists of the substituted perylene core. Similar effects for the dilution with solvent were previously reported¹⁶. If polymer **7** was used as a macroinitiator for the polymerization of 4-vinyl-triphenylamine **2**, the polydispersities were about 2 with a low molecular weight shoulder in GPC eluogram, which can be attributed to the macroinitiator. This result suggests that the solubility of the macroinitiator may limit this synthetic pathway, and therefore, the synthetic route starting from PvTPA macroinitiator was used (scheme 1).



Scheme 1. Living radical polymerization and block copolymerization of vTPA and PerAcr monomers via nitroxide mediated polymerization (NMP).

	M_n [g/mol] ^a	PDI^a	wt% of PerAcr^b	T_g [°C]^c	T_m [°C]^c	TGA -5% [°C]
4A: PvTPA1	15830	1.22	-	143.6	-	378
4B: PvTPA2	23210	1.19	-	145.3	-	376
6A: PvTPA1-bl-PperAcr1	17610	1.37	13.7	141.9	181.3	380
6B: PvTPA1-bl-PperAcr2	24170	1.47	40.3	137.7	187.7	391
6C: PvTPA1-bl-PperAcr3	37710	1.97	78.9	149.5	198.0	396
7: PPerAcr	19900	1.65	100	- ^d	189.8	404

Table 1. Overview of molecular weight and thermal properties of the homopolymers and block copolymers. ^a Measured against polystyrene standards via GPC. ^b Calculated from ¹H-NMR spectra. ^c heating rate 10 K/min, values taken from second heating curve. ^d T_g could not be observed down to -50 °C.

The macroinitiator PvTPA1 **4A** was used to synthesize the block copolymers PvTPA1-bl-PPerAcr **6A-6C**. All the block copolymerizations were performed in 1,2-dichlorobenzene with a 5 mol% excess of the free nitroxide **3**. The polymers exhibited polydispersities below 1.5 for dye contents up to 40 wt%. The composition of the block copolymers were determined by NMR-spectroscopy. The UV/vis spectra of this series of block copolymers **6A-6C** prepared from the same macroinitiator **4A** show the expected increase in perylene absorption proportional to the incorporation of perylene bisimide block as seen in fig. 2b. Additionally the dye content in **6A-6C** was also determined using UV/vis spectroscopy making use of the extinction coefficient of PPerAcr **7**. The dye contents were 13.0, 40.8, and 73.2 wt% for **6A**, **6B** and **6C** respectively. These values are in close agreement with the compositions calculated from NMR-spectroscopy.

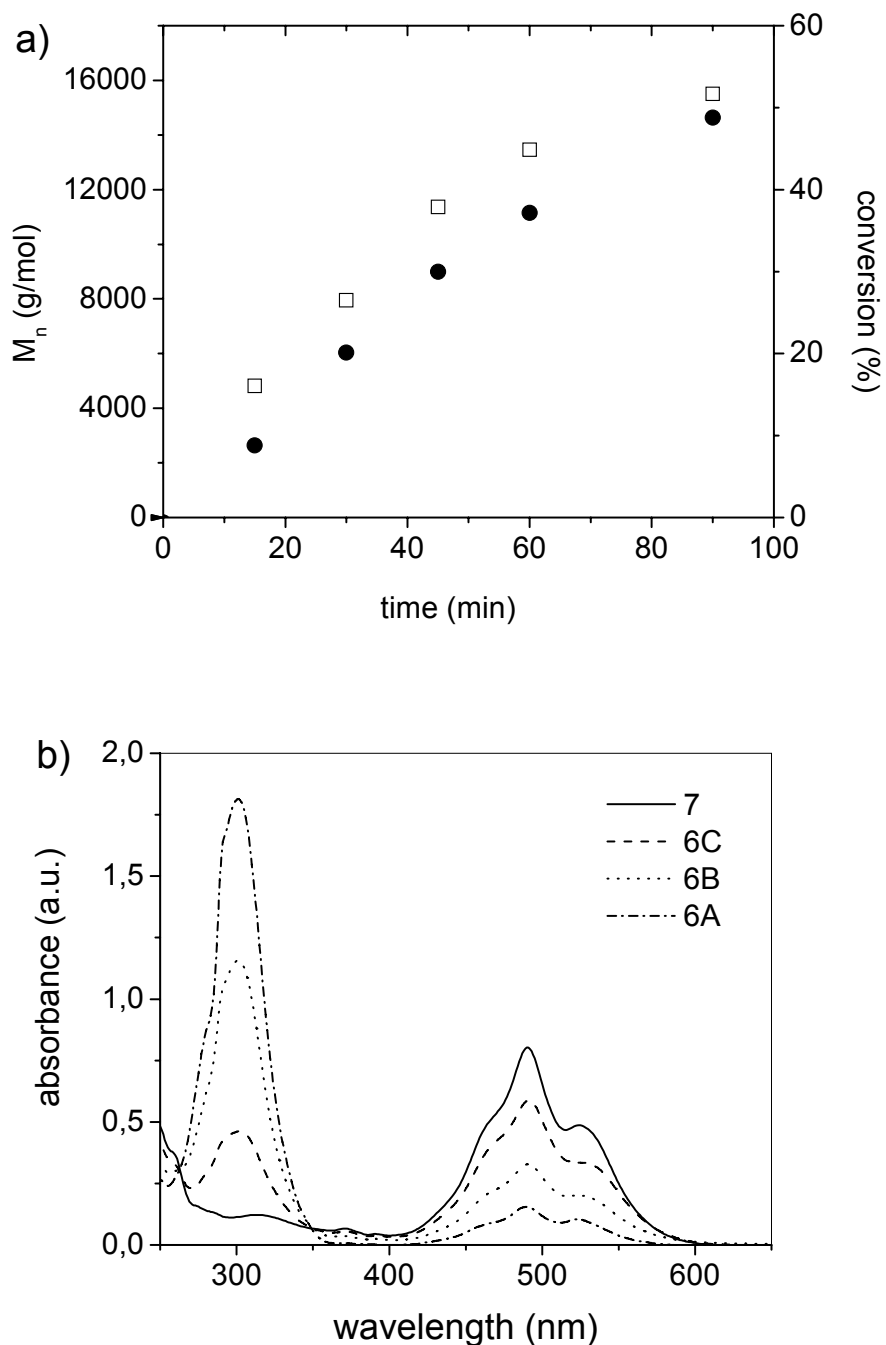


Figure 1. a) Evolution of molecular weight and conversion with time for nitroxide-mediated living polymerization of vTPA to PvTPA. Composition: 6 mmol **2**, 0.03 mmol **1**, 0.0015 mmol **3**, 600 μ l anisole; T = 125 °C and b) UV-Vis spectra of **6A-6C** measured in THF (concentration: 0.02 mg/ml)

The block copolymers **6A-6C** are thermally stable with T_{onsets} obtained from TGA well above 300 °C. DSC measurements showed that the glass transition temperatures and the melting points of the block copolymers **6A-6C** are in the same range as those of the corresponding homopolymers **4** and **7**. Those thermal properties and the fact that all block copolymers give optically clear films indicate a microphase separation. The final proof for microphase separation was achieved with transmission electron microscopy. TEM measurements were carried out on thin cross sections of relatively thick films (5-6 microns) obtained by melting down the polymer onto a glass substrate and subsequently tempering them at 200 °C for 1 hour. The TEM of **6A - 6C** show phase separation on nanometer scale. As the amount of dye block in copolymer increases, the perylene moieties in **6C** aggregate together to form nanowires, which are embedded into the PvTPA matrix (figure 2). The nanostructures are about 40-60 nm thick and 1-2 microns long, thus exhibiting high aspect ratios which favour a better percolation of charge transport. Moreover, the tempering process favours a vertical orientation of these nanowires on glass substrates as can be seen from fig. 2. We assume that the strong π - π interaction and crystallization of perylene moieties are the driving forces for the build up of nanowires in block copolymer **6C** with high perylene dye content. The situation here may be very similar to that in rod-coil polymers in which the stiff rod-like segments cause the nanostructures¹⁸.

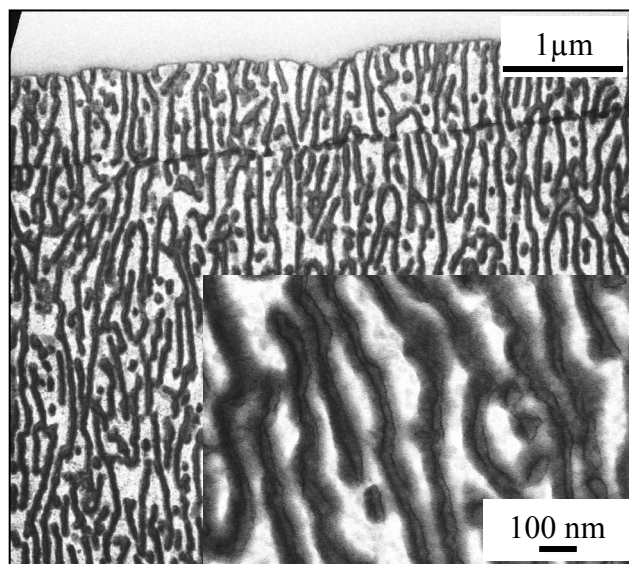


Figure 2. TEM of cross section of **6C** from relatively thick films (5-6 microns) obtained by melting down the polymers onto a glass substrate and subsequently tempering them at 200 °C for 1 hour.

Evidence for photoinduced charge transfer is provided by quenching of photoluminescence. After excitation at a wavelength of 492 nm, the homopolymer **7** shows an intense red fluorescence at 632 nm arising from perylene core. Using the same excitation wavelength, block copolymers **6A-6C** exhibit a quenching of this fluorescence with an efficiency of about 95%), which can be ascribed to an electron transfer from the excited state of perylene to PvTPA domains. The chance of energy transfer from perylene to TPA moieties is almost negligible due to the unfavourable HOMO/LUMO energy levels of the two species; TPA having a higher band gap energy than the perylene unit. Further studies of phase separation in thin films (<500 nm) and the application of such a nanostructured self-assembled film for photoinduced charge separation is underway and the results will be published later.

In summary, we have shown for the first time that the block copolymerization of 4-vinyl-triphenylamine and a perylene bisimide acrylate could be achieved by nitroxide-mediated living radical polymerization with control of molecular weight and low PDI. These fully functionalized block copolymers consist of one block with a hole transport moiety and a second block with an electron transport moiety having light absorption properties. In films these polymers show phase separation on nanometer scale and with increasing amounts of dye they build up nanostructures of perylene bisimide in a PvTPA matrix over a large area. Initial experiments show that charge transfer between the domains occurs, which is essential for the use in photovoltaic devices. The formation of oriented nanowires of an n-type organic semiconductor in a polymer matrix opens up new concepts not only in the field of existing electro-optics, but also in nanoscience and molecular electronics.

ACKNOWLEDGMENT. The financial support for this research work from German Research Council (DFG / SFB 481-Project B4) is gratefully acknowledged.

Supporting Information Available: Experimental procedures, characterization of materials and TEM cross sections of **6A** and **6B** are included. This material is available free of charge via the Internet at <http://pubs.acs.org>.

References and Notes

- (1) Shaheen, S.E.; Brabec, C. J.; Padinger, F.; Fromherz, T.; Hummelen, J. C.; Sariciftci, N. S. *Appl. Phys. Lett.* **2001**, *78*, 841-843.
- (2) Halls, J. J. M.; Walsh, C. A.; Greenham, N. C.; Marseglia, E. A.; Friend, R. H.; Moratti, S. C.; Holmes, A. B. *Nature* **1995**, *376*, 498-500.
- (3) Granström, M.; Petritsch, K.; Arias, A. C.; Lux, A.; Andersson, M. R.; Friend, R. H. *Nature* **1998**, *395*, 257-260.
- (4) Van Duren, J. K. J.; Yang, X.; Loos, J.; Bulle-Lieuwma, C. W. T.; Sieval, A. B.; Hummelen, J. C.; Janssen, R. A. J. *Adv. Funct. Mater.* **2004**, *14*, 425-434.
- (5) Sylvester-Hvid, K. O.; Rettrup, S.; Ratner, M. A. *J. Phys. Chem B* **2004**, *108*, 4296-4307.
- (6) Tang, C. W. *Appl. Phys. Lett.* **1986**, *48*, 183-185.
- (7) Stalmbach, U.; de Boer, B.; Videlot, C.; van Hutten, P. F.; Hadziioannou, G. *J. Am. Chem. Soc.* **2000**, *122*, 5464-5472.
- (8) Behl, M.; Hattemer, E.; Brehmer, M.; Zentel, R. *Macromol. Chem. Phys.* **2002**, *203*, 503-510.
- (9) Tew, G. N.; Pralle, M. U.; Stupp, S. I. *Angew. Chem.* **2000**, *112*, 527-531.
- (10) Peter, K.; Thelakkat, M. *Macromolecules* **2003**, *36*, 1779-1785.
- (11) Langhals, H. *Heterocycles* **1995**, *40*, 477-500.
- (12) Langhals, H.; Demmig, S.; Potrawa, T. *Journal f. prakt. Chemie* **1991**, *333*, 733-748.
- (13) Hawker, C. J.; Bosman, A. W.; Harth, E. *Chem. Rev.* **2001**, *101*, 3661-3688.

5. Appendix A3

- (14) Benoit, D.; Chaplinski, V.; Braslau, R. Hawker, C. J. *J. Am. Chem. Soc.* **1999**, *121*, 3904-3920.
- (15) Fischer, H. *Macromolecules* **1997**, *20*, 5666-5672.
- (16) Hawker, C. J.; Barclay, G. G.; Orellana, A.; Dao, J.; Devonport, W. *Macromolecules* **1996**, *29*, 5245-5254.
- (17) Lee, M.; Cho, B-K.; Zin, W-C. *Chem. Rev.* **2001**, *101*, 3869-3892.

Nanostructures of n-type Organic Semiconductor in a p-type Matrix via Self-Assembly of Block Copolymers

*Stefan M. Lindner and Mukundan Thelakkat**

Makromolekulare Chemie I, Universität Bayreuth, Universitätsstrasse 30, 95440 Bayreuth,
Germany

Supporting Information

General Information. The initiator **1** and the free nitroxide **3** were prepared according to literature¹. The monomer **5** was prepared in an adjusted synthesis for unsymmetrically substituted perylene bisimides according to literature^{2,3}. The free nitroxide **3** and P(^tBu)₃ were added as stock solutions in the solvent used for reaction. o-dichlorobenzene (water free) was purchased from Aldrich, anisole and toluene were distilled over sodium in an argon atmosphere and acetone was distilled over CaCl₂. Conversion and dye content were determined using ¹H NMR. ¹H NMR spectra were acquired on a Bruker AC 250 spectrometer (250 MHz). The molecular weights of polymers were determined by gel permeation chromatography (GPC) in THF + 0.25 wt% tetrabutylammonium bromide with UV and RI detectors (Waters) using polystyrene standards for calibration. UV-vis spectra were recorded using a Hitachi U-3000 spectrometer. Fluorescence spectra were recorded using a Shimadzu RF-5301 PC Spectrofluorophotometer. The thermal degradation of polymers was studied using a Mettler Toledo TGA/SDTA 851^e with a heating rate of 10 K/min under N₂.

atmosphere and the differential scanning calorimetry was carried out with a Perkin Elmer Diamond DSC with a heating rate of 10 K/min under N₂ atmosphere. TEM measurements were performed on a Zeiss 902 at 80 kV, the samples were stained with RuO₄.

Synthesis of 2. A mixture of diphenylamine (6.77 g, 40 mmol), 4-bromostyrene (8.79 g, 48 mmol), sodium tert-butoxide (5.00g, 52 mmol), Pd(OAc)₂ (90 mg, 0.4 mmol) and P(^tBu)₃ (0.324 g, 1.6 mmol) in 40 ml toluene under argon was heated at 100 °C for 1h. Column chromatography (silica gel, hexanes) afforded 9.22 g (85%) of product **2**.

Synthesis of 4A and 4B. A mixture of **1** (32.55 mg, 0.1 mmol), **3** (1.10 mg, 0.005 mmol), **2** (5.430 g, 20 mmol) and 1000 μl anisole were degassed by two freeze/thaw cycles, sealed under argon, and heated at 125 °C for 1h (**4A**) or 2h (**4B**). The reaction mixture was cooled, dissolved in THF and precipitated (2 times) in methanol. The white precipitate was filtered and dried to give the desired macroinitiator **4A** (2.438 g) or **4B** (3.910 g).

Synthesis of 6A and 6B. A mixture of **4A** (194 mg), **5** (495 mg, 0.6 mmol), **3** (0.11015 mg, 0.0005 mmol) and 250 μl o-dichlorobenzene were degassed by two freeze/thaw cycles, sealed under argon, and heated at 125 °C for 8h (**6A**) or 24h (**6B**). The reaction mixture was cooled, dissolved in THF and precipitated (3 times) in acetone. The red precipitate was filtered and dried to give the desired blockcopolymer **6A** (207 mg) or **6B** (298 mg).

Synthesis of 6C. A mixture of **4A** (194 mg), **5** (990 mg, 1.2 mmol), **3** (0.11015 mg, 0.0005 mmol) and 250 μ l o-dichlorobenzene were degassed by two freeze/thaw cycles, sealed under argon, and heated at 125 °C for 24h. The reaction mixture was cooled, dissolved in THF and precipitated (3 times) in acetone. The red precipitate was filtered and dried to give the desired block copolymer **6C** (479 mg).

Synthesis of 7. A mixture of **1** (6.51 mg, 0.02 mmol), **3** (0.2203 mg, 0.001 mmol), **5** (660 mg, 0.8 mmol) and 500 μ l anisole were degassed by two freeze/thaw cycles, sealed under argon, and heated at 125 °C for 24h. The reaction mixture was cooled, dissolved in THF and precipitated (2 times) in acetone. The red precipitate was filtered and dried to give the desired polymer **7** (384 mg).

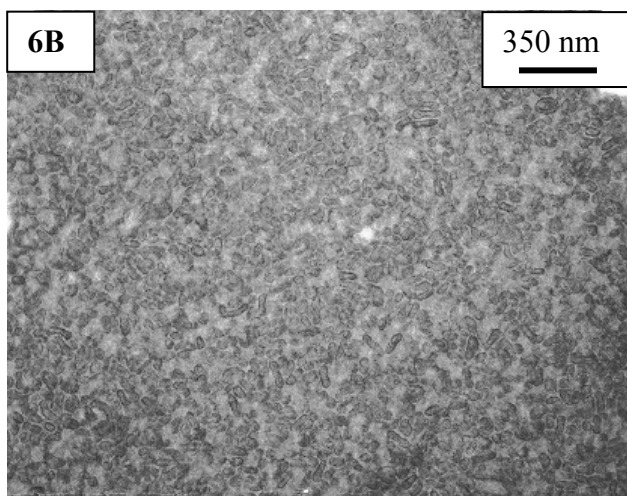
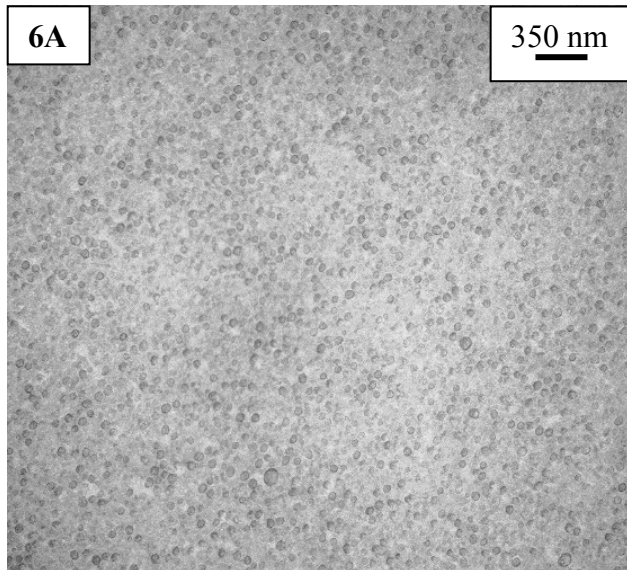


Figure 1. TEM of cross sections of **6A** and **6B** from relatively thick films obtained by melting down the polymers onto a glass substrate and subsequently tempering them at 200 °C for 1 hour. The growth of nanostructures can be seen from 6A to 6B in the order of increasing perylene dye content.

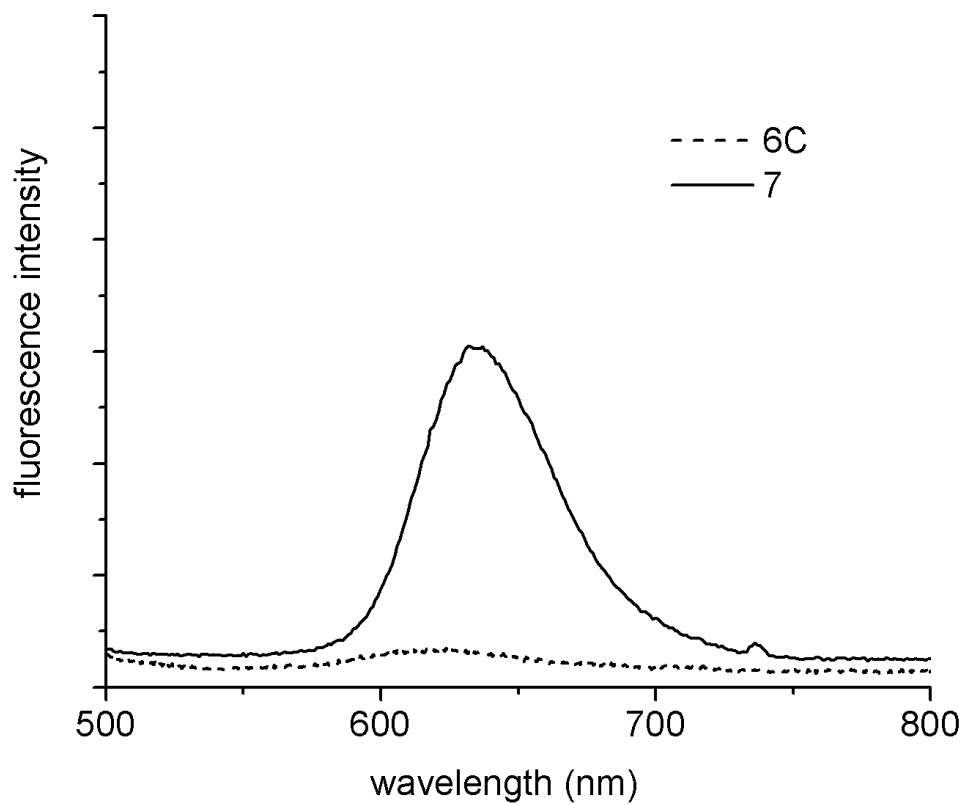


Figure 2. Fluorescence spectra of **7** and **6C** measured in film.

¹ Benoit, D.; Chaplinski, V.; Braslau, R.; Hawker, C. J. *J. Am. Chem. Soc.* **1999**, *121*, 3904-3920.

² Kaiser, H.; Lindner, J.; Langhals, H. *Chem. Ber.* **1991**, *124*, 529-535.

³ Langhals, H.; Saulich, S. *Chem. Eur. J.* **2002**, *8*, 5630-5643.

Nanostructured Semiconductor Block Copolymers: π - π Stacking, Optical and Electrochemical Properties

manuscript

*Stefan M. Lindner, Nadine Kaufmann, Mukundan Thelakkat**

Makromolekulare Chemie I, Universität Bayreuth, Universitätsstrasse 30, 95440 Bayreuth, Germany

ABSTRACT

The structural and optical properties of semiconductor block copolymers containing triphenylamine as hole transport material and perylene bisimide as dye and electron transport material are reported. The polymers were prepared by nitroxide mediated controlled radical polymerisation and characterized with GPC, DSC, and TGA. The electrochemical properties as determined by cyclic voltammetry show the HOMO and LUMO values of the block copolymers to be -5.23eV and -3.65eV respectively. The perylene bisimide units aggregate by π - π stacking which could be analyzed with wide angle x-ray scattering. The absorption and fluorescence properties of the perylene bisimide polymers and monomers in solution and film were investigated. It could be shown that they are strongly influenced by intramolecular coupling between different perylene bisimide units in polymers. The block copolymers exhibit a microphase separation on a nanometer scale with a constant perylene bisimide domain width of 13nm and lengths of up to several micrometers.

Keywords: organic semiconductor block copolymers; nanostructured bulk heterojunction; perylene bisimide polymer; vinyltriphenylamine polymer

* Corresponding author. Tel.: +49-921-553108; fax: +49-921-553206

e-mail address: mukundan.thelakkat@uni-bayreuth.de

1. Introduction

In organic electronic devices the interface between the hole transport material and the electron transport material is crucial for the performance as the charge separation (for organic solar cells) or the charge recombination (for organic light emitting diodes) occurs at this interface. As the exciton diffusion length is only in the order of some nanometers it is very important to get defined nanostructures in this range in the whole of the bulk for photovoltaic devices. The effect of the morphology in some systems has been studied experimentally [1] and by numerical simulations [2]. For this reason several methods were developed to control the thickness of the layers/domains precisely. The first organic heterojunction solar cells [3] were prepared by vacuum deposition, but the layer thickness in two-layer devices was too low to get sufficient absorption. In thicker layers the absorption would be better, but if they are thicker than the exciton diffusion length, the excitons cannot reach the interface. The efficiency would therefore not increase. In order to get high absorption with thin layers tandem cells were developed where the layers are adapted to the optical field intensity [4] to maximize the absorption. Another possibility widely used is the blending of polymers or polymers and small molecules. But the exact composition and morphology of such blends is difficult to control as for example, in the PPV-PCBM solar cells two domains occur with one pure PCBM domain and a mixed domain of PPV and PCBM [5,6]. We demonstrated that with the use of block copolymers nanostructured domain sizes between the hole and electron transport material can be achieved [7] and might be used for photovoltaic devices. Here we present a detailed study of the morphology of new block copolymers, the effect of molecular stacking in perylene bisimides and their electrochemical properties.

2. Experimental section

2.1 Materials

The initiator **1** and the free nitroxide **2** were synthesized according to literature [8]. The synthetic procedures of the monomers **3** and **5**, and those of the polymers **4C** and **7** were already published [7]. The macroinitiators **4A** and **4B** were prepared in a similar manner as **4C**, but varying the ratio of monomer to initiator. The block copolymers **6A-C** were synthesized via nitroxide mediated controlled radical polymerisation starting from macroinitiators **4A-C**. All solvents were distilled prior to use, anisole (anhydrous) and o-

dichlorobenzene (anhydrous) were purchased from Aldrich and used as received. **2** was added as a stock solution in the solvent used for the polymerisation.

*2.1.1 Poly(4-vinyltriphenylamine) **4A***

The initiator **1** (65.1 mg, 0.2 mmol), the free nitroxide **2** (2.20 mg, 0.01 mmol), the monomer **3** (5.46 g, 20 mmol) and 1 ml anisole were degassed three times and filled with argon. The reaction mixture was heated at 125 °C for 15 min. The polymer was purified by repeated precipitation from THF solution into methanol/acetone (1/1) to yield 350 mg of **4A**.

*2.1.2 Poly(4-vinyltriphenylamine) **4B***

The initiator **1** (65.1 mg, 0.2 mmol), the free nitroxide **2** (2.20 mg, 0.01 mmol), the monomer **3** (2.71 g, 10 mmol) and 1 ml anisole were degassed three times and filled with argon. The reaction mixture was heated at 125 °C for 45 min. The polymer was purified by repeated precipitation from THF solution into acetone to yield 2.62 g of **4B**.

*2.1.3 Synthesis of PvTPA-bl-PPerAcr **6A***

The macroinitiator **4A** (68 mg), the free nitroxide **2** (0.22 mg, 1 µmol), the PerAcr **5** (825 mg, 1 mmol) and 250 µl o-dichlorobenzene were degassed three times and filled with argon. The reaction mixture was heated at 125 °C for 24 h. The polymer was purified by repeated precipitation from chlorobenzene solution into acetone to yield 108 mg of **6A**.

*2.1.4 Synthesis of PvTPA-bl-PPerAcr **6B***

The macroinitiator **4B** (264 mg), the free nitroxide **2** (0.22 mg, 1 µmol), the PerAcr **5** (825 mg, 1 mmol) and 250 µl o-dichlorobenzene were degassed three times and filled with argon. The reaction mixture was heated at 125 °C for 24 h. The polymer was purified by repeated precipitation from chlorobenzene solution into acetone to yield 385 mg of **6B**.

*2.1.5 Synthesis of PvTPA-bl-PPerAcr **6C***

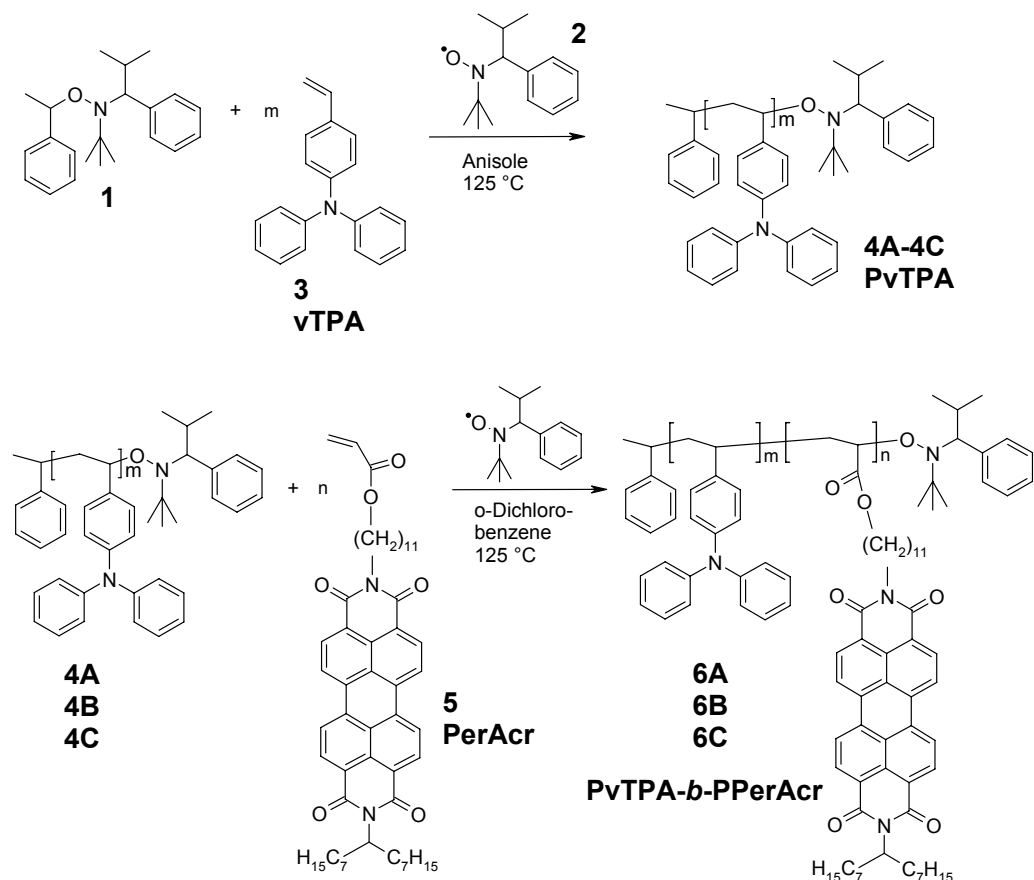
The macroinitiator **4C** (776 mg), the free nitroxide **2** (0.44 mg, 2 µmol), the PerAcr **5** (2970 mg, 3.6 mmol) and 1000 µl o-dichlorobenzene were degassed three times and filled with argon. The reaction mixture was heated at 125 °C for 24 h. The polymer was purified by repeated precipitation from chlorobenzene solution into acetone to yield 1857 mg of **6C**.

2.2 Instrumentation

The molecular weights of polymers were determined by gel permeation chromatography (GPC) in THF + 0.25 wt% tetrabutylammonium bromide with UV and RI detectors (Waters) using polystyrene standards for calibration. The dye content was determined with ^1H NMR spectroscopy using a Bruker AC 250 spectrometer (250 MHz). UV/vis spectra were recorded using a Hitachi U-3000 spectrometer and fluorescence spectra were recorded using a Shimadzu RF-5301 PC Spectrofluorophotometer. The wide angle X-ray scattering (WAXS) was performed on a Bruker-AXS D8 Advance in transmission geometry with $\text{CuK}\alpha$ radiation ($\lambda = 0.154$ nm). The samples were fixed on a tape for the measurement. For the cyclic voltammetry experiments a three-electrode assembly with a glassy carbon working electrode and a Ag/AgNO_3 reference electrode was used. THF containing 0.1 M tetrabutylammonium hexafluorophosphate was used as a solvent and each measurement was calibrated with ferrocene as internal standard.

3. Results and discussion

For the synthesis of the block copolymers nitroxide-mediated controlled radical polymerisation [9] was used (scheme 1). The advantage of this polymerisation is the controlled nature of polymerisation and the synthesis is metal free which is especially important for organic electronics. A variety of monomers with different functional groups can be used after the monomers were purified by column chromatography to remove any impurities. The monomer used for the first block was 4-vinyltriphenylamine (vTPA **3**) which acts as a hole transport material. The second monomer consists of a perylene bisimide substituted acrylate (PPerAcr **5**). The perylene bisimide acts as dye and as electron transport material. They are used due to their thermal, chemical and photochemical stability and they can easily crystallize via π - π stacking to form supramolecular structures [10]. The perylene bisimide is unsymmetrically substituted with an acrylate group for the polymerisation and a swallow-tail substituent [11] for the solubility. The monomer is very well soluble in organic solvents; even in a poor solvent such as hexane it is soluble. The block copolymer **6** consist of an amorphous hole transport block (PvTPA) and a semi-crystalline electron transport block (PPerAcr) which also absorb light intensively in the visible region. Thus all the function needed for organic solar cells are combined in this one block copolymer. With this approach not only the ratio of the blocks can be varied by the polymerisation conditions but also the length of each block. In our earlier work [7] we used **4C** as the macroinitiator to build up different lengths of perylene bisimide acrylate blocks, keeping the hole transport segment the same in all the block copolymers. Here different PvTPA macroinitiators **4A-C** with different molecular weights were used as macroinitiators in order to get block copolymers, PvTPA-b-PPerAcr **6A-C** with different PvTPA chain lengths after the second sequential polymerisation step. The perylene bisimide content is maintained between 60 and 80 wt%, in the range in which nanostructure formation is favoured. Thus, the block copolymers **6A** and **6B** have a comparable ratio of the two blocks, but the molecular weight of each block is very different. The PvTPA block in **6A** has a molecular weight of 2440 g/mol, but 11440 g/mol in **6B**. In this way, the influence of block lengths, composition and molecular weight on structural and physical properties can be elucidated. In scheme 1 the molecular weights, polydispersity (from GPC) and the thermal properties (from TGA and DSC) are given. The block copolymers **6A-C** exhibit a glass transition due to the PvTPA block and a melting peak due to PPerAcr segment. The perylenebisimide content was determined from $^1\text{H-NMR}$ spectroscopy and is also confirmed by UV-Vis spectroscopy.



	macro-initiator	M _n [g/mol]	PDI	wt% of PPerAcr	T _g [°C]	T _m [°C]	TGA-5%
4A	-	2440	1.21	-	111	-	311
4B	-	11440	1.11	-	138	-	362
4C	-	15830	1.22	-	144	-	378
6A	4A	9220	1.43	73	139	168	390
6B	4B	27850	1.47	64	136	194	389
6C	4C	26900	1.50	86	-	198	400
7	-	19900	1.65	100	-	190	404

Scheme 1. Controlled radical polymerisation of the macroinitiators **4A-4C** and the resulting block copolymers **6A-6C**. Overview of the prepared polymers and their properties.

5. Appendix A4

The electrochemical properties were determined with cyclic voltammetry. All the measured redox potentials and the HOMO/LUMO values obtained from those are tabulated in table 1. The measurements were conducted in THF containing 0.1 M tetrabutylammonium hexafluorophosphate as solvent.

Compound	$E_{\text{ox}1}$ vs Fc [V]	HOMO [eV]	$E_{\text{red}1}$ vs Fc [V]	LUMO [eV]
PvTPA 4	0.43	-5.23	---	---
PerAcr Monomer 5	---	---	-1.08	-3.72
PerAcr model 8	1.23	-6.03	-1.09	-3.71
PPerAcr 7	---	---	-1.17	-3.63
PvTPA- <i>b</i> -PerAcr 6	0.43	-5.23	-1.15	-3.65

Table 1. Redox potentials and HOMO/LUMO values determined from cyclic voltammetry in solution (Fc: Ferrocene)

The HOMO (highest occupied molecular orbital) and LUMO (lowest unoccupied molecular orbital) values were calculated with respect to ferrocene (HOMO: -4.8 eV). The PerAcr **5** monomer as well as the homo and block copolymers have two characteristic reversible reduction peaks of perylene bisimides; the first reduction peaks being at -1.08 V, -1.14 V and -1.15 V respectively with respect to ferrocene. From these values, the LUMOs can be calculated as -3.72 eV for the monomer **5**, -3.66 eV for the homopolymer **7** and -3.65eV for the block copolymers **6**. The HOMO value of the PvTPAs **4A-C** is -5.23 eV. These polymers are not soluble enough in CH_2Cl_2 to enable the study of the oxidation behaviour of perylene units which take place at higher potentials at which THF is not stable. For this reason we synthesized a highly soluble symmetrical N,N'-di(1-heptyloctyl)perylene-3,4:9,10-tetracarboxylic bisimide (**8**) as a model system (electrochemically more stable than the

monomer **5**) and measured it in CH_2Cl_2 containing 0.1 M tetrabutylammonium hexafluorophosphate. The first reduction peak being at -1.09 V and the first oxidation peak being at 1.23 V with respect to ferrocene, the LUMO can be calculated as -3.71 eV (very similar to those of block copolymer and perylene homopolymer) and the HOMO as -6.03 eV. The electrical gap between these states is 2.32 eV. In the case of block copolymers both the reduction peaks due to the perylene bisimide and the oxidation peak of the triphenylamine can be seen (see figure 1).

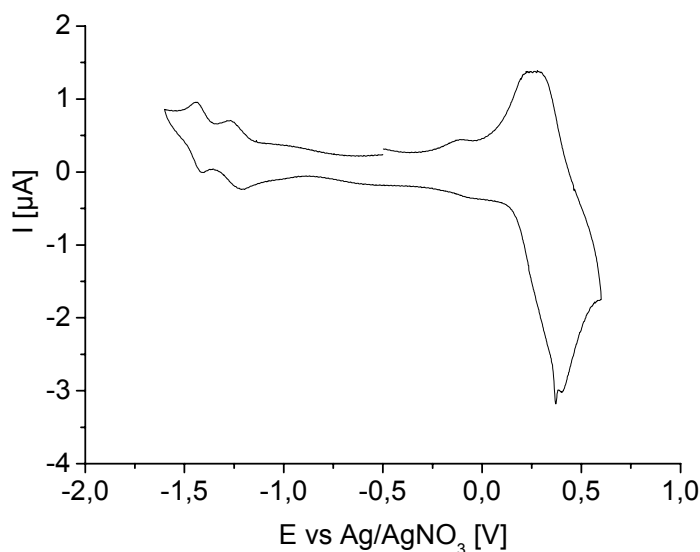


Figure 1. Example of a cyclic voltammogramm for a block copolymer with two reversible reduction peaks for the perylene bisimide unit and the oxidation of the triphenylamine unit. The spectrum was measured in THF containing 0.1 M tetrabutylammonium hexafluorophosphate.

The HOMO and LUMO values were determined as -3.65eV and -5.23eV respectively. This results in an electrical band gap of 1.58 eV for the block copolymers which decides the final photovoltage that can be obtained from this system.

Perylene bisimides exhibit a clear tendency to self-alignment via molecular π - π stacking which has a strong influence on their absorption and emission properties. The stacking property was investigated with wide angle x-ray scattering (WAXS) in powder. As an example, in figure 2 the spectra of the block copolymer **6C** and the monomer **5** are shown. Besides the amorphous halo, both spectra show a crystalline peak at 25.8° (2θ). The

crystallinity is conserved in the block copolymers, only the degree of crystallinity is lower than in **5**. The distance between two perylene bisimide units can be calculated as 3.45 Å which is very similar to the reported values for low molecular weight perylene bisimides [12]. For comparison, the layer distance in graphite is with 3.35 Å only 0.1 Å smaller. The stacking distance of the perylene bisimide is not strongly affected from the swallow-tail substituents which provide the solubility. This fact makes these compounds very promising for electro-optical applications as not only the absorption and emission properties are positively influenced by crystallinity but also the charge carrier mobility.

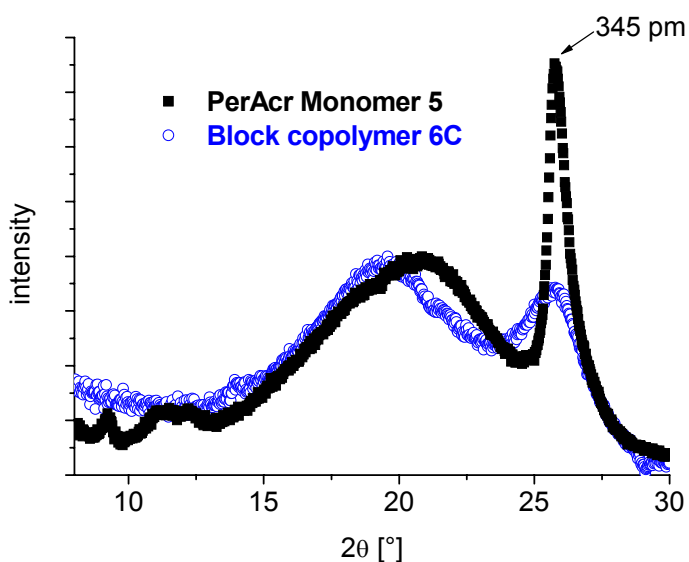


Figure 2. Wide angle X-ray scattering (WAXS) of the monomer **5** and the block copolymer **6C**.

In order to study the influence of π - π stacking of perylene bisimide units on optical properties, UV-Vis and photoluminescence measurements were carried out for the monomer and the various polymers. The difference in the optical properties of the monomer **5** and the homopolymer **7** is shown in figure 3A. The UV/vis absorption of the PerAcr monomer **5** is typical for isolated perylene bisimides without any π - π stacking. It reveals the vibronic transitions of the electronic S₀-S₁ transition (400-600 nm). In THF the absorption has a maximum at 521 nm with a high extinction coefficient (80800 cm²/mmol) and the second vibronic transition is at 485 nm. The monomer has a very strong photoluminescence at 528 nm.

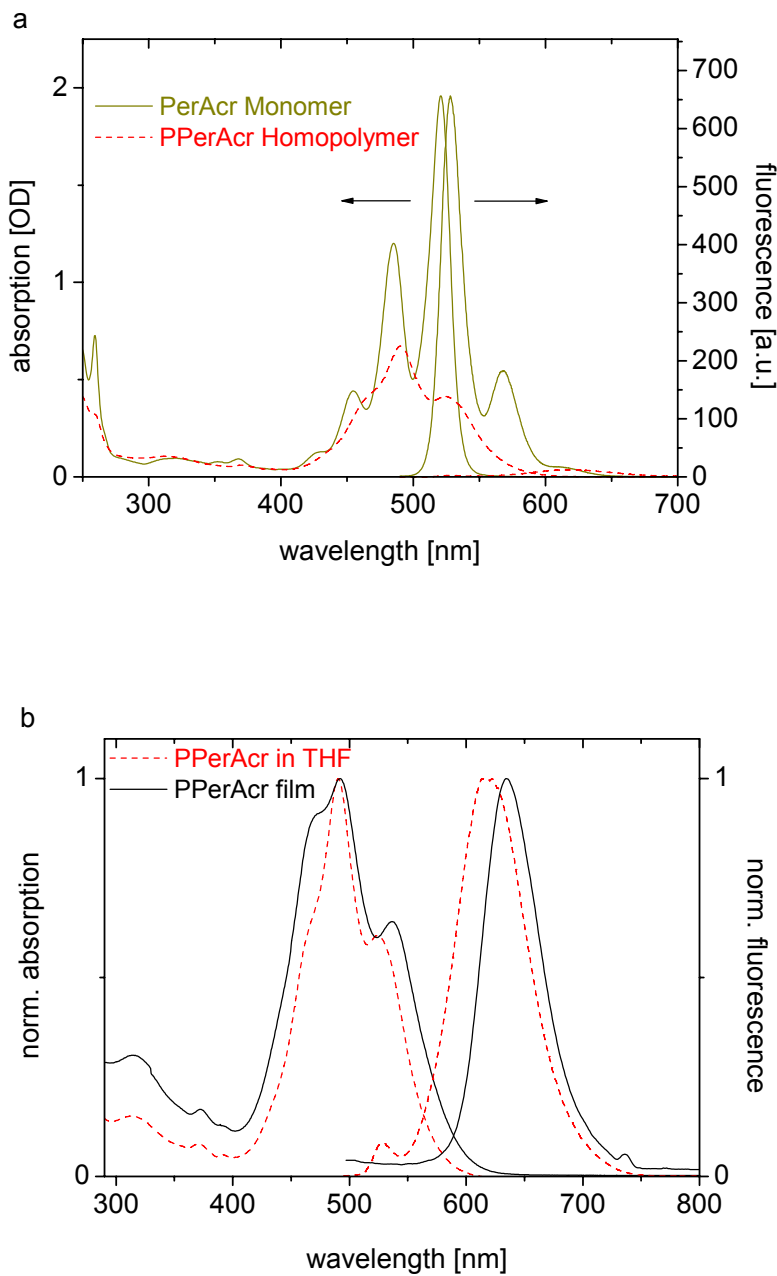


Figure 3.a) UV/vis and fluorescence spectra of the monomer PerAcr **5** and the homopolymer PPerAcr **7** in solution. The concentration for the UV/vis measurement is for both samples 0.02 mg/ml THF. b) UV/vis and fluorescence spectra of the homopolymer PPerAcr in THF solution and in film.

As the fluorescence quantum yield for swallow-tail substituted perylene bisimides is quantitative and not considerably affected by oxygen, they can be used as standards for the fluorescence yield [13]. If the UV/vis spectrum of the monomer **5** is compared to the spectrum of the perylene bisimide homopolymer PPerAcr **7** the difference is obvious. The

absorption gets broader and the intensities of the transitions change in polymer due to aggregation. The strongest absorption in perylene bisimide polymer **7** is the second vibronic transition at 490 nm. To express this change in the absorption, the quotient of the absorption at the second and the first vibronic transition is introduced. It changes from 0.61 for the monomer **5** to 1.63 for the homopolymer **7** in THF solution. Such optical parameters describe the degree of aggregation in perylene bisimide dyes [14]. It is also influenced by the solvent. For a chloroform solution with the same concentration the quotient is 1.07 and the fluorescence is shifted to 609 nm. The difference in absorption can also be seen as the colour of the monomer **5** changes from yellowish to red for the homopolymer **7**. The intramolecular coupling between the perylene bisimide units occurs in THF solution which can also be seen from the fluorescence. The fluorescence in the PPerAcr homopolymer is strongly reduced and it is red shifted to 618 nm. This behaviour is analogous to the interchain coupling in conjugated polymers and oligomers [15] but in our case it is an intramolecular coupling of two perylene bisimide units which are attached at the same polymer chain. We assign this behaviour to intramolecular coupling and not to intermolecular coupling as we could not observe any intermolecular aggregates in the GPC experiments. In films the red shift of the absorption is even stronger as can be seen in figure 3B and the fluorescence is further red shifted to 634 nm. In block copolymers also such a red shift in absorption is observed; the fluorescence of perylene bisimide being almost completely quenched, most probably due to electron transfer. Therefore the π - π stacking in the perylene bisimide segment is one of the major driving forces which can favour the nanostructure formation in these semiconductor polymers.

The interface between the electron and hole conductor is very important for organic solar cells as only there the exciton separation into a hole and an electron occurs. Block copolymers [16,17] are very interesting for this purpose as it is known that they show microphase separation on a nanometer scale exhibiting different morphologies. We investigated the morphology of the block copolymers **6A-6C** by transmission electron microscopy after melting the samples and cooling down to room temperature. In all our block copolymer samples which have a perylene content of 60-80 wt%, elongated nanowire-like structures occur except in **6A**. For **6A** as well as for the homopolymer **7** we could not observe any microphase separation using TEM.

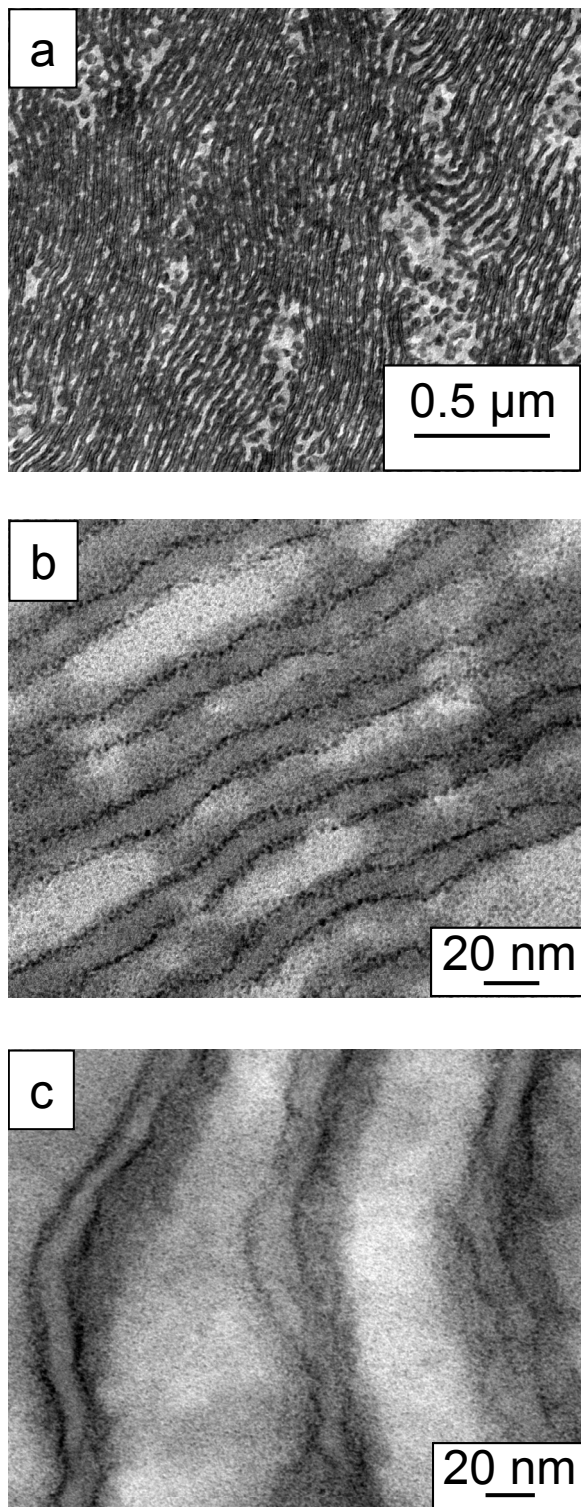


Figure 4. a) Overview of a TEM of the block copolymer **6B**. b) Magnification of the nanostructures in **6B**. c) Magnification of the nanostructures in **6C**. Samples were tempered for 1h at 200 °C, embedded into epoxy resin, cut and stained with RuO₄.

The building of these wire-like nanostructures seems to be stabilized by the PvTPA block. As in **6A** the PvTPA chain is very short, these structures are not favoured any more, most probably due to lack of enough amorphous domains which promote the segregation. In figure 4 the TEMs of the block copolymers **6B** and **6C** are shown. Both block copolymers show a microphase separation. It is interesting to note that both polymers show the same nanowire-like structure. The main driving force for this nanostructure formation is the crystallization of perylene bisimides via π - π stacking. It is important to note that these structures are non-equilibrium structures. In both cases, the perylene bisimide domains have a thickness of 13 nm with a length of up to several micrometers. The triphenylamine domains have no order or defined domain size with respect to the perylene bisimide domains which means that there is a minimal distance between the perylene bisimide wire structures. But the triphenylamine domains are flexible enough to cover also bigger distances. The samples shown here were stained with RuO₄ for approx. 5 minutes. With longer staining the structures seem to be larger than they actually are. The molecular stacking of the perylene bisimides which lead to such elongated structures with a constant thickness is still under investigation. In literature there are examples that perylene bisimides together with melamine form hexagonal structures by hydrogen-bonds [18,19]. We assume that in the case of the block copolymers **6** the nanostructures are induced by self-assembly of the perylene bisimides. As the domain size in the block copolymers is comparable to the exciton diffusion length these materials are very interesting for organic solar cells.

4. Conclusion

We have shown the synthesis and properties of block copolymers containing a perylene bisimide and a triphenylamine segment which were prepared by controlled radical polymerisation. The building of these nanostructures is induced by π - π stacking of the perylene bisimides. This stacking could be observed with WAXS. The changes in the optical properties from the monomer to the polymer could be explained as due to intramolecular coupling of the perylene bisimide moieties in polymers. The electrochemical properties together with the microphase separation on a nanometer scale are very interesting for organic electronics as the domain size is in the range of the exciton diffusion length.

Acknowledgement. The financial support for this research work from German Research Council (DFG/SFB 481 – Project B4) is gratefully acknowledged. We also thank Astrid Göpfert, University of Bayreuth, for the TEM measurement.

References

- [1] J. K. J. Van Duren, X. Yang, J. Loos, C. W. T. Bulle-Lieuwma, A. B. Sieval, J. C. Hummelen, R. A. Janssen, *J. Adv. Funct. Mater.* 14 (2004) 425.
- [2] K. O. Sylvester-Hvid, S. Rettrup, M Ratner, *J. Phys. Chem B* 108 (2004) 4296.
- [3] C. W. Tang, *Appl. Phys. Lett.* 48 (1986) 183.
- [4] J. Xue, S. Uchida, B. P. Rand, S. R. Forrest, *Appl. Phys. Lett.* 85 (2004) 5757.
- [5] S. E. Shaheen, C. J. Brabec; N. S. Sariciftci, F. Padinger, T. Fromherz, J. C. Hummelen, *Appl. Phys. Lett.* 78 (2001) 841.
- [6] H. Hoppe, M. Niggemann, C. Winder, J. Kraut, R. Hiesgen, A. Hinsch, D. Meissner, N. S. Sariciftci, *Adv. Funct. Mat.* 14 (2004) 1005.
- [7] S. M. Lindner, M. Thelakkat, *Macromolecules* 37 (2004) 8832.
- [8] D. Benoit, V. Chaplinski, R. Braslav, C. J. Hawker *J. Am. Chem. Soc.* 121 (1999) 3904.
- [9] C. J. Hawker, A. Bosman, E. Harth, *Chem. Rev.* 101 (2001) 3661.
- [10] F. Würthner, *Chem Commun.* 14 (2004) 1564.
- [11] H. Langhals, S. Demmig, T. Potrawa, *J. Prakt. Chem.* 333 (1991) 733.
- [12] E. Hädicke, F. Graser, *Acta Cryst. C* 42 (1986) 189. E. Hädicke, F. Graser, *Acta Cryst. C* 42 (1986) 195.
- [13] H. Langhals, J. Karolin, L. B. A. Johansson, *J. Chem. Soc., Faraday Trans.* 94 (1998) 2919.
- [14] B. A. Gregg, *J. Phys. Chem.* 100 (1996) 852.
- [15] J. Cornil, A. J. Heeger, J. L. Bredas, *Chem. Phys. Lett.* 272 (1997) 463.
- [16] M. J. Fasolka, A. M. Mayes, *Ann. Rev. Mat. Res.* 31 (2001) 323.
- [17] M. W. Matsen, F. S. Bates, *Macromolecules* 29 (1996) 1091.
- [18] L. E. Sinks, B. Rybtchinski, M. Iimura, B. A. Jones, A. J. Goshe, X. Zuo, D. M. Tiede, X. Li, M. R. Wasielewski, *Chem. Mater.* 17 (2005) 6295.
- [19] J. A. Theobald, N. S. Oxtoby, M. A. Philips, N. R. Champness, P. H. Beton, *Nature* 424 (2003) 1029.

Charge Separation at Self-Assembled Nanostructured Bulk Interface in Block Copolymers**

Angewandte Chemie International Edition, **2006**, *45*, 3364-3368.

Stefan M. Lindner, Sven Hüttner, Arnaud Chiche, Mukundan Thelakkat*, Georg Krausch*

Organic electronic devices and especially photovoltaics have attracted steadily increasing attention during the last years due to their potential in terms of cheap processing, large area application as well as the compatibility with flexible substrates [1,2]. In contrast to inorganic semiconductors, organic materials do not directly create free charge carriers on illumination, but leads to bound electron-hole pairs called excitons[3]. These excitons must be carried towards a donor-acceptor (DA) interface where they dissociate and then drift towards electrodes. Unfortunately, excitons travel only a few tens of nanometers before recombination. Therefore a very thin absorption layer is required for all the excitons to reach the DA interface[4]. At the same time the optical absorption length is in the order of a few hundreds of nanometers. Thus an efficient device also requires a thick absorption layer that is then not compatible with the very short diffusion length of an exciton. To solve this issue improvements of the original bilayer heterojunction device[4] have been developed by introducing concepts of multiple heterojunction[5] and bulk heterojunction [6-8] (Figure 1d). However, polymer-polymer blends usually result in macrophase separation limiting the

[*] S. M. Lindner, PD Dr. M. Thelakkat
Makromolekulare Chemie I
Universität Bayreuth
Universitätsstr. 30, 95440 Bayreuth, Germany
Fax: (+49) 921-55-3206
E-mail: mukundan.thelakkat@uni-bayreuth.de

S. Hüttner, Dr. A. Chiche, Prof. G. Krausch
Physikalische Chemie II
Universitätsstr. 30, 95440 Bayreuth, Germany
Fax: (+49) 921-55-2059
E-mail: georg.krausch@uni-bayreuth.de

[**] The authors are grateful to C. Kunert for the TEM images and to H. Hänsel as well as S. Haque, Imperial College London for fruitful discussions. This work was supported by the German Research Council (DFG/SFB 481-Project B4). AC acknowledges financial support from the European Community's "Marie-Curie Actions" under "Polyfilm" Research Training Network.

efficiency of charge separation and power conversion in a photovoltaic device [9,10]. Therefore, generating ‘nanostructured bulk heterojunctions’ which guarantee a proper percolation of charges is still a challenge to be taken.

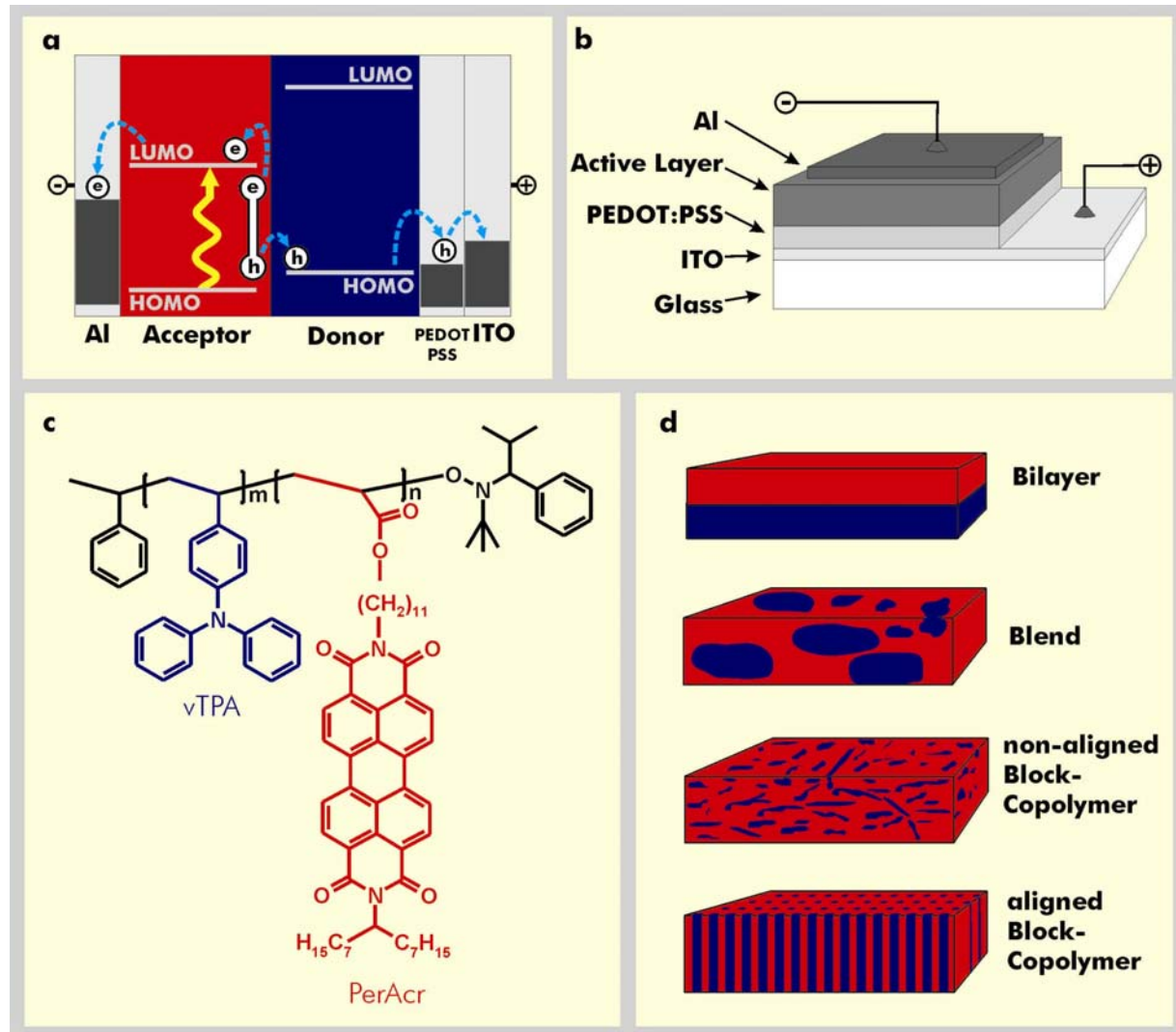


Figure 1. a) The upper drawing shows the physical processes in a bilayer donor/acceptor solar cell. The absorbed light generates excitons which drift in all directions. Those which reach the donor/acceptor interface separate into free charges. At the donor/acceptor interface an electron transfers into the LUMO of the acceptor and a hole into the HOMO of the donor. The separated charges are transported via hopping and collected at the respective electrodes. b) Schematic representation of device structure of a polymer solar cell. c) Chemical structure of block copolymer PvTPA-b-PPerAcr. d) Various morphologies in the active layer which can be utilized for the creation of DA interface for charge separation.

'Nanostructured bulk heterojunctions' can be realized using diblock copolymers made of two covalently linked polymers with suitable electronic properties (donor and acceptor blocks). The interplay between molecular connectivity and immiscibility leads to the spontaneous formation of ordered microdomains of molecular dimensions[11] and solves the issue of carrying excitons to the DA interface. The fundamentals of block copolymer self-assembly in thin films have been the subject of numerous studies throughout the last decade[12] in view of its enormous potential for nanotechnology applications[13]. This particularly involves the macroscopic alignment of the nanostructures by means of external fields [14,15], which potentially allows the control of the percolation paths mentioned above (Figure 1d). The obvious advantage of block copolymers for application in organic electro-optical devices has previously been recognized [16-18]. As for now, however, no working photovoltaic device based on 'nanostructured bulk heterojunction' has been demonstrated yet.

In the present contribution we describe a single active layer photovoltaic device obtained by the self-assembly of a diblock copolymer carrying all functionalities required for light absorption, charge separation and charge transport. The block copolymer self-assembles into a nanostructure, which provides charge separating interfaces at nanometer scale. As a proof of concept, we compare the performance of the block copolymer device with a device made from a blend of the two individual segment polymers of identical thickness and composition. We demonstrate that the photovoltaic properties (short circuit current, photovoltage, power conversion efficiency) of the block copolymer significantly surpass those of the blend device. Due to the nanostructured nature of the film, the photovoltaic properties are less dependent on the thickness of the polymer layer thereby enabling thicker devices with higher optical absorption without significant loss of efficiency. The considerable improvement in performance can be correlated via TEM and AFM of the active layers to the 'nanostructured bulk heterojunction' formed in block copolymers.

Recently, we have described the synthesis of fully functionalized tailor-made semicrystalline block copolymers carrying hole conductor, electron conductor and light absorption functionalities[19]. The hole transport function is taken care of by a poly(vinyltriphenylamine) segment (PvTPA, HOMO level ~5.2 eV), and both electron transport and light absorption occurs in a polyacrylate segment carrying perylene bisimide side groups (PPerAcr, LUMO level ~3.7eV) (Figure1c). The block copolymers were obtained with well-defined molecular weights in the range between 18 and 40 kg mol⁻¹. The composition and dye content can be varied to suit the requirements of light absorption and

balanced charge transport. It was also shown that such fully functionalized diblock copolymers phase-separate on nanometer scale. These block copolymers exhibit both a glass transition temperature T_g at about 150°C due to the amorphous PvTPA segment and a melting temperature T_m at about 200°C due to crystalline perylene bisimide side group stacking.

Thin films of PvTPA₂₁-b-PPerAcr₇₉ (79 wt% PPerAcr; $M_n = 37710 \text{ g mol}^{-1}$; $T_g = 149.5^\circ\text{C}$, $T_m = 198.0^\circ\text{C}$) with thicknesses around 250 nm were prepared by spin coating from chloroform solution onto a glass substrate initially coated with indium tin oxide (ITO) and an additional injection layer of PEDOT/PSS, to avoid short-circuit through the active layer. For means of comparison polymer blend cells were prepared in the same way by mixing homopolymers of PvTPA and PPerAcr (weight fractions: $\phi_{\text{PvTPA}} = 0.21$, $\phi_{\text{PPerAcr}} = 0.79$)[19]. Aluminium electrodes were evaporated onto the top of the polymer layers by vacuum deposition at 10^{-6} mbar (Figure 1b). The active area of a single device was 0.18 cm^2 . These single-layer devices were characterized by current-voltage measurements in the dark and under illumination with a white light source (AM 1.5 spectral conditions, 77 mW cm^{-2}). All measurements were performed at ambient conditions without any encapsulation or protection of the devices against degradation. Fig. 2 compares the current voltage characteristics of illuminated devices made of the polymer blend and the block copolymer. The data demonstrates quite convincingly that the block copolymer device exhibits significantly better performance than the blend device. The short circuit current J_{SC} is measured as 0.028 mA cm^{-2} for the blend and 0.19 mA cm^{-2} for the block copolymer. Accordingly, the open circuit voltage V_{OC} is increased from 525 mV for the blend to 865 mV for the block copolymer. The power conversion efficiency under white light exposure was improved by one order of magnitude from 0.007% in the polymer blend to 0.07% in the block copolymer device. The inset (fig 2) shows the energy level diagram of the donor and acceptor blocks. The energetic offset at the interface compels the charge separation and the desired flow of electrons to the respective electrodes. The values of HOMO/LUMO given here are determined from cyclic voltammetry measurements in solution.

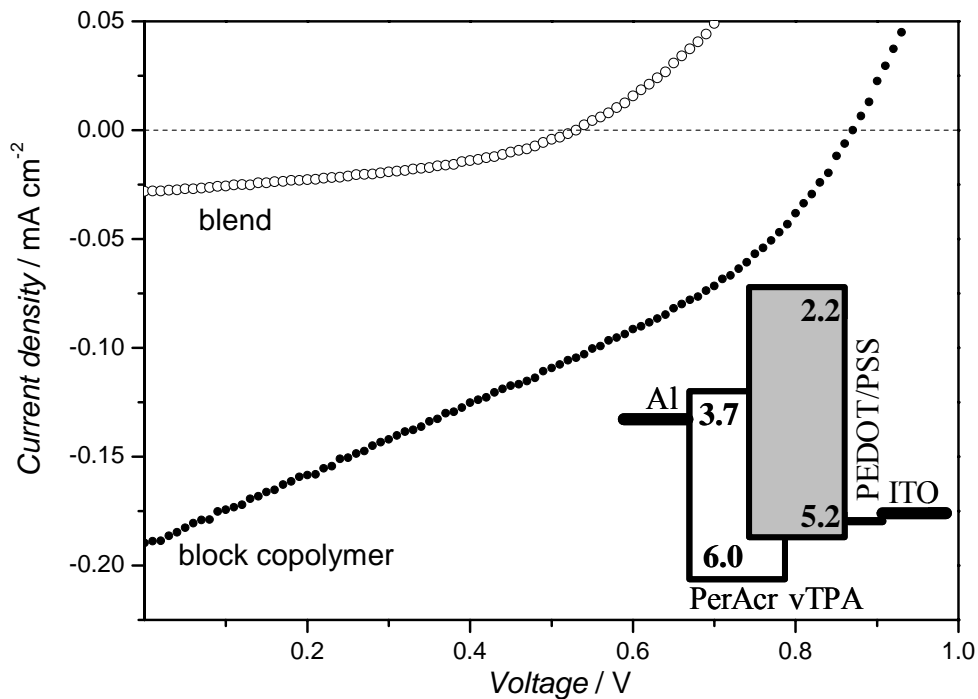


Figure 2. Current-voltage characteristics of a photovoltaic device using a polymer blend (open symbols) and a block copolymer (filled symbols) sandwiched between two electrodes. Thickness of active layer: 250 nm; the short circuit current (I_{sc}) and the open circuit voltage (V_{oc}) are 0.028 mA cm^{-2} and 0.525 V for the blend and 0.19 mA cm^{-2} and 0.865 V for the block copolymer, respectively. The power conversion efficiency was also improved by one order of magnitude from 0.007% in the polymer blend to 0.07% in the block copolymer device. Inset shows the energy level diagram of the donor and acceptor blocks ; the values representing the HOMO and LUMO levels being in eV as determined from cyclic voltammetry.

In order to rationalize this finding we investigated the phase morphology of the thin films as present in the solar cells. For this purpose cross sectional transmission electron microscopy (TEM) studies were carried out on the solar cells themselves. As PEDOT/PSS is water soluble, the active layer could be floated onto water, embedded into epoxy resin and cut revealing vertical cross sections through the active layer of the devices (Figure 3a, b). The dark domains result from stained perylene bisimide. It is obvious that the polymer blend is characterized by large, micron-sized domains whereas the block copolymer film exhibits a

nanoscopic structure. These results are also supported by tapping mode AFM topography images given in Figure 3c and 3d.

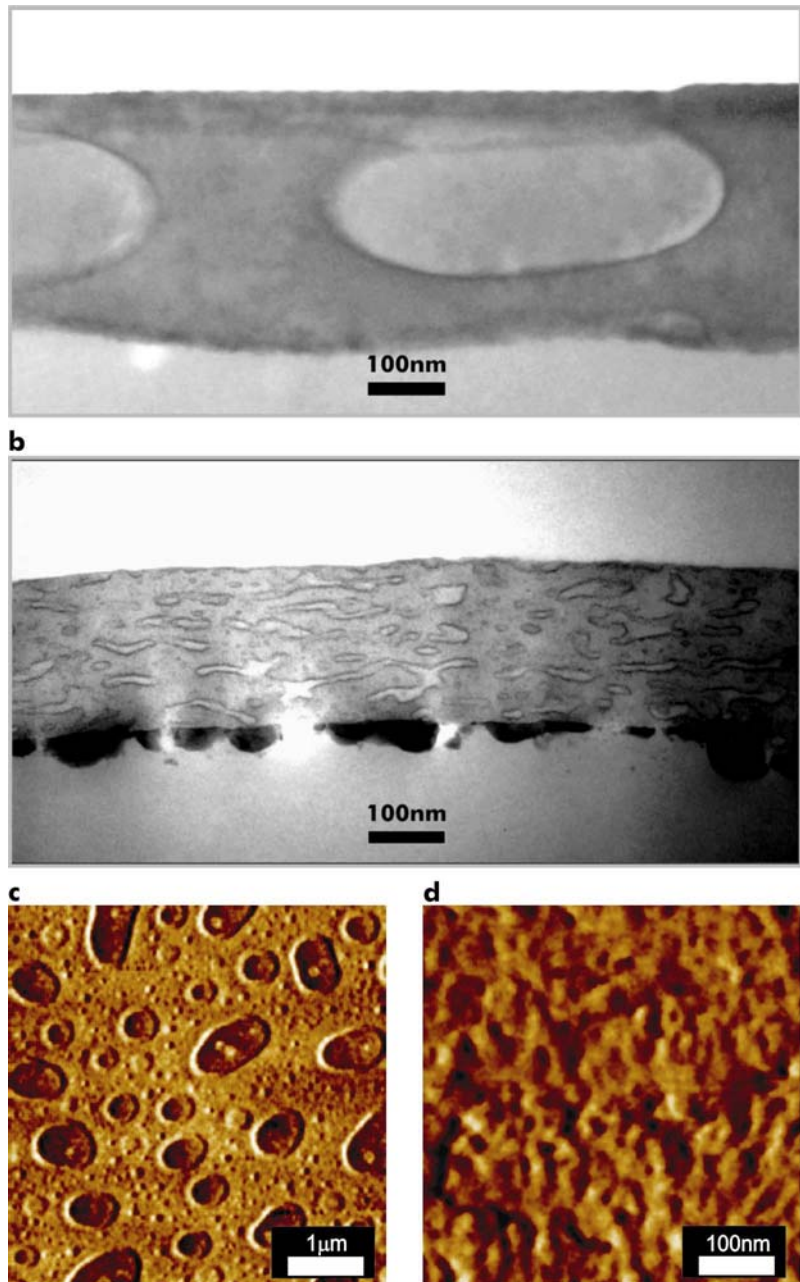


Figure 3. a) TEM cross sections of a polymer blend device with 20 wt% of PvTPA and 80 wt% of PPerAcr and b) of a block copolymer device ($\text{PvTPA}_{21}\text{-b-PPerAcr}_{79}$). The active layers were floated, embedded into epoxy and cut for TEM. TEM pictures were taken from the vertical cross sections of the same layers used for the preparation of the devices. c) AFM phase image in tapping mode of a polymer blend surface with 20 wt% of PvTPA and 80 wt% of PPerAcr (z range 2.5°) and d) of a block copolymer surface ($\text{PvTPA}_{21}\text{-b-PPerAcr}_{79}$) (z range 5.0°). Note that the scale bars differ by a factor of 10.

The characteristic width of the block copolymer microdomain structure (10 to 50 nm) is of the same order as the exciton diffusion length observed in similar perylene compounds[5]. This allows the excitons generated in the perylene bisimide domain to reach the DA interface (i.e. the PvTPA segment) more efficiently in a block copolymer layer than in the blend. Additional characterizations of the devices were performed to evaluate this explanation. Figure 4a presents the absorption curves of films of the blend and the block copolymer. The perylene dye units show strong aggregation (crystallization in confined nanometre domains due to segregation effects of segments in a block copolymer). This actually should favour the transport of electrons in these highly ordered structures and it also favour a small red shift in the absorption which is desired in solar cells. No obvious difference in these spectra can be noticed in both block copolymer and blend indicating the same amounts of absorbing material, in this case the vTPA and the perylene bisimide groups. This meets our expectations as the blend ratio and the block copolymer segment ratio are the same, and the polymeric layer has the same thickness around 250 nm. The same density of excitons should then be generated in both systems. These excitons can either reach a DA interface (and generate separated charges) or recombine, resulting in photoluminescence (PL). As suggested by the different performances of the cells (Figure 2) more excitons finally result in charge separation in the case of the block copolymer. This is confirmed by the PL quenching experiments carried out on both, the blend and the block copolymer (Figure 4a). The PPerAcr homopolymer exhibits intense PL at 620 nm on excitation with 470 nm light indicating that radiative decay is the main recombination pathway for the exciton. In the block copolymer the maximum PL intensity is quenched more efficiently than in the blend layer again indicating the more efficient charge transfer in nano-structured bulk heterojunction in a block copolymer. This is also supported by the wavelength dependent incident photon to current conversion efficiency (IPCE) measurements. The IPCE curves (Fig. 4b) are directly correlated with the absorption in both cases (Figure 4a), but the efficiencies are much lower for the blend devices. These results are also in agreement with the reported values of poor efficiency and quantum yield generally observed in polymer-polymer blend devices[10].

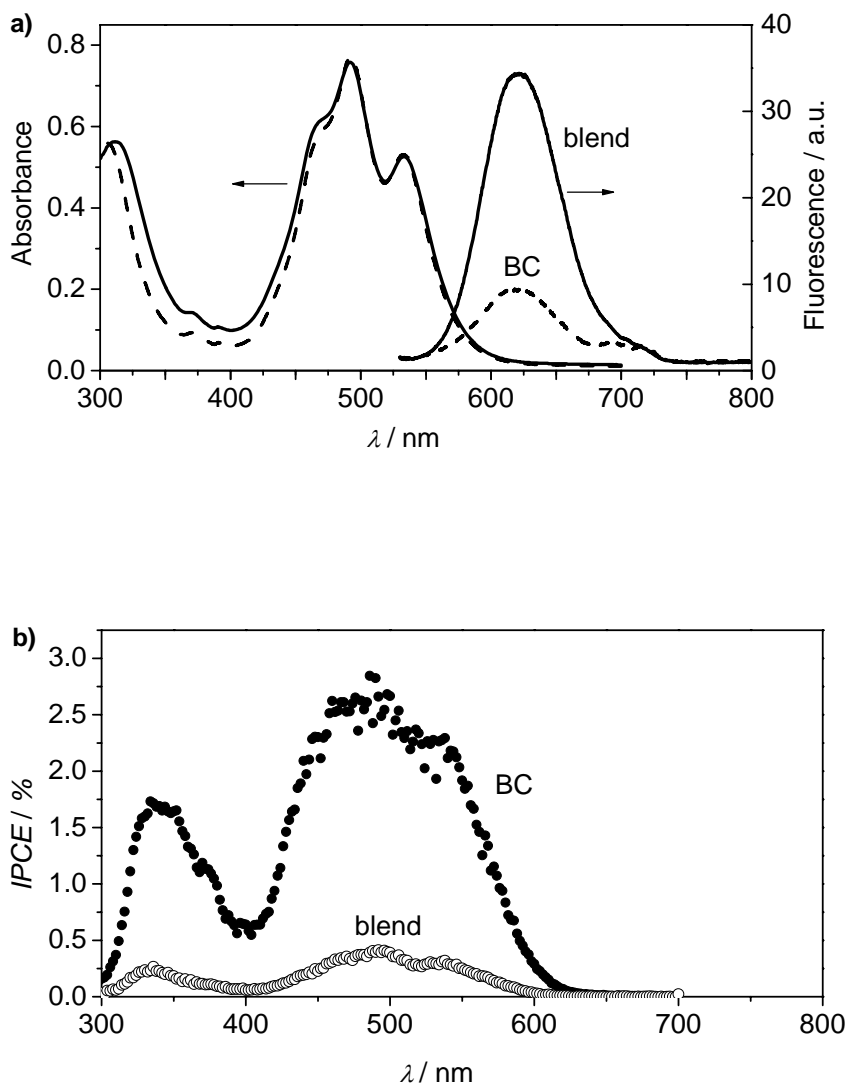


Figure 4. a) Absorption spectrum of both blend (solid line) and block copolymer (dashed line) and photoluminescence spectra of blend (solid line) and block copolymer films (dashed line) under an excitation wavelength of 470 nm, b) IPCE curves (external quantum efficiency) of both types of devices. The blend (open symbols) and the block copolymer (filled symbols) devices with 250 nm thickness are compared.

These are profound findings with positive consequences for polymeric devices. Using the concept of fully functionalized block copolymers single active layers can be used for efficient charge separation with the advantage that the majority of generated excitons reach the interface for charge separation. This is a first step towards efficient thicker layer devices designed for higher light absorption. Using a 580 nm thick block copolymer layer we have

already obtained a similar open circuit voltage V_{OC} (0.88 V) and a reasonable short circuit current J_{SC} (0.09 mA cm $^{-2}$).

From these results the use of a block copolymer with suitable electronic properties appears an elegant and a very promising solution to overcome the short diffusion length of an exciton formed in an organic semiconductor. Controlling the nano-domain alignment is the next challenge to be taken in order to improve the charge conduction toward the device electrodes. Indeed, the block copolymer domains displayed in Figure 3b do not exhibit a well-aligned structure, and if at all, appear to be preferentially aligned parallel rather than perpendicularly to the electrodes. Ideally, one would wish for rather defect-free microdomains being aligned perpendicularly to the plane of the film (Figure 1D). The orientation of PPerAcr nanostructures in particular will augment the flow of electrons towards the electrodes considerably. Current research work therefore concentrates on the combination of the above approach with one of the various techniques that have recently been devised for the creation of defect-free block copolymer structures and macroscopic domain alignment in thin block copolymer films. Potentially the most promising route may involve solvent induced alignment similar to what has recently been reported by the Russell group[20] as the films are prepared from solution anyway. Alternatively, electric field induced alignment of the domains may be striven for given that in most cases reported so far in the literature, the domains are aligned such that the interfaces lie parallel to the electric field vector[21,22]. In this case, particular care would have to be taken since the block copolymers under study are electrically (semi-) conducting, whereas the materials studied so far were insulators. While the absolute efficiencies of the devices studied in this work are still considerably smaller than the best state-of-the-art organic photovoltaic cells, we were able to give a proof-of-principle clearly showing that the concept of nanostructured bulk heterojunction devices based on block copolymers is a significant breakthrough in the design of more efficient organic devices. Moreover, the method of fabrication is compatible with current device preparation processes and with current schemes of defect removal and macroscopic domain alignment. This finding also gives large input into the field of fully functionalized self-organizing molecular devices and molecular electronics in general.

Experimental Section

UV/vis spectra were recorded on a Hitachi U-3000 spectrometer and fluorescence spectra were recorded on a Shimadzu RF-5301 PC Spectrofluorophotometer. The films were prepared by spin-coating from a 1.5 wt% CHCl₃ solution.

The photovoltaic devices were prepared by spin-coating PEDOT:PSS dispersion, obtained from Bayer AG, onto pre-cleaned, patterned indium tin oxide substrates (18 Ω per square). The active layer was deposited by spin-coating from a 1.5 wt% CHCl₃ solution. The aluminium electrode (100 nm) was deposited by vacuum evaporation at 10⁻⁶ mbar. The active area of the cell is 0.18 cm².

Current-voltage measurements were done with a constant intensity of 76.7 mW cm⁻² light under standard AM 1.5 G spectral conditions (Oriel set up with 150 W Xenon arc lamp and suitable filters). This set up is calibrated using a reference Si-cell from ISE Freiburg at the sample position and height.

Incident photon to current conversion efficiency (IPCE) is measured using a monochromator (Spex, Model 1681 B) with holographic grid (Lamp: 300 W Xenon arc lamp Model: 6259 Oriel) creating homogeneous illumination of a circular spot of 3.5 cm diameter (Power: <1 mW) for the wavelength range from 280 nm to 1000 nm.

Samples for TEM were floated with water, embedded into epoxy resin, cut vertical to get a cross section of the active layer and stained with RuO₄. The measurements were performed with a Zeiss 902 Transmission Electron Microscope. The AFM measurements were performed with a Dimension 3100 from Digital Instruments. Images were taken in tapping mode.

Keywords: block copolymer self-assembly, nanostructured bulk heterojunction, photovoltaic device, polymer solar cell.

Literature

- [1] G. Malliaras, R. Friend, Phys. Today 2005, 58, 53-58.
- [2] C.J. Brabec, J.A. Hauch, P. Schilinsky, C. Waldauf, MRS Bull. 2005, 30, 50-52.
- [3] B.A. Gregg, MRS Bull. 2005, 30, 20-22.
- [4] C. W. Tang, Appl. Phys. Lett. 1986, 48, 183-185.
- [5] P. Peumans, A. Yakimov, S.R. Forrest, J. Appl. Phys. 2003, 93, 3693-3723.
- [6] G. Yu, J. Gao, J.C. Hummelen, F. Wudl, A.J. Heeger, Science 1995, 270, 1789-1791.
- [7] C.J. Brabec, N.S. Sariciftci, J.C. Hummelen, Adv. Funct. Mater 2001, 11, 15-26.
- [8] J.J.M. Halls, C.A. Walsh, N.C. Greenham, E.A. Marseglia, R.H. Friend, S.C. Moratti, A.B. Holmes, Nature 1995, 376, 498-500.
- [9] A. C. Arias, J. D. MacKenzie, R. Stevenson, J. J. Halls, M., Inbasekharan, , E. P. Woo, D. Richards, R. H. Friend, Macromolecules 2001, 34, 6005-6013.
- [10] Y. Kim, S. Cook, S. A. Choulis, J. Nelson, J. R. Durrant, D. D. C. Bradley, Chem. Mater. 2004, 16, 4812-4818.
- [11] F.S. Bates and G.H. Fredrickson, Ann. Rev. Phys. Chem. 1990, 41, 525-557.
- [12] M.J. Fasolka and A.M. Mayes, Ann. Rev. Mat. Res. 2001, 31, 323-355.
- [13] C. Park, J. Yoon, E.L. Thomas, Polymer 2003, 44, 6725–6760.
- [14] Z.R. Chen, J.A. Kornfield, S.D. Smith, J.T. Grothaus, M.M. Satkowski, Science 1997, 277, 1248-1253.
- [15] T. Thurn-Albrecht, J. Schotter, G.A. Kastle, N. Emley, T. Shibauchi, L. Krusin-Elbaum, K. Guarini, C.T. Black, M.T. Tuominen, T.P. Russell, Science 2000, 290, 2126-2129.
- [16] J. Liu, E. Sheina, T. Kowalewski, R. D. McCullough, Angew. Chem. Int. Ed. 2002, 41, 329-332.
- [17] M. H. van der Veen, B. de Boer, U. Stalmach, K. I. van de Wetering, G. Hadzioannou, Macromolecules, 2004, 37, 3673-3684.

5. Appendix A5

- [18] J. P. Chen, D. Markiewicz, V. Y. Lee, G. Klaerner, R. D. Miller, J. C. Scott, *Synth. Met.* 1999, 107, 203-207.
- [19] S. M. Lindner, M. Thelakkat, *Macromolecules* 2004, 37, 8832-8835.
- [20] S.H. Kim, M.J. Misner, T.P. Russell, *Advanced Materials* 2004, 16, 2119-2123.
- [21] T. Thurn-Albrecht, J. DeRouchey, T. P. Russell, H. M. Jaeger, *Macromolecules* 2000, 33, 3250-3253.
- [22] A. Böker, H. Elbs, H. Hänsel, A. Knoll, S. Ludwigs, H. Zettl, V. Urban, V. Abetz, A.H.E. Müller, G. Krausch, *Phys. Rev. Lett.* 2002, 89, 135502.

Erklärung

Hiermit erkläre ich, dass ich die vorliegende Arbeit selbstständig verfasst und keine anderen als die von mir angegebenen Quellen und Hilfsmittel verwendet habe.

Ferner erkläre ich, daß ich weder anderweitig mit oder ohne Erfolg versucht habe, diese Dissertation einzureichen, noch eine gleichartige Doktorprüfung an einer anderen Hochschule endgültig nicht bestanden habe.

Bayreuth, 09. März 2006

Stefan Lindner